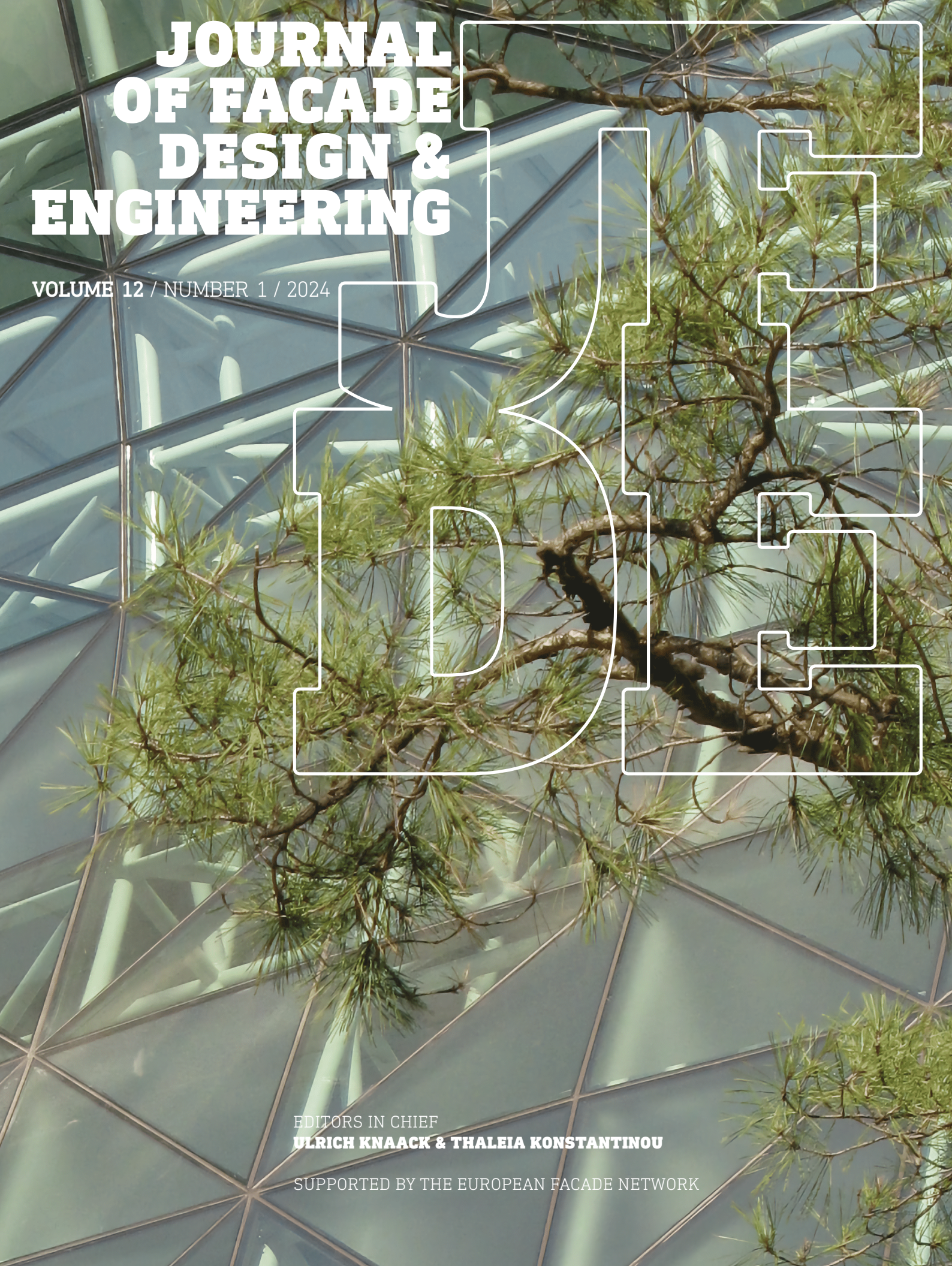

JOURNAL OF FACADE DESIGN & ENGINEERING

VOLUME 12 / NUMBER 1 / 2024

EDITORS IN CHIEF
ULRICH KNAACK & THALEIA KONSTANTINOU

SUPPORTED BY THE EUROPEAN FACADE NETWORK

JOURNAL OF FACADE DESIGN & ENGINEERING

VOLUME 12 / ISSUE 1 / 2024

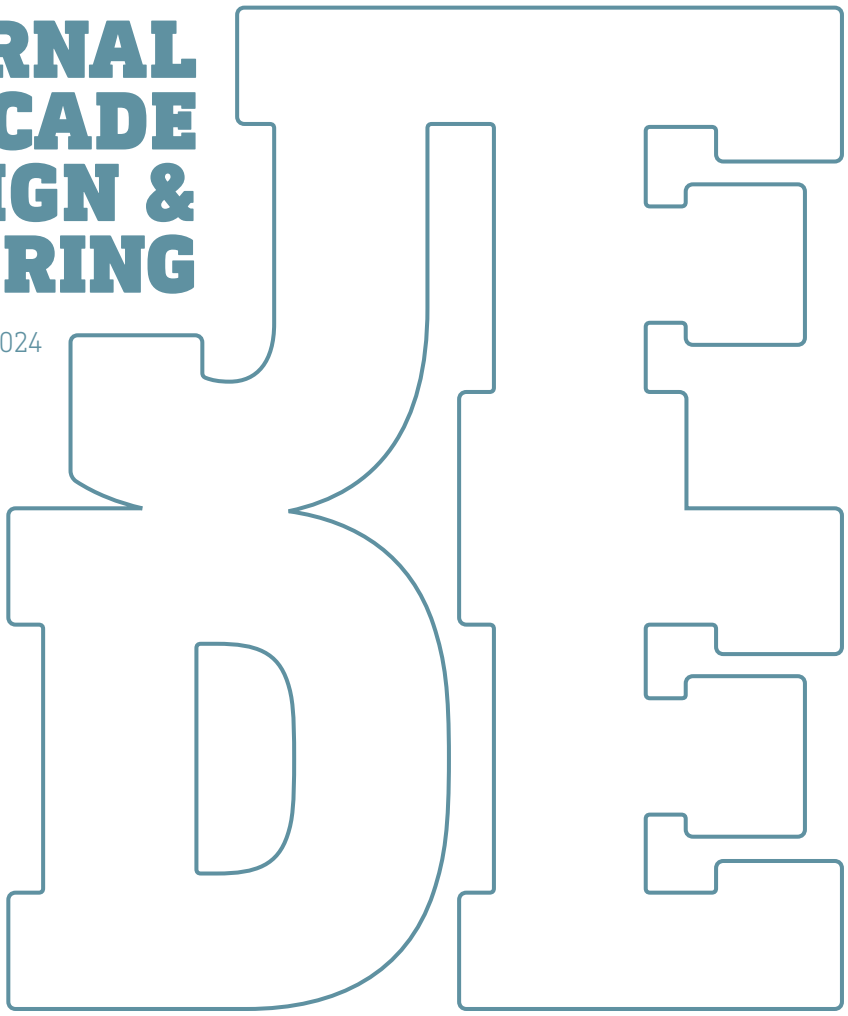

EDITORS IN CHIEF
ULRICH KNAACK & THALEIA KONSTANTINOU

SUPPORTED BY THE EUROPEAN FACADE NETWORK

JFDE Journal of Facade Design and Engineering

JFDE presents new research results and new proven practice of the field of facade design and engineering. The goal is to improve building technologies, as well as process management and architectural design. JFDE is a valuable resource for professionals and academics involved in the design and engineering of building envelopes, including the following disciplines:

– Architecture
– Building Engineering
– Structural design
– Climate design
– Building Services Engineering
– Building Physics
– Design Management
– Facility Management

JFDE is directed at the scientific community, but it will also feature papers that focus on the dissemination of science into practice and industrial innovations. In this way, readers explore the interaction between scientific developments, technical considerations and management issues.

Publisher
Stichting OpenAccess, Rotterdam

Owner
TU Delft / Faculty of Architecture and the Built Environment
Julianalaan 134, 2628 BL Delft, The Netherlands

Contact
Alessandra Luna Navarro
editors@jfde.eu
https://jfde.eu/

Policies
Peer Review Process – The papers published in JFDE are double-blind peer reviewed.
Open Access – JFDE provides immediate Open Access (OA) to its content on the principle that making research freely available to the public supports a greater global exchange of knowledge.

Indexation – JFDE is indexed in the Directory of Open Access Journals (DOAJ), Google Scholar, Inspec IET and Scopus.
Publication Ethics – Editors, authors and publisher adopt the guidelines, codes to conduct and best practices developed by the Committee on Publication Ethics (COPE).
Copyright Notice – Author(s) hold their copyright without restrictions.

Cover image
ENSNARE modular façade system combining RIVENTI's and ONYX's technologies. Image courtesy of Nuria Jorge.

Design & layout & proofreading
Design – Sirene Ontwerpers, Amsterdam
Layout & Open Access – Stichting OpenAccess, Rotterdam
Proof-reading – Usch Engelmann, Rotterdam

ISSN 2213-302X (Print)
ISSN 2213-3038 (Online)
ISBN 978-94-93439-16-0

Submissions
All manuscripts and any supplementary material should be submitted to the Editorial Office (editors@jfde.eu), through the Open Journal System (OJS) at the following link: https://jfde.eu/

Author Guidelines
Detailed guidelines concerning the preparation and submission of manuscripts can be found at the following link:
https://jfde.eu/index.php/jfde/about/submissions

Contents

Contents

EDITORIAL

Thaleia Konstantinou[1], Ulrich Knaack[1] (Eds.)

1 Delft University of Technology

The first issue of volume 11 of JFDE elaborates on several topics related to façade design and engineering, focusing on façade systems, their construction, properties, and performance.

The topic of prefabrication in façade construction is one of the themes emerging from this issue. The importance of prefabrication is growing in the building industry as it has the potential to improve productivity by allowing faster, high-quality, and cost-effective construction while reducing risks related to onsite construction. Different articles touch on this topic from varying perspectives. In the context of decarbonization and the large number of buildings to be renovated, prefabrication for energy retrofits is a relevant topic. One notable article presents the development and evaluation of prefabricated timber-based façade modules. The results showed significant energy savings and effective vapor release of the prefabricated façade system. Furthermore, prefabrication and pre-engineering of systems require a paradigm shift in design and engineering practices towards more integrated approaches. A Kit-of-Part (KoP) approach to façade design employed by the authors of a different article enables an architect-led design team to validate design options through digital design tools based on a pre-engineered set of components. Information about the products included in the tool includes performance, cost, and environmental impact.

Focusing further on the properties of façade components, a paper in this issue investigates large-scale applications in building design regarding the aluminum used in façades and underlines the environmental benefits to be gained from reducing the use of raw materials, with particular emphasis on a sustainable approach to façade design. Finally, the issue addresses shading as an essential component of façade function, examining the influence of different shading devices on both performance and aesthetic aspects of the façade.

Overall, the issue provides insights into contemporary trends in façade design, emphasizing the role of pre-engineering and evaluating façade components in contributing to the future of the construction industry.

The Editors-in-Chief,
Thaleia Konstantinou and Ulrich Knaack

DOI
http://doi.org/10.47982/jfde.2023.1.00

Data-driven and LCA-based Framework for environmental and circular assessment of Modular Curtain Walls

Luca Morganti [1,3], Peru Elguezabal Esnarrizaga [2,4], Alessandro Pracucci [3], Theo Zaffagnini [1], Veronica Garcia Cortes [2], Andreas Rudenå [5], Birgit Brunklaus [6], Julen Astudillo Larraz [2*]

* Corresponding author: julen.astudillo@tecnalia.com
1 University of Ferrara, Department of Architecture, Ferrara, Italy
2 TECNALIA, Basque Research and Technology Alliance (BRTA), Derio, Spain
3 Focchi S.p.A., Rimini, Italy
4 University of the Basque Country UPV/EHU, Department of Electrical Engineering, Bilbao, Spain
5 Paramountric A.B., Sweden
6 Research Institutes of Sweden, Division of Built Environment, Unit of Energy and Environmental System Analysis, Sweden

Abstract

To assist the sustainable development of the building sector, designers require tools illustrating the most viable design options. This paper, starting by presenting the opportunities and limitations of the Life Cycle Assessment (LCA) methodology and Digital Product Passport (DPP) instrument when applied to Custom Modules for Curtain Walls, proposes a Semantic Data-driven Framework to facilitate the design of low-carbon and circular façade modules. Based on literature and the practical outcome of the H2020 project Basajaun, this framework integrates computer-aided technologies that manufacturing companies commonly employ to automate an efficient sustainability assessment process using primary data. This solution innovates industrial process management and architectural design and supports the creation of greener products. It also facilitates the output of documents supporting end-of-life scenarios. The development methodology involves investigating required quantitative project data, environmental factors, and circularity information, as well as the definition of flowcharts for the Life Cycle Inventory, extending a best practice for the façade module's DPP. Furthermore, the methodology implicates data collection and IT implementation and organisation. This is through the definition of an ontology conceived for interconnection between digital systems. The findings shall contribute to implementing the LCA and DPP practices for custom prefabricated façade modules and suggest areas for further development. Challenges include obtaining and sharing data on environmental impacts and circularity, but involving stakeholders and addressing technical limitations can improve sustainability.

Keywords

Custom prefabricated Modules for Curtain Walls (CMCW), Life Cycle Assessment (LCA), Digital Product Passport (DPP), Semantic Data Framework, Eco-design tool, Production Management and Innovation

DOI

http://doi.org/10.47982/jfde.2024.305

1 INTRODUCTION

Among the most critical sustainability requirements that will have to be addressed in the coming decades, a renewer transformation of the building sector is inevitable (IPCC, 2023; UNEP & GABC, 2021). While the construction industry is hopefully moving in the green direction, it still needs to evolve to tackle the challenges of climate change, endurable use of resources, and water shortage. Therefore, it is fundamental to have a clearly defined picture of the design options that architects and designers own to minimise the environmental impact of their project's life cycle. However, current design tools are often limited in providing an accurate and comprehensive environmental and circular assessment. This study explores a data-driven approach to life cycle strategies in the sector of architectural building envelopes, which integrates the IT tools of Industry 4.0 for innovation, optimisation, and management of resources and processes.

Building façades are intricate components of architecture that interact with various disciplines and stages of the value chain. They have a shorter lifespan compared to the primary structure of a building (WGBC, 2019, p. 23). Consequently, it is both difficult and crucial to address the principles of the Circular Economy (CE) in façades. This transition is vital for shifting from the linear approach of take-make-waste to a more sustainable approach of reduce-reuse-recycle (Kragh & Jakica, 2022). This finding becomes even more stimulating in the case of prefabricated façade modules. Machado and Morioka (2021) systematically reviewed the literature to identify how modularity can contribute to a circular and sustainable economy. Fifteen advantages of commutability have been identified, which can positively impact the adoption of CE strategies, and five barriers have been recognised that may delay the process of incorporating these benefits. Examples of these advantages applicable to modular façade systems are reducing CO_2 emissions, assembly time, and production waste. Moreover, they facilitate disassembly, maintenance, product durability, and the entire reverse logistic process (López-Guerrero et al., 2022). However, a general assessment of these advantages remains challenging.

Considering all these factors, this paper will present the development and validation process of a Semantic Data-driven Framework (SDF) based on the Life Cycle Assessment (LCA) methodology for the environmental and circular evaluation of Custom prefabricated Modules for Curtain Walls (CMCW). This SDF is conceived to be integrated with manufacturing companies' software, such as computer-aided technologies, to automate the environmental assessment process using primary data. It can also facilitate better-defined product passports for End-of-Life (EoL) scenarios. Moreover, it can be perceived as a fundamental framework that can aid in corroborating software development of eco-design façade support tools. This type of circular construction necessitates the use of a novel set of design tools that can be seamlessly integrated into existing workflows (Heisel & McGranahan, 2024). Lastly, its connectivity could be further integrated with sensors and digital models, creating a framework for primary data towards supply chain stakeholders' collaboration and the work built on cross-platform unified standards.

The semantic data model proposed is being developed and tested within the European project H2020 Basajaun, one of the outcomes of which has been an industry 4.0 platform to ensure traceability and transparency of the engineering process. The method and the SDF have been applied to use-case in-line produced modules for an experimental building envelope (FIG. 1-3) to validate its development. The findings could contribute to implementing the LCA practice for CMCW and suggest areas for further development.

FIG. 1 In-line production of Basajaun's curtain wall modules (credit: Basajaun H2020, picture by Vandi, L.)

FIG. 2 *Basajaun's completed curtain wall modules (credit: Basajaun H2020, picture by Vandi, L.)*

FIG. 3 Basajaun's curtain wall modules' inner part installed on construction site. (credit: Basajaun H2020, picture by Vandi, L.)

2 STATE OF THE ART AND OPPORTUNITIES OF SDF

Ecological issues are driving market actors to pay more attention to the environmental impacts of their products. Since its definition, the LCA method has seen a growing diffusion in regulations and scientific research. Despite a lack of binding legislation, the European Union increasingly refers to LCA in its communication and policies (Sala et al., 2021). Generally, the LCA method applied in construction – intended as attributional in this research paper (Hauschild et al., 2018) – considers the environmental effects of resource usage associated with the lifespan of a building and its components. It also constructs a model of the analysed system based on these impacts, assisting in decision-making and identifying eco-design alternatives with a slighter environmental impact (Stijn, 2023). Succeeding in this field has notable expected impacts on the research and innovation of construction products that struggle to exhaustively implement the LCA method, such as the Custom prefabricated Modules for Curtain Walls (CMCW).

As mentioned, it is difficult to measure and compare the green and circular benefits of complex and custom systems due to the lack of comprehensive standards and benchmarks, difficulties in accessing correct data from suppliers and organisations, and the diversification of the certification schemes. Figure 4 summarises the promising sustainability requirements that façade engineers and manufacturers will have to demonstrate in the coming years in Europe, according to the

Commission's and WBCSD's view (European Commission et al., 2020; European Commission, 2021; WBCSD, 2023). This is a challenge for the CMCW industry, which needs to show its contribution to sustainable development. At this time, there are few examples of comprehensive analyses of these products on the market, merely some rare independently verified exceptions achieved after the installation (Scheldebouw, 2022), but even fewer regarding circularity. Moreover, to meet the demands of stakeholders who want to verify environmental targets, the industry needs a digital strategy that can quickly and accurately evaluate buildings using data analysis. The value proposition for companies is depicted by an improvement in process management and architectural design, with a gain in terms of time and economy beyond the creation of more virtuous and environmentally friendly products (Bach et al., 2019; Zaffagnini & Morganti, 2022).

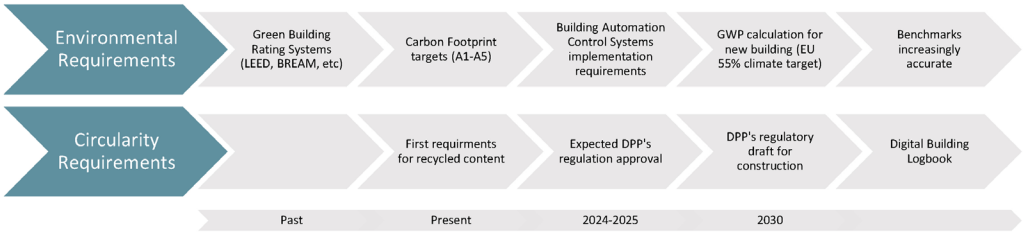

FIG. 4 Timeline of some of the upcoming possible environmental and circular requirements in the European construction sector (European Commission et al., 2020; European Commission, 2021; WBCSD, 2023)

That is why a Semantic Data-driven Framework (SDF) is proposed. It can help achieve these targets by enabling real-time data sharing among distinct departments with LCA-required data (e.g., quality and technical departments) and other data users (such as tender departments, project management, and design managers). In this way, the quantitative project data and environmental factors are always up to date when consulted (McAvoy, 2021) and related to relevant circularity information. The ultimate aim is to create optimal conditions for automatically linking the data across the existing computer-aided technologies, such as Enterprise Resource Planning (ERP) and Product Lifecycle Management (PLM) technologies, Common Data Environment (CDE) platforms and other specialised business databases if available.

Implementing this kind of SDF in support of companies' digital processes to perform data-driven LCA and DPP would offer several advantages:

A It would allow measuring the product's environmental impact using primary data based on the ISO EN standards. For that purpose, primary data are considered a key factor for accuracy (Silva et al., 2020). Moreover, it would aid in assessing and achieving other market requirements, such as using defined quantities of recycled materials or providing Environmental Product Declarations (EPDs) for the prefabricated modules. That rule-based compliance can be constantly verified during the project development.

B It would support ecological decision-making during several project stages, such as design, engineering, production, logistics, supply chain definition, assembly, and disassembly, by evaluating the impact of different options beforehand. In the future, this approach could also have the capacity to analyse the costs throughout the life cycle (Zeng et al., 2020).

C It would help create new and better strategies for the EoL of CMCWs to promote their circularity (Viscuso, 2021) and to enhance value creation after the dismantling stage. Moreover, by blending the entire supply chain within its digital framework and operation, it would be capable of integrating

and supporting production monitoring, shipping and transportation, delivery, inspection, and site installation monitoring for data traceability and reliability (Jang et al., 2022).

D It would help visualise LCA and circularity-related data, assisting managers and workers in extending the know-how of the processes in which they are involved, such as the production process, identify problems and opportunities, and make informed decisions. Visualisation instruments, such as dashboards, charts, and graphs, can present the data clearly and intuitively, highlighting the most relevant and actionable information (Uchil & Chakrabarti, 2013).
It is claimed that data-driven digital tools, plans that prioritise circularity and monitoring of dismantling are the most crucial categories for developing economies in construction (Oluleye et al., 2023). Despite being slow to adopt, these tools have the potential to revolutionize building design and construction (Sangiorgio et al., 2024). Comprehensively, developing instruments to make LCA practice and circular design the fastest and most accurate has considerable importance and value in the design and production of CMCW.

Furthermore, focusing on research and innovation beyond business development, the study of these digital systems would contribute to the redefinition of the main limits of the currently used LCA method and CE models for customised products:

E It would support the insufficient "what if" scenarios, updating the integration with BIM models in the environmental assessment and investigating the lack of time-dependent data for EoL stage management (Fnais et al., 2022). Besides LCA being a time-consuming method, there is a discrepancy between resolution detail and building description level, and results lack reproducibility (Jusselme et al., 2018). SDF can make these analyses faster and more reliable.

F It would contribute to achieving a CE in construction through the definition of metrics and key performance indicators to measure them, developing digitalisation initiatives and promoting materials passport, which are significant success factors for circular development (Oluleye et al., 2023).

G It would collect data that can be automatically organised in a Digital Product Passport (DPP) of the custom façade module to facilitate disassembly and reverse logistic actualisation in the future. For this purpose, blending STEP and BIM models offers possibilities for database integration and is increasingly being studied concerning data exchange solutions (Safari & AzariJafari, 2021). Moreover, it allows for complete tracking of the modules for the design and conception of the EoL (Llatas et al., 2022).

H It would help to implement a digital building logbook for construction collecting discussed data through time. This digital repository, or database, should contain comprehensive information about the building's materials and products throughout its lifecycle. The European Commission has recognised its potential as a tool to promote sustainability. Some experts believe that for the digital building logbook to be more widely adopted, there needs to be a systematic and improved approach to capturing, gathering, processing, exchanging, and storing information and data (European Commission et al., 2020).

All these issues and opportunities need to be addressed with a solution. Upon analysing the literature pertaining to digital tools, frameworks, or models that deal with data-driven circularity assessment approaches, as summarized in Table 1, it becomes apparent that some sources lay emphasis on circularity and concentrate solely on the requirements for DPP (or similar material passports), whereas others also focus on circularity but only address the requirements for Life Cycle Assessment (LCA).

TABLE 1 Summary of the literature reviewed regarding circularity assessment frameworks or models

Articles related to data-driven circularity digital tools, frameworks, or models						
References	Papers about tools, frameworks, or models					
	Generic Product Analysis	Related to construction, specifically:	Circular Assessment	Sustain-ability Assessment	Referred to DPP	Referred to LCA
Heinrich & Lang, 2019		Building products and buildings	x		x	
Jansen et al., 2023	x		x		x	
Mulhall et al., 2024	x		x		x	
Zabek et al., 2023		Mineral building materials	x	x		x
Klein et al., 2022		Building Products	x	x		x
Oluleye et al., 2023		Building construction industry	x			
Morganti et al., 2023		Building envelope components	x	x		x
Giovanardi et al., 2023a		Curtain Wall Façade	x		x	
Honic et al., 2024		Building products and buildings			x	
CWCT et al., 2022		Architectural Façades				x
European Commission et al., 2020		Built Environment	x		x	x

Interestingly, to the best of the authors' knowledge, there is no framework available that aligns with the new EU requirements, which includes both DPP and LCA for façades. Recognising this gap, this paper proposes the development of a novel SDF to address these dual requirements comprehensively. The primary aim of the SDF is to bridge the current gap in frameworks and provide an integrated solution tailored to the evolving regulatory landscape and the challenges associated with modular façade design.

3 METHODOLOGY

In the last decade, the idea of developing a tool for automatic or semi-automatic LCA-based analysis of industrial products has grown. Various methodologies have been formed which involve the development of semantic data frameworks (or models) that integrate computer-aided technologies (e.g. CAD, PLM, ERP, etc.) with Life Cycle Inventory (LCI) data to develop eco-design and management tools (Morbidoni et al., 2011; Tao et al., 2017; Mandolini et al., 2019; Rovelli et al., 2022). More recently, they have also been related to construction and beyond LCA, including computational methods and circularity indicators that can aid in assessing the effectiveness of circular design strategies (Dervishaj & Gudmundsson, 2024). This paper's aim and originality are based on the implementation and application of those methodologies in the CMCW context, as well as the reorganisation and performance of CE aspects in data-driven practices.

Overall, the proposed methodology can be summarised in five practical development steps:

1 Preparation and collection of data:
   a Investigation of the required CMCW data for Environmental and Circular assessment.
   b Description of the LCI flowcharts of the module's single components and operations.
2 Reception and organisation of data for the Life Cycle Impact Assessment (LCIA) and Digital Product Passport (DPP):
   a Identification of the data sources (Business departments and software) and collection.
   b Definition of the ontology and semantics of the data-driven framework.
3 Finalization of the data input and output, results, and setting sharing modalities:
   a Validation of the Semantic Data-driven Framework through testing the ontology on façade-related datasets.

The framework's overall functioning can be visualised through the schematic representation depicted in Figure 5. This representation shows three distinct phases: preparation of data, reception and organisation, and visualisation of results. These phases will be explained in detail in Chapter 4, which is dedicated to research and results analysis.

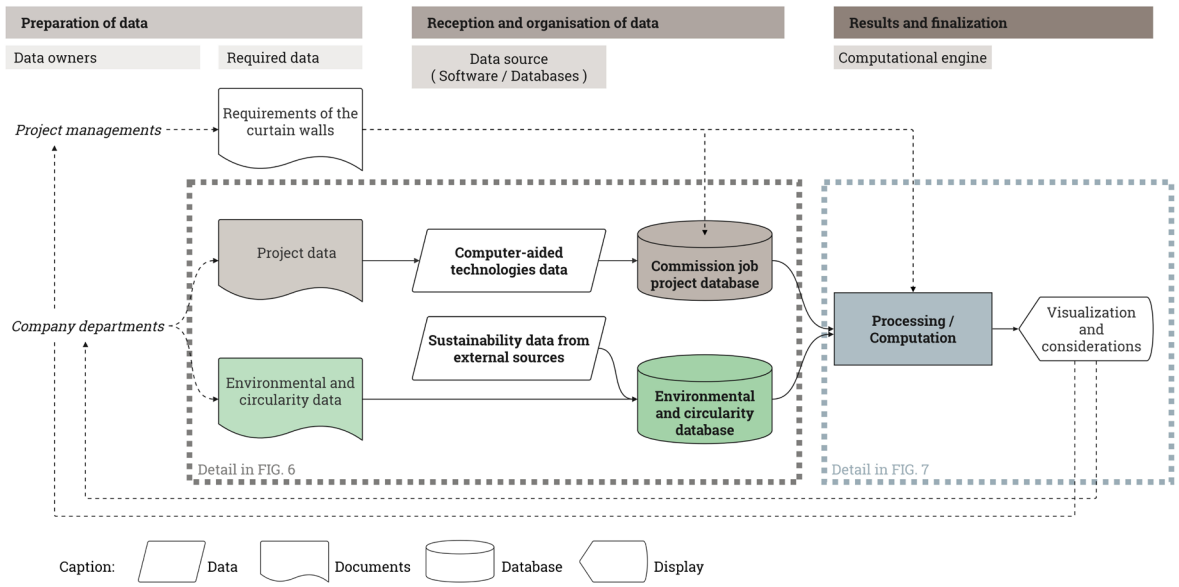

FIG. 5 *Schematic flowchart of the entire data processes according to the proposed semantic data-driven framework, from data preparation to finalisation. Figures 6 and 7 provide more detailed views of some steps.*

4 RESEARCH AND RESULTS

This chapter presents the methodology employed in the research and the consequential results that have emerged.

4.1 INVESTIGATION OF THE REQUIRED DATA

The first step involved in developing a Semantic Data-driven Framework (SDF) must be the definition of the information required to achieve its purpose, meaning assessing CMCWs according to their design. The concept of data here refers to a set of particular values that communicate information, such as those that characterise the subject of evaluation, for example, the weight of aluminium profiles or the surface area of glass. Additionally, it encompasses data that describes the environmental impact of these materials, such as the amount of carbon dioxide emitted per unit of aluminium or the percentage of recycled content present in the glass. To define the requirements, it is necessary to consider LCA impact categories, scoped label-specific rules and requirements of the most prevalent rating systems, as well as other certifications requested by clients (Rovelli et al., 2022; Zaffagnini & Morganti, 2022). These can serve as benchmarks for best practices defining products' impacts on the environment and circularity declarations. In addition, it should collect data that includes related input and output values from past events, actual sources or models (Venkatraj & Dixit, 2022). Lastly, organising these parameters in a hierarchy aids in assessing both short-term and long-term sustainability roadmaps. Once the SDF is operative, implementing target cascading makes it possible to seamlessly integrate innovative components and systems into parametric simulations. This approach tackles the challenge of exhaustively exploring diverse alternatives, as it allows for specific targets to be set at the system level (Jusselme, Rey & Andersen, 2018).

For the implementation of the SDF, three categories of data have been identified and collected: Project data, Environmental data, and Circularity data.

1. Project data describe the physical dimension of the construction module and its components and materials. Examples of project data can be the mass (kg) and surface (m^2) of the CMCW and the quantities of its framings, as well as architectural features. Beyond their related transportation distances (km), embodied electricity consumptions (kWh), and lifespan periods (years).
2. Environmental data represent the extent of the environmental damage related to each designed quantity. For instance, the Embodied Carbon Factors ($kgCO_2eq$/Functional Unit), water consumption (litre), or the Grid Carbon Factor ($kgCO_2eq$/kWh).
3. Circularity data are aimed at facilitating the assessment and communication of end-of-life scenarios, such as describing materials composition, percentages of pre- and post-consumer recycled content (%), or proposal for a reverse logistic stream.

For each data category, the annexes' tables A1-A4 concisely describe the identified project and environmental and circularity data to be collected that were identified in the research. The following subsections examine the necessary environmental and circularity data in more depth to conduct an effective analysis of these factors.

4.1.1 Required environmental assessment data for CMCW

Past literature reviews have examined the sustainability of industrialised building systems, primarily focusing on environmental factors and qualitative indicators. The primary reported indicators in evaluating the sustainability of building systems include Global Warming Potential (GPW) or Embodied Carbon (mass of equivalent CO_2 emitted), water consumption, waste generation, construction time, and productivity (López-Guerrero et al., 2022).

The Embodied Carbon Committee of the Centre for Window and Cladding Technology (CWCT) released a new type of report to introduce a peer-reviewed methodology for assessing specifically the embodied carbon of façades (2022). This procedure focuses on the GWP environmental impact indicator outlined in BS EN 15804 (2019) and aligns it with whole-life carbon assessment documents from other construction industry bodies. This proposed methodology, also aligned with BS EN 15978 (2011), has been considered a starting point for selecting the required environmental data for the presented research, considering the specific circumstances and requirements.

Even if, as a principle, designers and assessors must consider as many life cycle modules as possible, CWCT highlighted the minimum life cycle stages that must be included in the façade assessment. I.e. product stage (A1–A3), construction process stage (A4–A5), replacement stage (B4), and EoL stage (C1–C4). Table A2 in the annexe, named CMCW Environmental Data, presents a list of the information that must be retrieved for each project data depending on the stage of the façace's life cycle. In addition, further in the tool application, an off-site waste rate and a site waste rate must be defined. These are corrective factors (percentages) to be multiplied by the A3 and A5 façade GWP to consider the waste's impacts on the manufacturing and construction process. Furthermore, in developing the described SDF, it was decided not to exclude any component in the corporate IT system's bill of materials and components. This was due to the decision to validate the system with all the primary data relating to the use cases analysed.

4.1.2 Required circular assessment data for CMCW

Many circularity assessment methods and tools already exist not only in the construction field but are widespread in various manufacturing sectors. However, they often remained fragmented (Sassanelli et al., 2019) and focused on a single or a limited number of indicators. Thus, a comprehensive and quantitative assessment method is needed in the construction industry. An analysis of existing literature by Sposito and Scalisi (2020), focused on assessing the life cycle of materials and buildings, has shown limited research on the process-related aspects. Furthermore, Cambier et al. (2020) found that while there are general guidelines for building circular design, there is still a lack of specific policies for construction components.

This encompasses various types of façade-related data, including static and dynamic information such as administrative documents (e.g., assembly and use and maintenance manuals), building detail drawings describing the technical systems, components and material characteristics, performance data, and connections to building ratings and certificates.

When assessing complex building components, such as CMCW, it is important to inventory them as a combination of different parts and materials. This inventory should differentiate materials with varying use cycles and lifespans. Additionally, all value retention processes and use cycles should

be documented (Stijn, 2023; Kedir et al., 2021; McDonough & Braungart, 2013). This can facilitate the end-of-life management of the module and its components. For that reason, the data collection of components processing information of the LCA must be designed in such a way as to collect the data not only considering their impact as a component of the façade module but also as a future element/material that can be repaired, reused, recycled or efficiently disposed of. As a digital repository, the Digital Product Passport (DPP) report is being proposed by the European Commission to increase transparency and promote circularity throughout the product lifecycle. Moreover, the construction sector is one of the eight priority industries with a Commission's Action Plan, which should end with the definition of a DPP by 2030. Nonetheless, further development is required for data storage, carrier, access, and governance requirements (WBCSD, 2023)

Mulhall et al. (2022) and Jansen et al. (2023) identified the requirements for a DPP system through stakeholder involvement, consultations with industry experts, and current literature science. They conducted a state-of-play analysis and developed an overview of the current discussion on requirements. In addition, they formulated problem statements based on the analysis and created a template and guidance to improve circularity data sharing efficiency. Furthermore, Heinrich & Lang (2019) and Zabek et al. (2023) incorporated performance indicators derived from legal frameworks and LCA methodology. They summarised these indicators, including a description and recommended actions for product manufacturers to achieve the targets. Nevertheless, all of them provide a foundation for further research on DPP system requirements.

The research results present a best practice summary of the required circularity data for generic CMCWs and their possible DPP in the annexe section, table A3-A4.

4.2 DESCRIPTION OF THE LCI FLOWCHARTS

To move forward with this semantic framework development, the second step of the methodology consists of creating a clear and simplified Life Cycle Inventory (LCI) plan. This plan has to include all possible flowcharts for each component and operation within the analysed productive processes and the required environmental and circular design details for an accurate LCA. That implies defining categories of components and operations through the life cycle. Some will denote physical product elements (e.g. extruded profiles, glass), and others will denote the operations and organised activities (e.g. manufacturing, varnishing) associated with the product entity (Tao et al., 2017). This is by identifying physical dimensions compatible with the calculation of the impact categories of the LCA that will characterise the following data collection (Famiglietti et al., 2022; Rovelli et al., 2022). This methodological step is important in the development of the SDF because it aims to lay the basis for the forthcoming executive structure of the data to be collected and suggests the ontology with which the data are to be related to each other.

Afterwards, once the SDF is integrated into a performing tool, design parameters must be established by designers based on their interests or on the impact of the outcome, either through research or previous use of the method. Each parameter's values should be qualified or quantified within specified boundaries, chosen in accordance with the designer's expertise (Jusselme et al., 2018). Moreover, considering the scope of the tool, in the first phase, it is also important to identify the standards that the customer and general contractor have requested, which must be considered during all the further project stages.

4.3 IDENTIFICATION OF THE DATA SOURCES AND COLLECTION

At this stage of development, the preparatory phase is considered complete, and the data collection necessary for the analyses can begin. To do this, the first step consists of the breakdown and analysis of project commission jobs, identifying the business departments that manage the required data for the assessment and the departments that need the data. It is crucial to determine the pieces of information that can be directly obtained from business commissioning management systems and through databases, spreadsheets and documents from the company (Zaffagnini & Morganti, 2022; Rovelli et al., 2022). Instead, data that cannot be acquired directly from these systems must be implemented from literature and external databases or estimated using average values (Famiglietti et al., 2022). Typical data references for any required information have been identified and listed in tables A1 to A4 in the annexes.

The method proposed in this paper involves a data retriever from different sources in two feature-based databases to support the SDF, prepared for integration according to the LCI (Tao et al., 2017), which has been developed in the second step. This can also be done through ETL processes (Extract, Transform, Load), which involve extracting data from one or more sources with different structures or formats, transforming it as needed, and loading it into a unified target database. This replication approach is useful when real-time synchronisation or high availability is required.

There were various reasons for transferring the data to the two different databases instead of linking the SDF directly to the identified sources, such as computer-aided technologies:

1. It allows for more user-friendly management by operators who may need to interact directly with this data but do not have the necessary technical skills to understand all the sources from which these data come (e.g., an IT technician who is unable to comprehend a complex technical drawing).
2. It allows the customisation of data collection databases to be compatible with the unique semantic languages production companies utilise in their operational processes. Additionally, the database architecture, storage capacity, and processing power can be adapted to handle the growing volume and complexity of data without relying on external providers.
3. It allows for consolidating data from external databases and private production datasheets, which may contain confidential information, e.g. about suppliers. By creating a dedicated database, companies can implement necessary compliance measures to ensure control over data privacy and meet requirements imposed by data protection laws and intellectual property rights.
4. It allows for more protection than relying on third-party solutions. With a dedicated database, companies can implement encryption techniques and access controls and authentication protocols to safeguard sensitive information.
5. It allows for the necessary measures to be taken to meet legal standards, particularly for production companies that deal with sensitive information and must comply with strict regulations within their respective industries.

As mentioned, the proposed methodology implies the development of two databases, one to organise the project data related to each production company's commission job and the other to collect the environmental and circularity data in one single place (FIG. 6). The environmental and circularity database is designed to be unique for each production plant or industry and contains at least four datasets. (1) The first dataset must contain information about each possible single component of CMCWs relating to phases A1, C3, and C4 of the life cycle. Likewise, (2) the dataset related to the construction site options must contain data about all the working activities that the module can refer to. (3-4) The transport and production data can be stored in two different datasets.

On the other hand, project data needs to be separated into different databases for each commission job. That is due to the need for datasets for each type of CMCW designed, containing its bill of materials, components, and processes. Moreover, a dataset for each module is needed to contain information on its construction activities. The other two datasets related to project data are unique for commission jobs and contain information about the logistics and production of the modules. In order to ensure the effective management of data in various datasets, each data string is assigned a unique code (@id) associated with the relevant information. This code may also coincide with the alphanumeric codes utilized by the manufacturing companies in their computer-aided technology systems. Such a practice is crucial for accurate data identification and retrieval, thereby enhancing the overall efficiency of data management processes.

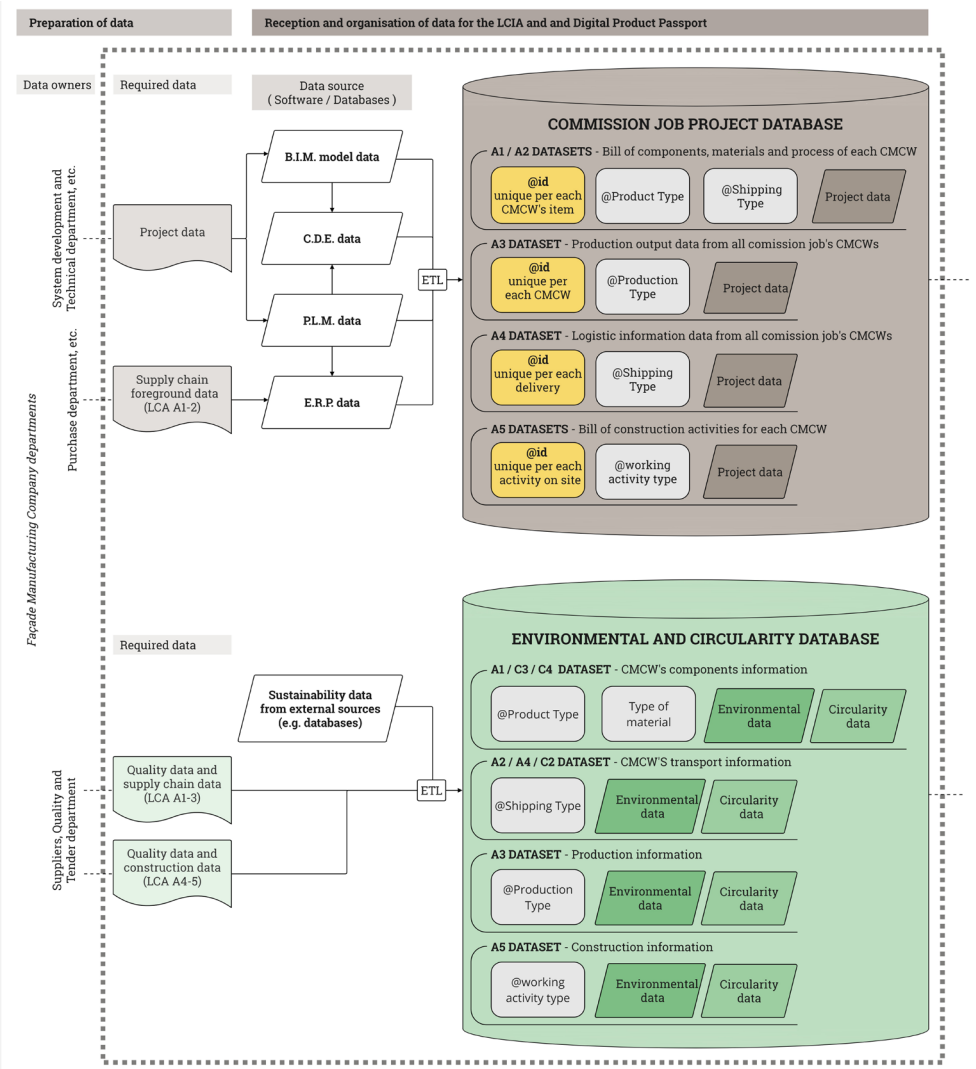

FIG. 6 Schematic flowchart of Project, Environmental, and Circularity data flow to the databases and their related datasets on which the SDF is based. It is a more detailed representation of Figure 5 concerning the stage of receiving and organising data.

The difference between the proposed databases and a data warehouse–in computing known as a reporting system used for data analysis essential in business intelligence–is that their data cannot be "read-only", because for some kind of components or processes, an update or delete action could be necessary for that step (Dedić & Stanier, 2016).

4.4 ONTOLOGY AND SEMANTICS OF THE DATA-DRIVEN FRAMEWORK

To best describe the next step of the methodology, it is helpful to examine the flowchart concerning the processing and computation of the collected data (FIG. 7).

The SDF is designed to start with the input of the identification module code of the CMCW that has to be analysed. In the computer-aided technology software typically used by companies operating the code of a CMCW, it is possible to trace back all its life cycle characterisations. As an illustration, the aforementioned module code may be utilised to identify the CMCW in the corporate Product LifeCycle Management (PLM) software. But also its components and processes, how it will be produced, how it will be shipped, and what activities it will be subjected to on the construction site. All attributes of these pieces of information must be related to the correct environmental data. Under the designer's supervision, this can be done automatically if there is an unambiguous correspondence or manually if the database contains more than one option. To develop this system, it is necessary to define ontology classes for the procedure, both during the collection of information in the respective databases and later during the development of the framework.

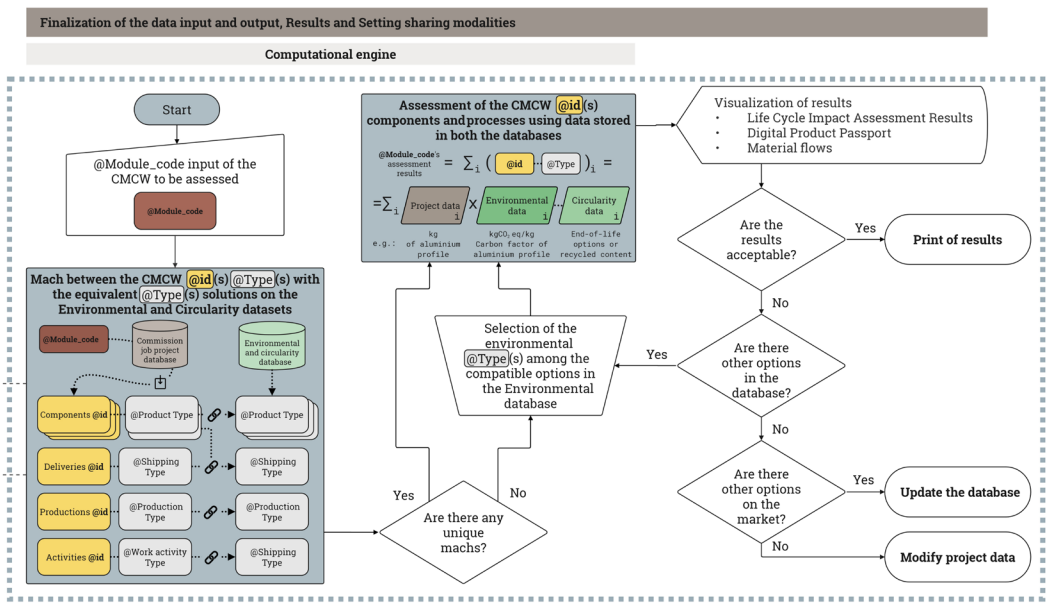

FIG. 7 *Schematic flowchart of the final stage of the SDF, in which data are correlated to obtain the results of the analysis. It is a more detailed representation of Figure 5 concerning the stage of finalisation and results visualisation.*

Ontologies are conceptual vocabularies used to represent knowledge and facilitate data exchange and interoperability across multiple databases. They provide a level of abstraction above specific database designs, enabling data to be exported, queried, and unified across independently developed systems (Gruber, 2008).

In order to achieve efficient management and evaluation of project and environmental data, it is crucial to comprehend their interconnection. This stage establishes the groundwork for acquiring valuable insights. During the SFD creation, it is essential to opt for features and advancements that correspond with the metrics the designer intends to analyse (Jusselme et al., 2018). This applies not only to LCA engines but also to circularity assessment tools. Moreover, regarding circular aspects, Kedir et al. (2021) have developed an ontology-based framework to gather DPP-related information

for industrialised construction products. They have found that it is essential to identify the functional levels of buildings and collect their property attributes at each level. Additionally, property attributes may have varying values during different stages of the building's life cycle, so it is crucial to fill in the corresponding life cycle for each value. Typically, representational primitives comprise classes, attributes, and relationships among class objects. Therefore, for each dataset included in project and environmental databases must be defined classes that facilitate database integrations through their attributes and the definition of rules depending on the kind of component or material.

A structured framework for data collection for comparative design evaluations defined by Mandolini et al. (2019) aims to manage and share life cycle information along the product development process. Their framework defines classes and attributes that represent the product structure. Attributes, describing relevant characteristics such as the data that have been previously identified and collected, define a list of features necessary to uniquely identify a class and allow mapping the relation with others linked. For instance, this can mean functional units with which to relate design data and carbon factors or end-of-life documents. Furthermore, the list of attributes can be customised by adding or removing attributes to suit the specific product and application context. In this SDF, classes are called types (@type), which include @product type, @shipping type, @ production type, and @work activity type.

Interoperable connections between data sources internally and externally need proper semantic methods to ensure unambiguous and consistent mapping. Going towards automation in Industry 4.0, the interconnections between systems are central. One of the challenges facing the use of data templates and DPPs is the absence of standardisation, which could promote the implementation of passports, but aligning existing concepts and identifying overlaps remains challenging (Honic et al., 2024). Open Platform Communications Unified Architecture (OPC UA) evolved around companion information models to align the industry and create an extensible framework to enable continuous integrations. Furthermore, additions to the OPC UA standard (Part 14 "PubSub") promote IoT connectivity over the Internet, extending the Operational Technology (OT) from on-site factory data pipelines to distributed and decentralised architectures. Connections between OT and IT departments are increasingly common and unlock the potential to break up vertical silos for business operations and supply chain collaboration on the information system level. When OT connects to the channels of decentralised infrastructure, great opportunities emerge for data-driven solutions, such as dynamic value chain evaluation networks. This also increases the need for semantic interoperability using namespace prefixes as the semantic meaning of data payloads is likely different between systems or actors in an extended network and consequently cannot be controlled like the manufacturing company of CMCW itself. Several standards are emerging to leverage IoT messaging using semantic JSON payloads.
After thoroughly analysing IT-related protocols and their connection to OPC UA and industrial operations, a clear correlation has been established between the world of semantic web technology standards and various systems utilised in manufacturing operations, such as Computer-aided technologies (e.g. ERP, MRP, and CRM). The compatibility of many of these systems with the REST API over HTTP protocol using JSON serialisation has caused a recent surge in integration solutions, showcasing the potential for further development. Moreover, the concept of "context broker" is used in the area of connected digital twins as a concept of sharing the data with the metadata needed to distribute the context together with the universally identified mechanism required (W3C, 2020).

The JSON-LD standard is a way to contextualise JSON properties with namespaces to identify entities and their types. Looking at the @id and the @type handles to define identities and pointing to a specific instance is possible to further the semantic connections. Data from relational databases,

spreadsheets or graph data structures can be hooked into a mapping process of either "knowing" or "not yet knowing" item's identity, iteratively working towards an agreement between actors and data sources to formalise the connections. More significantly, in this framework, the semantic model is not modelled top-down but instead aims at an increasingly better understanding using data contexts. As the semantic structures of various processes become confident and additional data sources, actors, and products are incorporated into the decision-making process, automation can be extended to more tasks.
Using the @id and @type, a row in a database or spreadsheet is a well-defined entity in the context of well-known operations. The next step would be to harmonise and align with other datasets to see if this represents the same or similar thing in these vocabularies. Using ontologies, the formal definition of contextual descriptions, and machine-readable logic can assist with this validation. Furthermore, the ontologies must be made understandable by users as the conceptualisation of "real things". This is how workers from different departments or companies with different backgrounds will understand each other in the collaboration to improve the sustainability implications of operations, processes, and LCA between co-workers, executives, and stakeholders. Utilising pre-existing ontologies is highly desirable as it covers many domains and promotes better interoperability and automation with greater industry convergence. However, the human knowledge process in collaborative efforts is often overlooked as ontologies are typically created and used by a small group of experts, leading to accessibility issues for the industry. Hence, the proposed framework prioritises knowledge acquisition and collaboration through co-creating information models instead of mandating ontologies from the outset.

Moreover, emerging trends in ontology layering indicate a preference for starting at the first level closest to the application and moving towards strict formal descriptions using first-order logic. This approach enables the establishment of principles for ontology connections rather than the unnecessary expansion of ontologies. A modular approach can be taken, using domain-level ontologies to cover various phenomena along the supply chain. However, a local scope can be maintained at the application level to address specific problems and proposed solutions.
The application-level ontologies can be connected to domain-level ontologies or the more abstract middle-level ontologies, which are aligned with top-level ontologies that are mathematically proven to be consistent.

4.5 VALIDATION OF THE FRAMEWORK TESTING THE ONTOLOGY

To validate the presented methodology and the SDF architecture, an assessment of CO_2eq emissions associated with the manufacturing, transportation, and installation of the modular façade system was carried out. The assessment was performed through the GWP A1-A5 calculation of some demo CMCWs and related circularity data collection. This phase aimed to evaluate the framework by defining the appropriate @type for each process category or component to be assessed and defining an ontology that binds them together in a workable manner.

The object of the analysis was the curtain wall modules façade of the demo house built during the H2020 Basajaun project, to be constructed in the village of Le Pian-Médoc (Nouvelle-Aquitaine, France). For this, eight different types of CMCWs were designed and fabricated for the building (Figure 8). Two of these were used to validate the proposed SDF: an Opaque Vertical Module without any glazing and a Window Module containing both glazed and opaque elements. Finally, a Glazed Vision Module, primarily composed of glass and designed for another demo building that was planned to be built, was also used to validate the framework.

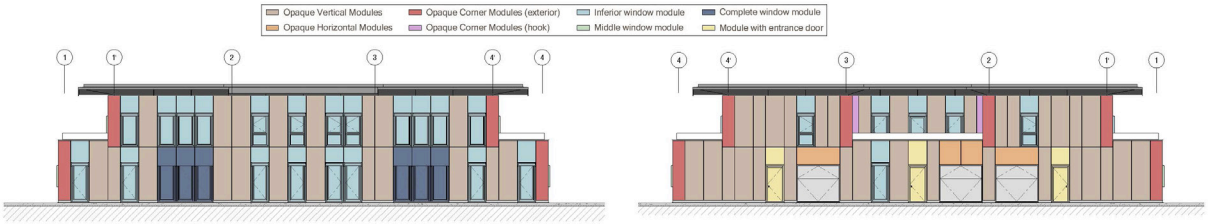

FIG. 8 *Schematic representation of the French demo building elevations showing the CMCWs developed in the Basajaun project. The two module types used in the validation depicted here are the ones named "Opaque Vertical Module" and "Inferior window module".*

According to the methodology logic, two databases were manually constructed, containing essential data for the analysis: one pertaining to design data and the other to environmental and circular data. No ETL systems were used during the validation phase of the framework. Instead, the users re-processed the information collected in the databases themselves.

The Project Database comprised six datasets:

A Three "A1 / A2" datasets corresponding to components within the selected CMCW for framework validation. These datasets included supplier information along with transportation details.
B An "A3" dataset detailing the assembly of modules in the manufacturing facility, including the average energy consumption in kWh per square meter of the assembled module (or Factory Energy Intensity).
C An "A4" dataset containing information related to module transportation to the construction site, including the transported weight and the distance.
D An "A5" dataset encompassing details of on-site operations necessary for module installation and related energy consumptions.

On the other hand, the Environmental and Circularity Database consisted of four datasets:

A An "A1" dataset containing Embodied Carbon Factors (ECF) or GWP Unit values related to the analysed module's possible components. In addition to these, information related to the circularity of products and processes was also collected. Where applicable, for example, an attempt was made to keep track of the presence or absence of product EPDs, percentages of recycled material, and description of the disassembly procedure recommended by suppliers. For products for which EPDs were available, data on other environmental impacts (e.g., water consumption) were also collected.
B An "A2 & A4" dataset containing the Transport Emission Factor (TEF) of the transportation mode used.
C An "A3" dataset and an "A5" dataset with respective Grid Carbon Factor (GCF) values for the module manufacturing facility and the construction site.

Due to their complexity, the three Basajaun CMCWs proved to be an ideal use case. Upon exporting the bill of materials for each module from the Enterprise Resource Planning (ERP) and Product Lifecycle Management (PLM) systems, the Opaque Vertical Module revealed 44 unique components, the Window Module 81 and the Glazed Vision Module 52. These components (and processes) consist mostly of frame profiles, insulation equipment, glass, and seal systems. It is worth noting that some of these components share the same characteristics but appear in different modules. Each component and process is linked to a database string associated with a unique @id. An ontology was developed to simplify the association of strings, and @type assignments were made for each data

string in both databases. Additionally, Reference Measurement Units were defined in both datasets to facilitate the correlation of Functional Units.

The subsequent tables provide concise summaries of the @types defined for each lifecycle stage during the validation process and the mandatory Reference Measurement Units needed to calculate the GWP depending on the database. Lastly, it is critical to underscore that the quantity (Qi) at which a particular component or process is employed in the production of the façade module must be explicitly stated, even though it may be a straightforward notion.

4.5.1 A1 - Components supply and related processes

TABLE 2 Summary of the identified @product type(s) related to phase A1 of the life cycle

@product type	Mandatory UoM (Project data)	Mandatory UoM (Environmental data)	Notes
PreassembledProduct or CommercialProduct	none	A1-A5 GWP [kgCO2eq /quantity] or, alternatively: ECF for the material [kgCO2eq /quantity]	As a Preassembled Product (or as a single commercial product), the unique factor is the quantity. During the finalisation, it will probably be necessary to consult technical drawings or product sheets to select adequate corresponding @types.
IGU	UoM Surface [m2]	A1-A5 GWP [kgCO2eq /m^2] or, alternatively: ECF for the material [kgCO2eq/m^2]	It will probably be necessary to consult technical drawings to determine the composition of the Insulated Glass Unit because it is not always specified in framework references (e.g., ERP).
Finishing or Machining	UoM Surface [m2]	A1-A5 GWP [kgCO2eq/m^2] or, alternatively: ECF for the material [kgCO2eq /m^2]	If the treatment is applied to a profile with a channel section, UoM thickness indicates the profile's thickness and length and width indicate its max dimensions.
Extruded&Pultruded	UoM Mass [kg], UoM Height [mm]	A1-A5 GWP [kgCO2eq /kg] or, alternatively: ECF for the material [kgCO2eq /kg]	
Panels&Materials	UoM length [mm], UoM width [mm], UoM thickness [mm]	A1-A5 GWP [kgCO2eq /m^3] or, alternatively: ECF for the material [kgCO2eq /m^3]	Mostly rectangular blocks made of singular or composed materials.
Tapes&Sealants	UoM width [mm], UoM Height [mm]	A1-A5 GWP [kgCO2eq /m^2] or, alternatively: ECF for the material [kgCO2eq/m^2]	This could also include sheets.

$$GWP_{A1} = \sum_i [Q_i \times_{component} UoM \times GWP_{A15i}] + \sum i [Qi \times_{component} UoM \times ECF_{A13i}] \quad (1)$$

Equation 1 calculates the total A1 GWP by summing the contributions of each @product type, considering the quantity, the specific reporting unit factor for that @product type, and the corresponding A1-A5 GWP or A1-3 ECF for each component.

4.5.2 A2 - Transport to factory

TABLE 3 Summary of the identified @shipping type related to phase A2 of the life cycle

@product type	Mandatory UoM (Project data)	Mandatory UoM (Environmental data)	Notes
Components_Lorry_avg	Transport Distance (TD) [km]	Average km TEF [kgCO2eq /km] (Transport Emissions Factors = TEF)	No specific data about the type of large goods vehicle (lorry) used for the components' supply have been collected for the validation assessment. A standard lorry has been assumed for all the components.

$$GWP_{A2} = \sum_i [Q_i \times TD \times TEF] \quad (2)$$

Equation 2 calculates the total A2 GWP associated with transporting components to the façade manufacturing plant using an average large goods vehicle. It considers the quantity of each component, the transport distance, and the Total Emission Factor associated with the average large goods vehicle used for transportation.

4.5.3 A3 - Manufactory (fabrication and assembly)

TABLE 4 Summary of the identified @production type related to phase A3 of the life cycle

@product type	Mandatory UoM (Project data)	Mandatory UoM (Environmental data)
Production_line_2021	UoM Surface (S) [m2], Average Consumption per m^2 [kWh/m2]	Generated electricity carbon factor (GECF) [kgCO2eq/kWh], Off-site waste emissions [%]

$$GWP_{A3} = (Q_i \times S \times Average\_Consumption\_per\_m^2 \times GECF) + Off\text{-}site\_waste\_emissions \quad (3)$$

Equation 3 assesses the environmental impact of the assembly and production process of the CMCW by considering the energy consumption per square meter, carbon factor associated with electricity generation, and off-site waste emissions.

4.5.4 A4 - Transport to site

TABLE 5 Summary of the identified @shipping type related to phase A4 of the life cycle

@product type	Mandatory UoM (Project data)	Mandatory UoM (Environmental data)
Lorry_Euro_5_avg	Transport Distance [km], UoM Mass [kg]	TEF (km•Kg) kgCO2eq /km•kg] (Transport Emissions Factors = TEF)

$$GWP_{A4} = \sum_i [Q_i \times TD \times mUoM \times TEF] \quad (4)$$

Equation 4 calculates the total GWP associated with the transportation process using an average Euro 5 large goods vehicle. It considers the quantity, transport distance, mass of shipped items, and the emission factor specific to the type of lorry and the mass of items transported.

4.5.5 A5 – Construction

TABLE 6 Summary of the identified @working activity type related to phase A5 of the life cycle

@product type	Mandatory RMU (Project data)	Mandatory RMU (Environmental data)
Pallet_truck_use	Machine or plant usage time (MT) [hours], Ren. Energy cons. [kW], Non-Ren. Energy cons. [kW], Fuel consumption (uFC) [litre]	Generated electricity carbon factor (GECF) [kgCO2eq /kWh], or, alternatively: Grid carbon factor (GCF) [kgCO2eq /kWh] site waste emissions [%]
Pick&Carry_Crane,2t	Machine or plant usage time (MT) [hours], Ren. Energy cons. [kW], Non-Ren. Energy cons. [kW], Fuel consumption (uFC) [litre]	Generated electricity carbon factor (GECF) [kgCO2eq /kWh], or, alternatively: Grid carbon factor (GCF) [kgCO2eq /kWh] site waste emissions [%]
Boom_lifter_use	Machine or plant usage time (MT) [hours], Ren. Energy cons. [kW], Non-Ren. Energy cons. [kW], Fuel consumption (uFC) [litre]	Generated electricity carbon factor (GECF) [kgCO2eq /kWh], or, alternatively: Grid carbon factor (GCF) [kgCO2eq /kWh] site waste emissions [%]

$$GWP_{A5} = \sum_i [Q_i \times m_{Average\_Consumption} \times GECF] + site\_waste\_emissions \quad (5)$$

Equation 5 comprehensively assesses the environmental impact of different working activities, considering both energy consumption and on-site waste emissions. The summation of different working activities allows for a holistic evaluation of the overall contribution to global warming potential associated with the specified activities. It is possible to calculate the GWPA15 result by summing the GWPs obtained from applying all five equations.

The simplification of the company's practice has had a significant impact on the analysis, especially in the life cycle stage A1. Previously, 177 unique objects with individual article numbers, as translated by @id, were identified in the first dataset. However, the process has now been streamlined to six categories with unique rules (i.e., @product types), which include components and processes. Meanwhile, on-site installation activities have been reduced from four @id to one @ working activity type. As this was the first time the framework was defined for the manufacturing company, data had to be manually searched for within the company software. The tables in annexes' Tables A1-A4 provided the typical data reference for each data type. However, with the systematization of the framework, this data transposition can now be automated with an ETL system, further increasing the time saved during assessments. Additionally, organising data in this manner makes it easier for non-technical personnel to access information related to environmental impacts and circularity.

5 DISCUSSIONS

Measuring a product's environmental impact through primary data has been confirmed as a best practice (Silva et al., 2020). However, retrieving project data has been found to require less effort than environmental data. This is because project data is readily available in the company's software systems, whereas environmental data may be more demanding to obtain due to various factors such as data availability, reliability, and accessibility. Integrating project data and primary data declared directly by suppliers can significantly enhance the environmental assessment process and make it more cost-effective compared to relying solely on tools available in online databases

(Morganti et al., 2023). While suppliers may have access to data that can contribute to a more holistic assessment, these are typically limited and require additional verification and integration; they often lack comprehensive LCA data on several impact factor indicators besides global warming potential. An ecological approach can be easily implemented during various stages of the product's life cycle. By considering environmental factors from the early design phase to manufacturing, distribution, and end-of-life (EoL) management, companies can identify opportunities for reducing environmental impacts and promoting sustainability. Moreover, one of the challenges lies in including information about costs associated with each stage of the product's life cycle (Amon et al., 2021). Without sellers involved in the data collection, economic data related to the supply chain would be typically retrieved from Enterprise Resource Planning Software, which tends to be focused on past purchases and may not accurately reflect current market variations. This can lead to misleading cost analyses and hinder the integration of cost considerations into environmental and circularity assessments.

Improving strategies for the EoL management of construction products is crucial for promoting their circularity and increasing value creation after dismantling (Giovanardi et al., 2023b). Actors who play a vital role in Digital Product Passports (DPPs) should be identified and assigned responsibilities. By involving stakeholders throughout the product's life cycle, such as designers, manufacturers, and managers, companies can ensure comprehensive data collection and utilisation for circular industrialised construction products, such as CMCW. For instance, the Material Passport Ontology provides a structure that offers guidance to industrialised construction firms on how to design, produce, and manage circular products effectively (Kedir et al., 2021). An outcome DPP should include specific data for its components and materials and instructions for repairing and disassembly. This comprehensive information can incentivise the creation of closed life cycles for product components, increasing the overall circularity of the entire module. Additionally, a digital building logbook can be utilised to document relevant information about buildings, their components, and maintenance activities, supporting ongoing sustainability efforts. The type of data selected and represented in annexe Tables A3 and A4, related to the design data according to a precise ontology within the proposed Semantic Data-driven Framework (SDF), would facilitate all these developments of the DPP and draft its semi-automatic realisation for both façade models and their components. Furthermore, the development of qualitative or quantitative circularity Key Performance Indicators (KPIs) can be linked to the circularity information values captured in the product passport. This will allow companies to track and measure their progress towards circularity goals, providing insights into the effectiveness of their sustainability initiatives.

Regarding data portability, further research is needed to establish common technical standards that facilitate seamless data transfer from one data controller to another. This can include the ability to export data into user-accessible local files, promoting interoperability between different systems, and enabling searchability through sophisticated tools. By addressing data portability challenges, companies can enhance the accessibility and usability of environmental data, fostering collaboration and knowledge sharing within the industry. As mentioned, in Industry 4.0, the connectivity between systems is crucial for moving towards automation. Open Platform Communications Unified Architecture (OPC UA) has developed companion information models to bring the industry together and establish a scalable framework that allows for seamless integration. Implementing such standardised languages can accelerate the processes of environmental data evaluation and dissemination.

The primary limitations that need to be addressed for its successful implementation are mainly technical. One of the primary technical limitations is the need of the involved companies to acquire computational-aided technologies aimed at managing the commission job and its specific

aspects if the company does not already have it. This requirement can pose a challenge for small enterprise organisations that do not already possess the necessary software infrastructure or have insufficient financial resources. Additionally, developing the implementation framework requires interdisciplinary skills from the technicians or team responsible for its design and ontology development. These skills include a deep understanding of the business organisation, environmental impact assessment, circular economy approach, and some expertise in the software involved. Furthermore, the approach necessitates the involvement of IT engineers responsible for managing the data workflow, organising and structuring the data, and establishing relationships between different data elements following the Life Cycle Inventory needs. The success of this process relies on extensive collaboration among all roles and departments within the company. Effective communication and cooperation are essential to ensure a cohesive and integrated approach. This could also be extended to the supply chain actors besides the company's internal departments. It is important to acknowledge the initial commitment of time and resources required to set up the design software system. This includes incorporating both standard and eco-design tools to enable the reading, completion, storage, and collaboration of the life cycle standard data model. The company needs to allocate sufficient resources to implement and maintain this system effectively.

Although the proposed approach offers significant benefits in framing environmental impact reduction options in the life cycle of façade modules, it is currently hardly applicable on an entire building scale. The complexity and uncertainties associated with large-scale building projects make it challenging to implement this approach effectively. Because it would require the retrieval of detailed data from the entire supply chain of all contractors involved in the construction, it would be a compelling development for the future. However, it can be already highly valuable for early eco-design assessments, where there is a higher degree of control over the supply chain. During the initial stages of the design process, the approach can provide helpful insights and inform decision-making regarding sustainability concerns.

Considerations of temporal aspects play a significant role during the commissioning process, influencing the dynamic modelling of systems and impacts (Beloin-Saint-Pierre et al., 2020). This includes understanding the differences and establishing links between preliminary studies, ongoing flowcharts, and practical completion flowcharts. As the project develops, the source of data may change, and it is crucial to account for these potential variations. Flexibility in the approach is necessary to accommodate evolving data sources and ensure the accuracy and relevance of the analysis throughout the project lifecycle.

Another critical factor to consider in the field of industrial innovations is the marketability of software implemented using the SDF. Currently, it is difficult to envision a readily available digital product tool in the market that can undertake the comprehensive analysis required for sustainable design with omni-comprehensive data. The complexity arises from the need to integrate and analyse data from various databases, which could be public, owned by individual production companies, or subject to licensing agreements. In the absence of a standardised approach or shared database, it is more likely that each company involved in complex custom-building products will develop its own databases to meet its specific requirements. Therefore, they are not set up for the automatic and semi-automatic data exchange as proposed here. However, if environmental database owners were to share their data more openly, it would facilitate the establishment of more precise benchmarks for sustainable future development. Collaboration and data sharing among stakeholders could lead to a more comprehensive understanding of the environmental impact of building materials and processes, fostering a collective effort towards sustainable practices.

6 CONCLUSIONS

This study has presented a comprehensive methodology for developing and implementing a semantic data-driven and LCA-based framework (SDF) to develop low-carbon and circular Custom prefabricated Modules for Curtain Walls (CMCW). This framework can be considered a fundamental part of developing digital eco-design tools to support design. The findings highlight the importance of a primary data recovery framework and collection through integration with the project and environmental data stored in the manufactory company's computer-aided technology software—in addition to adopting an ecological approach throughout the product's life cycle. By obtaining primary data directly from their IT management systems and suppliers, companies can enhance the assessment process and obtain more reliable and detailed information about the environmental impacts and circular End-of-Life options of CMCWs. This approach allows for a more comprehensive and precise evaluation of impact factors such as Global Warming Potential (GWP), water consumption, waste generation, construction time, and productivity. At the same time, it would gather data that can be automatically organised into a Digital Product Passport (DPP) for the custom façade module and its components and materials. In the future, disassembly and reverse logistics will be simplified with this kind of approach. Additionally, it will aid the development of a Digital Building logbook to keep track of buildings.

Integrating semantic web technology standards and ontologies offers significant potential for facilitating collaboration, automating processes, and improving sustainability implications in operations and supply chains. The use of ontologies and semantic models enables the effective management and exchange of data between different systems and actors involved in the assessment process. However, it is important to acknowledge the technical limitations and challenges associated with implementing such a system, ensuring data portability, and establishing common technical standards. Moreover, at this research stage, the SDF is designed to assess and support Façade Design for production and construction management and innovation. Implementing it on a building scale presents challenges due to the complexity and uncertainties associated with large-scale projects. Further research and adaptation of the methodology are needed to address these challenges and enable the assessment of sustainability implications at a broader scale. Additionally, the proposed methodology and framework rely on the availability and reliability of data from various sources. Obtaining comprehensive and up-to-date data can be challenging, and data collection processes may require significant effort and resources. Furthermore, the marketability and widespread adoption depend on the willingness of companies to share data and collaborate transparently. Overcoming these data-related challenges and fostering a culture of data sharing and collaboration within the construction industry is crucial for realising the full potential of data-based ecological approaches, such as the one presented.

In conclusion, this study contributes to the field of sustainable design and assessment of CMCW by providing a development methodology for an eco-design framework aimed at evaluating environmental and circular aspects. The integration of primary data, project data, and an ecological approach enables a comprehensive analysis of the environmental impacts of CMCWs throughout their life cycle. Despite the acknowledged limitations, this research provides a foundation for future developments in data-driven sustainability assessments and circularity in construction façade technologies, with the potential to drive positive environmental and economic outcomes in the industry.

Credit author statement

- Luca Morganti: Conceptualization, Methodology, Formal analysis, Validation, Investigation, Data Curation, Writing - Original Draft, Writing - Review & Editing, Visualization
- Peru Elguezabal Esnarrizaga: Resources, Writing - Review & Editing, Supervision
- Alessandro Pracucci: Conceptualization, Methodology, Resources, Supervision, Writing - Review & Editing
- Theo Zaffagnini: Conceptualization, Methodology, Resources, Supervision, Writing - Review & Editing
- Veronica Garcia Cortes: Resources, Supervision, Writing - Review & Editing
- Andreas Rudenå: Software, Formal analysis, Writing - Review & Editing
- Birgit Brunklaus: Formal analysis, Validation, Writing - Review & Editing
- Julen Astudillo Larraz: Resources, Supervision

Data Availability Statement

The datasets collected during the validation of the framework and openly available have been published in the Zenodo repository under the title: "Project Database and Environmental and Circularity Database containing information on Basajaun Façade System Modules" (DOI: https://doi.org/10.5281/zenodo.10557349).

Furthermore, the results of the validation step concerning Global Warming Potential measurement of modules' life cycle stages from cradle to practical completion (A1–A5) and their related circularity insights have been published in a paper titled: "A1–A5 Embodied Carbon Assessment to Evaluate Bio-Based Components in Façade System Modules" (DOI: https://doi.org/10.3390/su16031190).

Acknowledgements

The results and the study described here are part of the results obtained in the BASAJAUN project: "Building a Sustainable Joint Between Rural and Urban Areas Through Circular and Innovative Wood Construction Value Chains" (2019–2024). This information reflects only the author's views, and neither the Agency nor the Commission are responsible for any use that may be made of the information contained therein.
EC CORDIS website https://cordis.europa.eu/project/ id/862942 (accessed on 1 March 2022).

References

Amon, F., Dahlbom, S., & Blomqvist, P. (2021). Challenges to transparency involving intellectual property and privacy concerns in life cycle assessment/costing: A case study of new flame retarded polymers. Cleaner Environmental Systems, 3, 100045. https://doi.org/10.1016/J.CESYS.2021.100045

Bach, R., Mohtashami, N., & Hildebrand, L. (2019). Comparative Overview on LCA Software Programs for Application in the Façade Design Process. Journal of Facade Design and Engineering, 7(1), 13–26. https://doi.org/10.7480/jfde.2019.1.2657

BASAJAUN - Building A SustainAble Joint between rurAl and UrbaN Areas Through Circular And Innovative Wood Construction Value Chains [Grant agreement ID: 862942]. BASAJAUN Project | Fact Sheet | H2020. (n.d.). CORDIS | European Commission. Retrieved July 20, 2023, from https://cordis.europa.eu/project/id/862942

Beloin-Saint-Pierre, D., Albers, A., Hélias, A., Tiruta-Barna, L., Fantke, P., Levasseur, A., Benetto, E., Benoist, A., & Collet, P. (2020). Addressing temporal considerations in life cycle assessment. Science of The Total Environment, 743, 140700. https://doi.org/10.1016/j.scitotenv.2020.140700

British Standards Institute. (2019). Sustainability of construction works. Environmental product declarations. Core rules for the product category of construction products (EN 15804:2012+A2:2019).

British Standards Institute. (2011). Sustainability of construction works. Assessment of environmental performance of buildings. Calculation method (BS EN 15978:2011).

Cambier, C., Galle, W., & De Temmerman, N. (2020). Research and Development Directions for Design Support Tools for Circular Building. Buildings, 10(8), 142. https://doi.org/10.3390/buildings10080142

CWCT Embodied Carbon Committee, Ladipo, T., & Wild, W. (2022). How to calculate the embodied carbon of facades: A methodology. https://www.cwct.co.uk/pages/embodied-carbon-methodology-for-facades

Dedić, N., & Stanier, C. (2016). An Evaluation of the Challenges of Multilingualism in Data Warehouse Development. In Hammoudi, S., Maciaszek, L., Missikoff, M., Missikoff, M., Camp, O., & Cordeiro, J. (eds.). Proceedings of the 18th International Conference on Enterprise Information Systems (ICEIS 2016), 1. (pp. 196–206). SciTePress. 25–28 April 2016, Rome, Italy. https://doi.org/10.5220/0005858401960206

Dervishaj, A., & Gudmundsson, K. (2024). From LCA to circular design: A comparative study of digital tools for the built environment. Resources Conservation and Recycling, 200, 1–19. https://doi.org/10.1016/j.resconrec.2023.107291

European Commission, Executive Agency for Small and Medium-sized Enterprises, Volt, J., Toth, Z., Glicker, J. (2020). Definition of the digital building logbook – Report 1 of the study on the development of a European Union framework for buildings' digital logbook, Publications Office. https://data.europa.eu/doi/10.2826/480977

European Commission, (2021), "Proposal for a DIRECTIVE OF THE EUROPEAN PARLIAMENT AND OF THE COUNCIL on the energy performance of buildings (recast)", 2021/0426 (COD), Brussels, https://eur-lex.europa.eu/legal-content/EN/TXT/?uri=CELEX-%3A52021PC0802&qid=1641802763889

Famiglietti, J., Toosi, H. A., Dénarié, A., & Motta, M. (2022). Developing a new data-driven LCA tool at the urban scale: The case of the energy performance of the building sector. Energy Conversion and Management, 256, 115389. https://doi.org/10.1016/j.enconman.2022.115389

Fnais, A., Rezgui, Y., Petri, I., Beach, T., Yeung, J., Ghotoghi, A. and Kubicki, S. (2022), The application of life cycle assessment in buildings – Challenges, and directions for future research, The International Journal of Life Cycle Assessment, 27, 627-654. https://doi.org/10.1007/s11367-022-02058-5

Giovanardi, M., Konstantinou, T., Pollo, R., & Klein, T. (2023a). Internet of Things for building façade traceability: A theoretical framework to enable circular economy through life-cycle information flows. Journal of Cleaner Production, 382(135261). https://doi.org/10.1016/j.jclepro.2022.135261

Giovanardi, M., Konstantinou, T., Pollo, R., & Klein, T. (2023b). The Internet of Things for circular transition in the façade sector. TECHNE - Journal of Technology for Architecture and Environment, (25), 243–251. https://doi.org/10.36253/techne-13707

Gruber, T. (2008). Ontology. In Liu, Ling; Özsu, M. Tamer (eds.). Encyclopedia of Database Systems. Springer-Verlag.

Hauschild, M. Z., Rosenbaum, R. K., & Olsen, S. I. (2018). Life cycle assessment: Theory and practice. In Life Cycle Assessment: Theory and Practice. https://doi.org/10.1007/978-3-319-56475-3

Heinrich, M., & Lang, W. (2019). Materials passports - best practice. Innovative Solutions for a Transition to a Circular Economy in the Built Environment. Technische Universitat Munchen, BAMB. https://www.bamb2020.eu/wp-content/uploads/2019/02/BAMB_MaterialsPassports_BestPractice.pdf

Heisel, F. & McGranahan, J. (2024). Enabling Design for Circularity with Computational Tools. In C. De Wolf, S. Çetin, & N. M. P. Bocken (Eds.), A Circular Built Environment in the Digital Age (pp. 97–110). Springer International Publishing. https://doi.org/10.1007/978-3-031-39675-5_6

Honic, M., Magalhães, P. M., & Van den Bosch, P. (2024). From Data Templates to Material Passports and Digital Product Passports. In C. De Wolf, S. Çetin, & N. M. P. Bocken (Eds.), A Circular Built Environment in the Digital Age (pp. 79–94). Springer International Publishing. https://doi.org/10.1007/978-3-031-39675-5_5

IPCC: Intergovernmental Panel on Climate Change, (2023). Synthesis report of the IPCC sixth assessment report (AR6), [Core Writing Team, H. Lee et al.]. IPCC. https://report.ipcc.ch/ar6syr/pdf/IPCC_AR6_SYR_SPM.pdf

Jansen, M., Meisen, T., Plociennik, C., Berg, H., Pomp, A., & Windholz, W. (2023). Stop Guessing in the Dark: Identified Requirements for Digital Product Passport Systems. Systems, 11(3), 123. https://doi.org/10.3390/systems11030123

Jang, Y., Lee, J.-M., & Son, J. (2022). Development and Application of an Integrated Management System for Off-Site Construction Projects. Buildings, 12(7), Article 7. https://doi.org/10.3390/buildings12071063

Jusselme, T., Rey, E., & Andersen, M. (2018). An integrative approach for embodied energy: Towards an LCA-based data-driven design method. Renewable and Sustainable Energy Reviews, 88, 123–132. https://doi.org/10.1016/j.rser.2018.02.036

Kedir, F., Bucher, D. F., & Hall, D. M. (2021). A Proposed Material Passport Ontology to Enable Circularity for Industrialized Construction. Proceedings of the 2021 European Conference on Computing in Construction, 2, 91–98. https://doi.org/10.35490/EC3.2021.159

Klein, T., Aguerre Azcarate J., & Voet E. van der (2022). Expert Workshop on Reverse Logistics for Circular Building Products [MOOC]. TU Delft. https://online-learning.tudelft.nl/courses/expert-workshop-on-reverse-logistics-for-circular-building-products/

Kragh, M. K., & Jakica, N. (2022). 21 - Circular economy in facades. In E. Gasparri, A. Brambilla, G. Lobaccaro, F. Goia, A. Andaloro, & A. Sangiorgio (Eds.), Rethinking Building Skins (pp. 519–539). Woodhead Publishing. https://doi.org/10.1016/B978-0-12-822477-9.00016-4

Llatas, C., Soust-Verdaguer, B. and Passer, A. (2020), Implementing life cycle sustainability assessment during design stages in building information modelling – From systematic literature review to a methodological approach, Building and Environment, 182, 107164, 1-14. https://doi.org/10.1016/j.buildenv.2020.107164

López-Guerrero, R. E., Vera, S., & Carpio, M. (2022). A quantitative and qualitative evaluation of the sustainability of industrialised building systems: A bibliographic review and analysis of case studies. Renewable and Sustainable Energy Reviews, 157, 112034. https://doi.org/10.1016/j.rser.2021.112034

Mandolini, M., Marconi, M., Rossi, M., Favi, C., & Germani, M. (2019). A standard data model for life cycle analysis of industrial products: A support for eco-design initiatives. Computers in Industry, 109, 31–44. https://doi.org/10.1016/j.compind.2019.04.008

Machado, N., & Morioka, S. N. (2021). Contributions of modularity to the circular economy: A systematic review of literature. Journal of Building Engineering, 44, 103322. https://doi.org/10.1016/j.jobe.2021.103322

McAvoy, S., Grant, T., Smith, C., & Bontinck, P. (2021). Combining Life Cycle Assessment and System Dynamics to improve impact assessment: A systematic review. Journal of Cleaner Production, 315, 128060. https://doi.org/10.1016/j.jclepro.2021.128060

McDonough, W., & Braungart, M. (2013). The Upcycle: Beyond Sustainability--Designing for Abundance (1st ed.). New York, NY: North Point Press

Morbidoni, A., Favi, C., & Germani, M. (2011). CAD-Integrated LCA Tool: Comparison with dedicated LCA Software and Guidelines for the Improvement. In J. Hesselbach & C. Herrmann (Eds.), Glocalized Solutions for Sustainability in Manufacturing (pp. 569–574). Springer. https://doi.org/10.1007/978-3-642-19692-8_99

Morganti, L., Demutti, M., Fotoglou, I., Coscia, E. A., Perillo, P., & Pracucci, A. (2023). Integrated Platform-Based Tool to Improve Life Cycle Management and Circularity of Building Envelope Components. Buildings, 13(10), Article 10. https://doi.org/10.3390/buildings13102630

Mulhall, D., Ayed, A.-C., Schroeder, J., Hansen, K., & Wautelet, T. (2022). The Product Circularity Data Sheet—A Standardized Digital Fingerprint for Circular Economy Data about Products. Energies, 15(9), 3397. https://doi.org/10.3390/en15093397

Oluleye, B. I., Chan, D. W. M., Antwi-Afari, P., & Olawumi, T. O. (2023). Modeling the principal success factors for attaining systemic circularity in the building construction industry: An international survey of circular economy experts. Sustainable Production and Consumption, 37, 268–283. https://doi.org/10.1016/j.spc.2023.03.008

Rovelli, D., Brondi, C., Andreotti, M., Abbate, E., Zanforlin, M., & Ballarino, A. (2022). A Modular Tool to Support Data Management for LCA in Industry: Methodology, Application and Potentialities. Sustainability, 14(7), 3746. https://doi.org/10.3390/su14073746

Safari, K. and AzariJafari, H. (2021), Challenges and opportunities for integrating BIM and LCA – Methodological choices and framework development, Sustainable Cities and Society, 67, 102728, 1-18. https://doi.org/10.1016/j.scs.2021.102728

Sala, S., Amadei, A. M., Beylot, A. and Ardente, F. (2021), The evolution of life cycle assessment in European policies over three decades, The International Journal of Life Cycle Assessment, 26, 2295-2314. [Online] Available at: https://doi.org/10.1007/s11367-021-01893-2

Sangiorgio, A., Bogdanova, A., Globa, A., Jacob, C., Vela, V., & Bianchini, M. (2024). Testing Digital Workflows on Building Renovations: The Case Study of F10 New Law Building for the University of Sydney. In P. Ruttico (Ed.), Coding Architecture: Designing Toolkits, Workflows, Industry (pp. 141–166). Springer Nature Switzerland. https://doi.org/10.1007/978-3-031-47913-7_8

Sassanelli, C., Rosa, P., Rocca, R., & Terzi, S. (2019). Circular economy performance assessment methods: A systematic literature review. Journal of Cleaner Production, 229, 440–453. https://doi.org/10.1016/j.jclepro.2019.05.019

Scheldebouw bv - Permasteelisa Group (2022) Curtain wall FT01a of "n2" London [EPD] https://www.mrpi.nl/epd/scheldebouw-b-v-permasteelisa-group-curtain-wall-ft01a-of-n2-london/

Silva, F. B., Reis, D. C., Mack-Vergara, Y. L., Pessoto, L., Feng, H., Pacca, S. A., Lasvaux, S., Habert, G. and John, V. M. (2020), Primary data priorities for the life cycle inventory of construction products – Focus on foreground processes, The International Journal of Life Cycle Assessment, 25(6), 980-997. https://doi.org/10.1007/s11367-020-01762-4

Sposito, C., & Scalisi, F. (2020). Built environment and sustainability. Recycled materials and Design for Disassembly between research and good practices. AGATHÓN | International Journal of Architecture, Art and Design, 8, 106–117. https://doi.org/10.19229/2464-9309/8102020

Stijn, A. van (2023). Developing circular building components: Between ideal and feasible. A+BE | Architecture and the Built Environment, 05, 1–740. https://doi.org/10.7480/abe.2023.05.6975

Tao, J., Chen, Z., Yu, S., & Liu, Z. (2017). Integration of Life Cycle Assessment with computer-aided product development by a feature-based approach. Journal of Cleaner Production, 143, 1144–1164. https://doi.org/10.1016/j.jclepro.2016.12.005

Uchil, P., & Chakrabarti, A. (2013). Communicating life cycle assessment results to design decision makers: Need for an information visualization approach. DS 75-5: Proceedings of the 19th International Conference on Engineering Design (ICED13) Design For Harmonies, 5: Design for X, Design to X, Seoul, Korea 19-22.08. 2013.

UNEP: United Nations Environment Programme, & GABC: Global Alliance for Building and Construction (2021). 2021 Global Status Report for Buildings and Construction: Towards a Zero-emission, Efficient and Resilient Buildings and Construction Sector. UNEP publications.

Venkatraj, V., & Dixit, M. K. (2022). Challenges in implementing data-driven approaches for building life cycle energy assessment: A review. Renewable and Sustainable Energy Reviews, 160, 112327. https://doi.org/10.1016/j.rser.2022.112327

Viscuso, S. (2021), Coding the circularity – Design for the disassembly and reuse of building components, Techne | Journal of Technology for Architecture and Environment, 22, 271-278. https://doi.org/10.36253/techne-10620

WBCSD: World Business Council For Sustainable Development (2023). The EU Digital Product Passport shapes the future of value chains: What it is and how to prepare now. https://www.wbcsd.org/Pathways/Products-and-Materials/Resources/The-EU-Digital-Product-Passport

WGBC: World Green Building Council (2019). Bringing embodied carbon upfront: Coordinated action for the building and construction sector to tackle embodied carbon. [Core Writing Team, A. Matthew et al.]. WGBC. https://worldgbc.s3.eu-west-2.amazonaws.com/wp-content/uploads/2022/09/22123951/WorldGBC_Bringing_Embodied_Carbon_Upfront.pdf

W3C: World Wide Web Consortium (2020). JSON-LD 1.1: A JSON-based Serialization for Linked Data. https://www.w3.org/TR/json-ld/

Zabek, M. E., Konstantinou, T., & Klein, T. (2023). Digital and physical incremental renovation packages enhancing environmental and energetic behavior and use of resources (AEGIR EU Project Deliverable D2.3: Sustainable requirement).

Zaffagnini, T., & Morganti, L. (2022), Data-Driven LCA for green industrial innovation of custom curtain walls, Agatón | International Journal of Architecture, Art and Design, 12, 94-105. https://doi.org/10.19229/2464-9309/1292022

Zeng. R., Chini, A. and Ries, R. (2020), Innovative design for sustainability – Integrating embodied impacts and costs during the early design phase, Engineering, Construction and Architectural Management, 28(3). https://doi.org/10.1108/ECAM-09-2019-0491

ANNEXES

TABLE ANNEX. A1 Summary of the required CMCW project data

CMCW PROJECT DATA				
Information required	**Information Description**	**Physical Dimension**	**Typical data reference**	**Ref.**
A1 - COMPONENTS SUPPLY				
Curtain wall framing (Qty)	Transom, Mullion, Intermediate transom, Cover caps, Trims, Beads, Thermal breaks, Gaskets, Others.	Qty, m, kg, ...	Company's PLM and ERP, Technical drawings, BIM model	1, 2, 3
Glass (Qty)	Glazing (inner laminate), Glazing (outer laminate), Spacer, Others.	Qty, m^2, m, kg, ...	Company's PLM and ERP, Technical drawings, BIM model	1, 2, 3
Mechanical joints (Qty)	Sealant, Glue, Gaskets, Others.	Qty, kg, ...	Company's PLM and ERP, Product's Datasheet, Technical drawings, BIM model	1, 2, 3
Spandrel (Qty)	Insulation, Aluminium panel, Steel back panel, Acoustic board, Fixings, Trims, Beads, Others.	Qty, m^2, m, kg, ...	Company's PLM and ERP, Technical drawings, BIM model	1, 2, 3
Architectural features (Qty)	Petal fins, Horizontal fins, Vertical fins, Support brackets, Spigots, Trims, Caps, Others.	Qty, m^2, m, kg, ...	Company's PLM and ERP, Product's Datasheet, Technical drawings, BIM model	1, 2, 3
Others used on site (Qty)	Fire floor-stop, Support bracket (plate, cast-in channels, anchors, bolts), Fixings, Membranes, Sealing tape, Coping, Weather protection, Others.	Qty, m^2, m, kg, ...	Company's PLM and ERP	1, 2
A2 - TRANSPORT TO FACTORY				
Component / Material transportation distances	Distances covered by components and materials to reach the factory. Different kinds of assessment are required for trains, roads and boats.	km	Company's PLM and ERP, DDT, Departments worksheets	1, 2, 3
A3 - MANUFACTORY (FABRICATION + ASSEMBLY)				
Factory energy intensity per assembled module (mFEI)	Energy consumed during production and assembling of the module.	kWh/module, kWh/m2	Electricity bill kWh data divided by the number of modules or m^2 produced	1, 2, 3
A4 - TRANSPORT TO SITE				
Module transport distance	Distances covered by the modules to the construction site Different kinds of assessment are required for train, land and ship.	km	Company's PLM and ERP, DDT, Departments worksheets	1, 2, 3
A5 - CONSTRUCTION / INSTALLATION (SITE EMISSIONS)				
Machine or plant usage time per module installed (MT)	Assumed and real construction site hours. Considering machinery rental and construction site's Gant chart.	h	Production and construction company	1, 2, 3
Fuel consumption per module installed (mFC)	Litres or kWh of consumption over the entire duration of activity. Considering vehicle rental and construction site's Gant chart.	kWh, litre	Production and construction company	1, 2, 3
B2 - MAINTENANCE				
Cleaning rate (CR)	Number of times the module will be cleaned in the future (e.g. glass) each year	Qty/years	Production company, use and maintenance regulations	1, 2, 3
Maintenance rate (MR)	Number of times the module is the object of maintenance operations each year	Qty/years	Production company, use and maintenance regulations	1, 2
Reference study period (RSP)	Representative of typically required service lives of the different building types	years	Production company, use and maintenance regulations	1, 2, 3
C2 - WASTE / DECONSTRUCTION TRANSPORT				
Materials and components (Qi)	Same list of the A1 - components supply	Qty, m^2, m, kg, ...	Company's PLM and ERP, Technical drawings, BIM model	1, 2, 3
C4 - DISPOSAL OF NON-RECYCLABLE / REUSABLE MATERIALS				
Materials and components (Qi)	Same list of the A1 - components supply	Qty, m^2, m, kg, ...	Company's PLM and ERP, Technical drawings, BIM model	1, 2, 3

TABLE ANNEX. A2 Summary of the required CMCW environmental data.

CMCW ENVIRONMENTAL DATA (e.g. data related to GWP)				
Information required	**Information Description**	**Physical Dimension**	**Typical data reference**	**Ref.**
A1 - COMPONENTS SUPPLY				
Global Warming Potential from EPDs (GWPA13,i)	Module A1-3 Global Warming Potential (GWP) of the materials (This is more reliable than ECFA13,i).	kgCO2eq/Qty, kgCO2eq/m2, kgCO2eq/kg	Supplier Components' EPD	1, 2
Embodied carbon factor for the material (ECFA13,i)	Module A1-3 Embodied Carbon Factor (ECF) of the materials.	kgCO2eq/Qty, kgCO2eq/m2, kgCO2eq/kg	Internal information or external databases (e.g. ecoinvent, ICE, CWCT)	1, 2, 3
A2 - TRANSPORT TO FACTORY				
Trasport emission factor (TEFmode)	Transport emission factor of the transportation used. Trains, roads and boats, but also if it is electric, by gas or by other fuels.	kgCO2eq/km	Internal information or external databases (e.g. ecoinvent, ICE, CWCT)	1, 2, 3
A3 - MANUFACTORY (FABRICATION + ASSEMBLY)				
Generated electricity carbon factor (GECF)	Measured as mass of CO2 equivalent emitted for each kWh of electricity generated by a local energy source or by the manufacturing plant.	kgCO2eq/kWh	Electricity production sensors (e.g. linked to photovoltaic panels)	1, 2
Grid carbon factor (GCF)	Measured as mass of CO2 equivalent emitted for each kWh of electricity generated on the National Grid.	kgCO2eq/kWh	Internal information or external databases (e.g. ecoinvent, or defra)	1, 2, 3
A4 - TRANSPORT TO SITE				
Trasport emission factor (TEFmode)	Distances covered by the modules to the construction site. Different kinds of assessment are required for trains, roads and boats.	kgCO2eq/km	Internal information or external databases (e.g. ecoinvent, ICE, CWCT)	1, 2, 3
A5 - CONSTRUCTION / INSTALLATION (SITE EMISSIONS)				
Fuel carbon factor for fuel source (FCFs)	Measured as mass of CO2 equivalent emitted for each kWh or litre of fuel per machinery activity.	kgCO2eq/kWh kgCO2eq/litre	Internal information or external databases (e.g. ecoinvent, GaBi)	1, 2, 3
Fuel consumption per module installed (mFC)	Litres or kWh of consumption over the entire duration of activity. Considering vehicle rental and construction site's Gant chart.	kWh, litre	Production and construction company	1, 2, 3
B2 - MAINTENANCE				
Cleaning emissions factor (CEF)	Measured as mass of CO2 equivalent emitted for each cleaning activity.	kgCO2eq/Qty	Internal information or external databases (e.g. ecoinvent, GaBi)	1, 2, 3
Maintenance emissions factor (MEF)	Measured as mass of CO2 equivalent emitted for each maintenance activity.	kgCO2eq/Qty	Internal information or external databases (e.g. ecoinvent, GaBi)	1, 2
C2 - WASTE / DECONSTRUCTION TRANSPORT				
Global Warming Potential from EPDs (GWPC2,i)	Module C2 Global Warming Potential (GWP) of the materials (This is more reliable than ECF).	kgCO2eq/Qty, kgCO2eq/m2, kgCO2eq/kg	Supplier Components' EPD	1, 2
Embodied carbon factor for the material (ECFC2,i)	Module C2 Embodied Carbon Factor (ECF) of the materials.	kgCO2eq/Qty, kgCO2eq/m2, kgCO2eq/kg	Internal information or external databases (e.g. ecoinvent, ICE, CWCT)	1, 2, 3
C4 - DISPOSAL OF NON-RECYCLABLE / REUSABLE MATERIALS				
Global Warming Potential from EPDs (GWPC4,i)	Module C2 Global Warming Potential (GWP) of the materials (This is more reliable than ECF).	kgCO2eq/Qty, kgCO2eq/m2, kgCO2eq/kg	Supplier Components' EPD	1, 2
Embodied carbon factor for the material (ECFC4,i)	Module C2 Embodied Carbon Factor (ECF) of the materials.	kgCO2eq/Qty, kgCO2eq/m2, kgCO2eq/kg	Internal information or external databases (e.g. ecoinvent, ICE, CWCT)	1, 2, 3

ANNEXES PROJECT AND ENVIRONMENTAL DATA REFERENCES LEGEND
References
[1] EN 15978:2011
[2] EN 15804:2012+A2:2019
[3] CWCT, et al., 2022

TABLE ANNEX. A3 Summary of the required CMCW circularity data

CMCW CIRCULARITY PASSPORT DATA

Information required	Type of data	Information description	Typical data reference	Ref.
GENERAL INFORMATION				
Module name	Short Text, Alphanumeric data	Name of the façade module (e.g. a short description).	Production Company	3
Supplier Company	Short Text, Alphanumeric data	Name of the façade module manufacturer.	Production Company	1, 3, 5
Company contacts and production site	Long Text (Memo), Large amounts of alphanumeric data	Information that should help future stakeholders to contact the manufacturer eventually.	Production Company	3
Production date	DateTime, Date	Date in which the façade module has been produced.	Company's PLM and ERP	1, 8
Certifications	Hyperlink, Link address to the certifications of the object	Link to the environmental certification related to the module (e.g. ISO:14001, BES:6001, EPD).	Quality and Sustainability Department	1, 6, 8
Data portability	Hyperlink, Link address	Information to ensure that module data are transferable from one software system to another.	e.g., blockchain, centralised databases, centralised ledgers, OPC UA	2, 8
PHYSICAL DATA				
Dimensions and weight	Number, Numeric data	Physical dimensions useful to describe the façade module (i.e. dimensions and weight).	Company's PLM and ERP, Technical drawings, BIM model	1, 8
Bill of components/ materials	Hyperlink, Link address to the list of the objects	Detailed list of the components and materials part of the façade module. Those should be linked to their own DPP data sheets.	Company's PLM and ERP	1, 4, 5, 7
Technical drawings and 3D model	Hyperlink, Link address to the technical drawings of the object	Any kind of drawing or 3D model that can be useful in the life cycle stages of the module after the installation at the construction site.	Company's PLM and ERP	1, 7, 8
U-value of the module	Number, Numeric data	Factory thermal transmittance of the façade module (i.e. IGU, spandrel, etc.)	Production Company	8
INFORMATION ABOUT CIRCULARITY				
Disassembly methods, specialised knowledge	Long Text (Memo), Large amounts of alphanumeric data or Hyperlink	Description of the connection systems to building. Construction practices that prioritise the ability to disassemble and remove components.	Quality and Sustainability department, Technical drawings, BIM model	1, 2, 3, 4, 5, 7
Maintenance/Warranty	Number, Numeric data	Asset reference period (e.g. Every how many years maintenance is required).	Production Company, manuals of use and maintenance	4, 5
Reuse potential and recyclability	Long Text (Memo), Large amounts of alphanumeric data	Description of the second life options foreseeable during the design stage.	Production company, Quality and Sustainability depart.	1, 3, 4, 5, 7
Life span period	Datetime, Date	Date beyond which façade module becomes obsolete or unusable.	Production Company, manuals of use and maintenance	1, 4, 8
OTHER				
Products exposure history	Hyperlink, Link address to the technical drawings of the object	Information to enable real-time data (if needed), and report and documentation for prediction.	Facade Digital-Twin, sensors, owner, leasing service.	1, 2, 6, 7
Financial concepts for multiple life cycles	Long Text (Memo), Large amounts of alphanumeric data	Information about incentives or budget allocation for companies or end users to extend module lifespans through services or take-back agreements.	Production company, owner, leasing service.	4, 5, 6

TABLE ANNEX. A4 Summary of the required CMCW's components and materials circularity data.

CMCW'S COMPONENTS AND MATERIALS CIRCULARITY PASSPORT DATA

Information required	Type of data	Information description	Typical data reference	Ref.
GENERAL INFORMATION				
Product name	Short Text, Alphanumeric data	Name of the component (e.g. a short description or a commercial name).	Component supplier's company	3, 7
Supplier Company	Short Text, Alphanumeric data	Name of the component supplier.	Component supplier's company	1, 3, 7
Source mill	Geographic data, location or area data	Geographic data about where the component materials come from.	Component supplier's company	1, 3, 4, 8
Certifications	Hyperlink, Link address to the technical drawings of the object	Link to the environmental certification related to the module (e.g. ISO:14001, BES:6001, FSC®/PEFC®, EPD, CRADLE TO CRADLE, VOC)	Component supplier's company	1, 7, 8
Data portability	Hyperlink, Link address to the technical drawings of the object	Information aimed to ensure that component data are transferable from one software system to another.	E.g., blockchain, centralised databases, centralised ledgers	2, 7, 8
PHYSICAL DATA				
Material and product composition	Long Text (Memo), Large amounts of alphanumeric data	Description of the product's material (e.g. monolytical material, chemical substance, potentially harmful substances, health risks)	Component supplier's company	1, 3, 4, 5, 6, 7, 8
Applied coatings or furniture	Short Text, Alphanumeric data	Description of the product's coatings or furniture (e.g. varnishing, etc.)	Company's PLM and ERP, Technical drawings, BIM model	1, 7
Relevant Physical properties	Number, Numeric data	Physical dimensions useful to describe the type of the component (e.g. weight, length, volume, surface, etc.)	Company's PLM and ERP, Technical drawings, BIM model	1, 7, 8
Technical drawings and 3D models	Hyperlink, Link address to the technical drawings of the object	Any kind of drawing or 3D model that can be useful in the life cycle stages of the component.	Company's PLM and ERP	1, 8
Pre-consumer recycled content	Percentage, Numeric data	Percentage of the pre-consumer content in the component.	Component supplier's company	3, 4, 6, 7
Post-consumer recycled content	Percentage, Numeric data	Percentage of the post-consumer content in the component.	Component supplier's company	3, 4, 6, 7
Bio-composite quantity	Percentage, Numeric data	Percentage of the bio-composite content in the material.	Component supplier's company	
INFORMATION ABOUT CIRCULARITY				
Expected material reverse stream / Waste category	Long Text (Memo), Large amounts of alphanumeric data	Description of a feasible reverse logistic foreseeable during the design stage.	Component supplier's company	5, 6, 7, 8
Reuse potential and recyclability	Long Text (Memo), Large amounts of alphanumeric data	Description of the second life options foreseeable during the design stage.	Component supplier's company	1, 3, 4, 5, 6, 7
Compostability	Yes/No or True/False	Information about the quick and complete breakdowns in a composting environment, leaving no harmful residues or by-products.	Component supplier's company	4
Life span period	Datetime, Date	Information about incentives for companies or end users to extend component lifespans through services or take-back agreements.	Component supplier's company	1, 4, 8

ANNEXES CIRCULARITY PASSPORT DATA REFERENCES LEGEND

References	Papers about tools, frameworks, or models					
	Generic Product Analysis	Specific analysis for Buildings	Circular Assessment	Sustainability Assessment	Referred to DPP	Referred to LCA
[1] Heinrich & Lang, 2019		x	x		x	
[2] Jansen et al., 2023	x		x		x	
[3] Mulhall et al., 2022	x		x		x	
[4] Zabek et al., 2023		x	x	x		x
[5] Klein et al., 2022		x	x	x		x
[6] Oluleye et al., 2023		x	x			
[7] Morganti et al., 2023		x	x	x		x
[8] European Commission et al., 2020		x	x		x	x

Façade Design Pattern Optimisation Workflow Through Visual Spatial Frequency Analysis and Structural Safety Assessment

Martin Ivanov[1*], Jun Sato[1]

* Corresponding author: martin.ivanov359@gmail.com
1 The University of Tokyo, Department of Socio-Cultural Environmental Studies, Japan

Abstract

As the demand for highly efficient yet aesthetically pleasing, complex building envelope structures is rising worldwide, computational analysis and generative design tools are becoming ever so relevant. Previous methods for achieving a natural distribution of structural or shading elements in non-uniform façades are mostly based either on computer-generated pseudo-randomness or a literal biomorphic approach where a naturally occurring pattern is directly projected on the façade surface. As an alternative, this research introduces a novel technique for optimisation that utilises a two-dimensional Power Spectrum Analysis, suitable for numerically assessing the alignment of designed geometry with natural patterns. By integrating this optimisation method into the design process, the façade pattern generation can be automated and optimal design can be selected by evaluating multiple design solutions. Instead of using repetitive geometrical patterns or generated pseudo-randomness, patterns objectively similar to those occurring in nature can be created without directly copying natural structures.
The distribution of the structural and shading elements controls the way natural light permeates the building and, considering the data gathered from images of natural scenes, this method can be used to design structures not only with optimal structural and energy performance but also with visual and psychological occupant comfort in mind.

Keywords

Generative Façade Design, 2D Power Spectrum Analysis, Computational Design Tools, Non-uniform Façades, Structural Optimisation, Natural Light Control, Naturalness

DOI

http://doi.org/10.47982/jfde.2024.299

1 INTRODUCTION

The design process of façade structures requires many considerations like structural and energy efficiency, solar gain, visual and thermal comfort. The performance of a façade system regarding most of these aspects can be objectively measured through computer simulations with clear values, which can then be used to improve the façade design through various optimisation algorithms (Huang & Niu, 2016). Computational design tools enable semi-automatic façade design generation, where the designer sets constraints and the algorithm automatically creates and evaluates a large number of potential solutions.s (Heusler & Kadija, 2018). Designing a façade structure algorithmically offers adaptability and easy reconfiguration of the structure and its elements based on the input parameters, and computational analysis tools aid the designer in their decision-making process.

Structural performance can be studied by the Finite Element Method (FEM) with linear and non-linear analysis tools (Sato, 2010), and methods such as daylight analysis and glare analysis are effectively utilised for solar gain and visual comfort (Larson & Shakespeare, 1998). There is a multitude of proposed metrics to measure visual comfort by evaluating daylight levels and distribution, exposure to direct sunlight, and glare intensity (Tabadkani et al., 2021) such as the established Daylight Glare Probability metric (Wienold & Christoffersen, 2006). To assess the window view quality in terms of view content, access, and clarity, there is a proposed framework (Ko et al., 2021), an integral part of which is the analysis of the visual features and aesthetic qualities of the view (Matusiak & Klöckner, 2015).

Quantifying the aesthetic appeal of façade designs with objective metrics presents challenges, often leading architects to draw inspiration from natural forms. In achieving a natural distribution of structural or shading elements within non-uniform façade structures, architects generally adopt one of two main strategies: employing stochastic geometry or generated pseudo-randomness (Verbeeck, 2006) or directly incorporating natural shapes through a biomorphic approach (Vincent, 2009). While the randomness employed in generative art or architecture can foster creativity, it may result in uncontrollable and unpredictable outcomes that necessitate further design evaluations. Conversely, the biomorphic approach, which involves the direct application of natural patterns to structural designs, tends to be labour-intensive and might limit design flexibility by typically producing a single design solution based on a singular reference.

To address these challenges, this research proposes a novel approach: the utilisation of a Power Spectrum Analysis (PSA) technique suitable for implementation within automated and semi-automated structural design generation and optimisation systems. Defining "naturalness" in objective terms is challenging, which is why this research explored the potential of 2D PSA, a proven method to evaluate visual scenes (Oliva et al., 1999; Torralba & Oliva, 2003), their perceived aesthetics (Redies et al., 2007; Spehar et al., 2003) and visual comfort (Juricevic et al., 2010; O'Hare & Hibbard, 2011). PSA has seen successful application in evolutionary art systems as a tool to derive a mathematical value conducive to optimisation (Gircys & Ross, 2019). The principal goal of this study is to determine the feasibility of incorporating PSA into a generative design process, specifically for enhancing façade designs by ensuring their spectral alignment with a selected natural pattern. Within a generative design framework, the proposed analysis technique, when paired with optimisation algorithms, enables the automated generation and evaluation of diverse design solutions.

This method can reference either a single natural image or an entire image category, offering a novel alternative to the conventional biomorphic approach. Unlike direct mimicry of natural phenomena, this method employs statistical analysis to evaluate the designed geometry, offering a numeric assessment of how closely a design's pattern aligns with those observed in nature.

The proposed methodology was assessed through two generative design experiments. The initial experiment focused on a double-skin glazed curtain wall system, targeting the singular objective of achieving spectral similarity to a predetermined natural pattern over successive generations through model-based and metaheuristic optimisation solvers. The subsequent experiment demonstrated the utility of incorporating the PSA-based method with other structural optimisation techniques in a Multi-Objective Optimisation (MOO) framework, integrating linear structural analysis via the FEM to simultaneously address structural feasibility and safety.

This methodology presents an alternative form-finding strategy for natural-form façade design, diverging from the conventional biomorphic approach that primarily depends on visual similarities. It aims to strike a balance between emulating natural characteristics and maintaining design control, potentially leading to innovative architectural solutions that embody the essence of natural structures while adhering to practical and functional requirements. This endeavour seeks to bridge the gap between human-made and naturally occurring structural forms, fostering the creation of built environments that resonate with the inherent qualities of the natural world.

1.1 PERCEPTION OF THE BUILT AND NATURAL ENVIRONMENTS

Biological perceptual systems have evolved in response to the physical properties of natural environments, adapting to the statistical patterns observed in natural scenes (David et al., 2004; Field, 1987; Olshausen & Field, 1996; Párraga et al., 2000; Simoncelli & Olshausen, 2001). The psychological effect of environmental stimuli precedes cognition. It is well-proven that natural environments are greatly preferred over artificial ones, and scenes with higher visual complexity are mostly preferred over simple ones in both natural and built environments (Kaplan et al., 1972). This preference is often attributed to the fact that humans evolved over a much longer period in natural settings, which predisposes us to react positively to nature as opposed to built content. Apart from the aesthetic preferences of natural environments, it is also proven that, especially in urbanised societies, the connection to natural environments benefits people emotionally and psychologically (Ulrich, 1983).

A defining feature of the natural environment is the presence of flicker or 1/f-noise, which is the most commonly occurring signal in both physical and biological systems (Szendrő et al., 2001; Bak et al., 1988). Contrary to white noise, which is an expression of mathematical randomness, flicker noise has equal energy per octave of frequency. From plants, water, and clouds, this can be observed at any scale from atomic structures to galaxy formations as well (Gisiger, 2001). Flicker noise in nature is scale-invariant and appears multi-dimensionally. Examples of one-dimensional flicker noise in nature include the sound of waves crashing on the shore and the rustling of leaves in the wind. Two-dimensional flicker noise has equal energy per octave in both the horizontal and vertical dimensions – it has more low-frequency energy and less high-frequency energy than white noise in both dimensions. It typically appears to a different degree in any two-dimensional image of a natural scene.

For the human visual cortex, it is easy to distinguish between built and natural scenes and to what extent a natural scene contains artificially built objects. In computer graphics, however, we need a reliable classification method to achieve this task with high accuracy. The information in images can be encoded through various techniques, and one way to study the statistics of natural images is by analysing their frequency composition (Field, 1987). To convert an input signal from its temporal or spatial domain into the frequency domain we can apply the Fast Fourier Transform (FFT), which is a common technique in a large variety of fields in signal processing and analysis (Cooley et al., 1969; Brigham, 1988). The FFT is a highly efficient algorithm that can be performed in multiple dimensions, and in the case of image analysis, a 2D FFT can be performed, which results in the 2D power spectrum of the image. Following the Fourier transformation, the frequency composition of the image can be analysed. Research consistently demonstrates that the frequency composition of a scene has a direct influence on visual perception and is related to aesthetic preference (Spehar & Taylor, 2013; Hagerhall et al., 2004; Spehar et al., 2003) and visual comfort (Fernandez & Wilkins, 2008; Juricevic et al., 2010; O'Hare & Hibbard, 2011. Consequently, analysing the frequency composition is hypothesised to be well-suited for aesthetic computational image generation and has been successfully applied in generative art systems (Gircys & Ross, 2019). This is further detailed in the following section, which discusses the implications for architectural design.

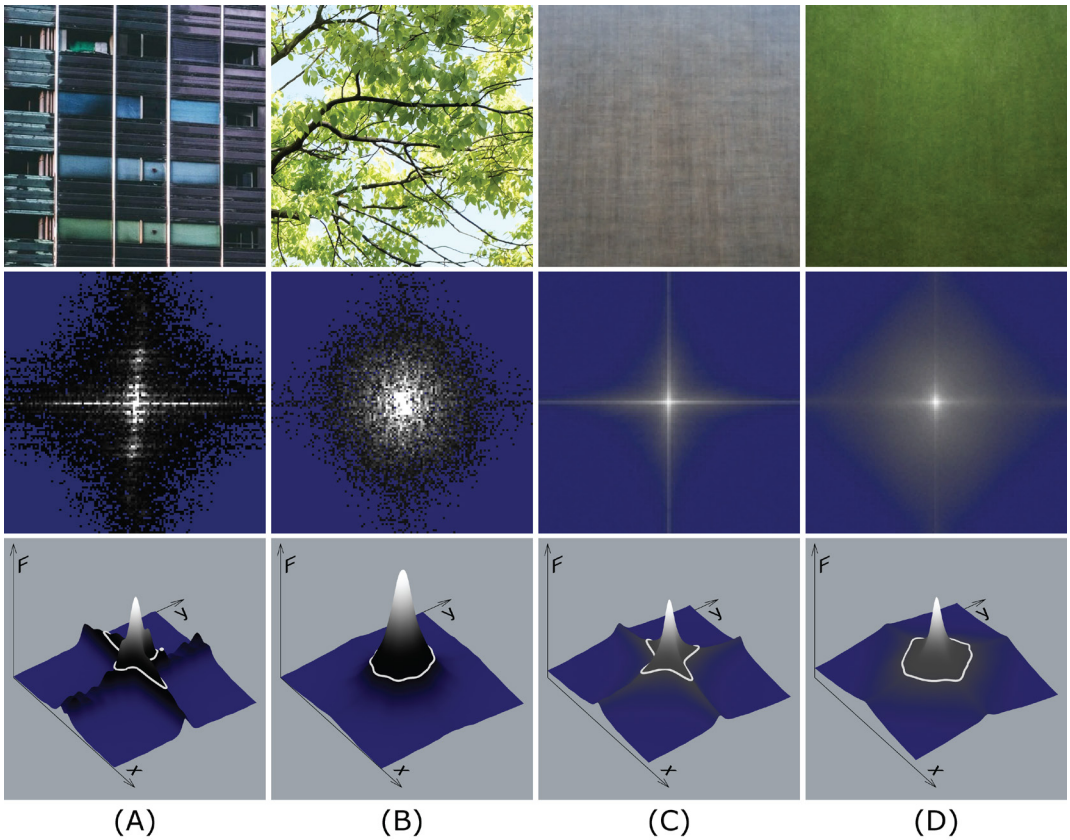

FIG. 1 Comparison of the power spectra of images of built and natural environment scenes (Based on (Torralba & Oliva, 2003)

Analysing the frequency composition of images is a key method for scene evaluation, allowing for the extraction and study of their low-level features. Statistical analysis of thousands of images demonstrates that natural images have a specific output very distinct from images of artificial structures (Ruderman & Bialek, 1994; Oliva et al., 1999; Torralba & Oliva, 2003).

The natural world is distinguished from the one built by humans, for which the term "carpentered world" is often used in literature. Characteristics of the carpentered world, especially in an industrialised society, are straight and parallel lines, right angles, and even planes. Such geometrical features typically lead to scenes whose frequency composition exhibits limited and pronounced directionality, predominantly in horizontal and vertical orientations. On the other hand, for structures occurring in nature, the variability of directionality and, therefore, the uniformity of power distribution is a lot more common. FIG. 1. illustrates these distinct differences in the power spectra of images of natural and built structures. Sets (A) and (B) show the difference in the 2D power spectra of single images of a building and a natural scene. The zero values of the power spectra are recoloured from black to dark blue for a better visual representation of the spectral shape. The power spectra are also plotted on a 3D graph to visualise the magnitude F on the vertical axis. Set (C) of FIG. 1. shows the mean average collected from 100 random pictures from the "Building" category of a public domain image classification database, and the mean average of their power spectra is plotted in 2D and 3D. In the same manner, 100 random images from the "Forest" category were processed in Set (D). This study illustrates the statistically verified spectral disparities between artificial and natural scenes, highlighting 2D PSA's significant utility in distinguishing natural imagery from artificial constructs. Based on these observations, 2D PSA is recognised as a robust technique for assessing the inherent natural qualities in digital images, establishing it as a powerful instrument for scene evaluation.

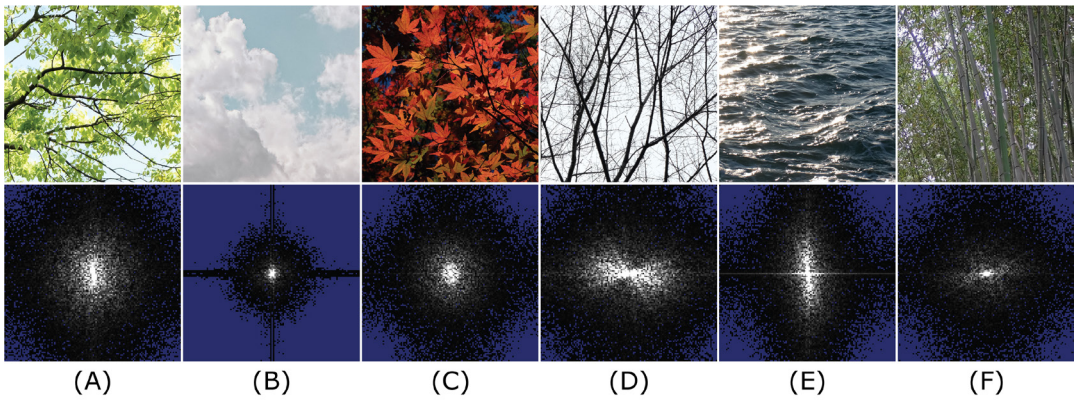

FIG. 2 Catalogue of natural scenes power spectra.

Natural images are also very distinguishable from randomly generated images due to the appearance of specific structures of the flicker noise as opposed to the randomness of white noise (Ruderman, 1994). The power spectra of a variety of naturally occurring structures or phenomena can be studied and used as an inspiration for visual arts and architectural design. FIG 2. presents a part of a custom catalogue of power spectra of different examples of natural scenes, which all contain flicker noise but also display some distinct features. Image set (A) shows a flicker noise distribution observable both in lower and higher frequencies of the power spectrum, while due to its relatively higher uniformity (B) is limited to the lower frequencies of the power spectrum. Image set (C) shows a power spectrum most similar to the pure $1/f^2$ noise. In (D), (E), and (F), we observe some dominant directionality in the power spectra caused by repetitiveness in the directions of some of the natural scene components.

1.2 IMPLICATIONS FOR FAÇADE DESIGN

Structural patterns like those occurring in nature are often considered a suitable reference in architectural design, especially in the design of complex building envelopes. Inspiration from natural structures is implemented in many façade projects using a biomimetic approach, which can prove useful for energy efficiency (Nagy & Osama, 2016). Façade structures act as an environmental filter as they control what permeates in and out of the building, and façade design is directly responsible for the building occupants' experience (Pastore & Andersen, 2022). Aiming to improve the occupants' experience, this study introduces a numerical method to assess and enhance aspects such as aesthetic appeal and visual and psychological comfort by integrating natural environment statistics into a generative design approach.

The visual system of higher mammals is finely tuned to optimally process information from natural stimuli, a capability shaped by evolution, development, and adaptation to the statistical patterns of natural scenes. Studies indicate that humans exhibit a consistent aesthetic preference for images exhibiting scale invariance, regardless of whether these images are derived from natural, human-made, or computer-generated sources (Hagerhall et al., 2004; Spehar et al., 2003. This propensity suggests scale invariance as a possibly universal trait in visual art, with the exception of some modern art forms deviating from aesthetic pursuits to explore alternative artistic tenets (Redies et al., 2007). A variety of aesthetically appealing images, spanning Western and Eastern art to graphic novels, exhibit shared statistical properties in their power spectra, such as the $1/f^2$ characteristic, which aligns with the scale-invariant structure found in complex natural scenes. This parallelism implies that aesthetic images harmonise with the statistical patterns found in nature (Graham & Field, 2007; Field, 1987; Tolhurst et al., 1992). Consequently, it is theorised that artists may instinctively or deliberately align their creations with the mammalian visual system's efficient processing of natural scenes, potentially explaining the universal appeal of certain artistic styles and compositions (Melmer et al., 2013).

Other than the aesthetic appeal, research shows that images closer to the statistical properties of natural scenes are more comfortable, while those that stray from these natural scene statistics may induce visual discomfort (Juricevic et al., 2010; O'Hare & Hibbard, 2011). It is empirically proven through human participant research that discomfort ratings can be predicted by the amplitude of the Fourier spectrum at specific spatial frequencies (Fernandez & Wilkins, 2008). These studies support the notion that the human visual system is optimised for processing natural scenes and can find certain unnatural statistics physiologically stressful. Such insights could help by guiding the selection of images in sensitive settings, such as public art in hospitals, to ensure they are appropriate and comfortable for viewers. Aesthetic preference and visual comfort extend to any visual scene, and as such, the PSA can be considered a suitable tool for evaluating architectural design as well.

For the built environment, the power spectrum was used to analyse structures and patterns as a design consideration. It has already been utilised in the design process of a variety of experimental and commercial projects. A couple of examples in FIG. 3 can serve to explore the power spectra of a transparent glass structure (A), experimentally built during a Stanford University seminar and workshop in 2015 (Choe & Sato, 2016) and a timber façade structure (B), built for a commercial building in Aoyama, Tokyo (Kengo Kuma and Associates, 2013). The power spectra of those structures have visual similarity to the power spectra of natural image scenes such as those occurring in a forest – the Komorebi phenomenon (the permeation of light through the leaves in a forest).

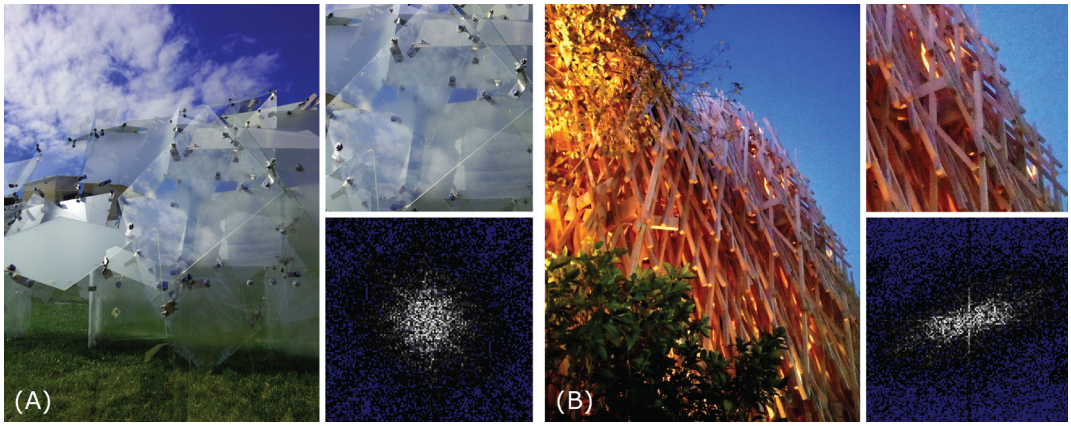

FIG. 3 Examples of experimentally and commercially built structures with their power spectrum analysis: (A) Transparent structure as a perceptual filter, Stanford University workshop project (Choe & Sato, 2016); (B) Sunny Hills Aoyama, commercial building in Tokyo (Kengo Kuma and Associates, 2013).

The validated efficacy of using 2D PSA for assessing aesthetic properties in images suggests its applicability as a fitness measure in generative design systems. By conducting a 2D Fourier analysis on a target image, essential spatial features can be identified and leveraged to guide the development of new images that exhibit similar characteristics. Such a strategy is successfully employed in creating procedural textures and evolutionary art (Gircys & Ross, 2019). Focusing on prominent frequencies and orientations allows evolutionary art systems the flexibility to create variations that resonate visually with the target image without exact replication. Within a genetic programming framework, a fitness metric based on PSA can be applied to evolve images that reflect the spectral qualities of chosen target images or image categories.

The evolutionary generation of images and textures, however, faces significantly fewer limitations when compared with the generative design of architectural structures. Therefore, creating an efficient PSA-based generative design method for building elements necessitates tight control over the geometric and physical properties of the patterns, ensuring the generated structures are both feasible and safe. Consequently, a flexible methodology that can integrate PSA into a broader Multi-Objective Optimisation (MOO) workflow is essential.

2 METHODOLOGY

The goal of the current research was to devise a PSA method suitable for automated and semi-automated structural design optimisation. For this case, computer graphics tools were used to process images and measure spectral similarity to extract a numeric value for the difference between natural input and computer-generated images. This result can be used in the proposed workflow (FIG. 4.), which aims to automate design optimisation based on 2D PSA in combination with other structural analysis methods.

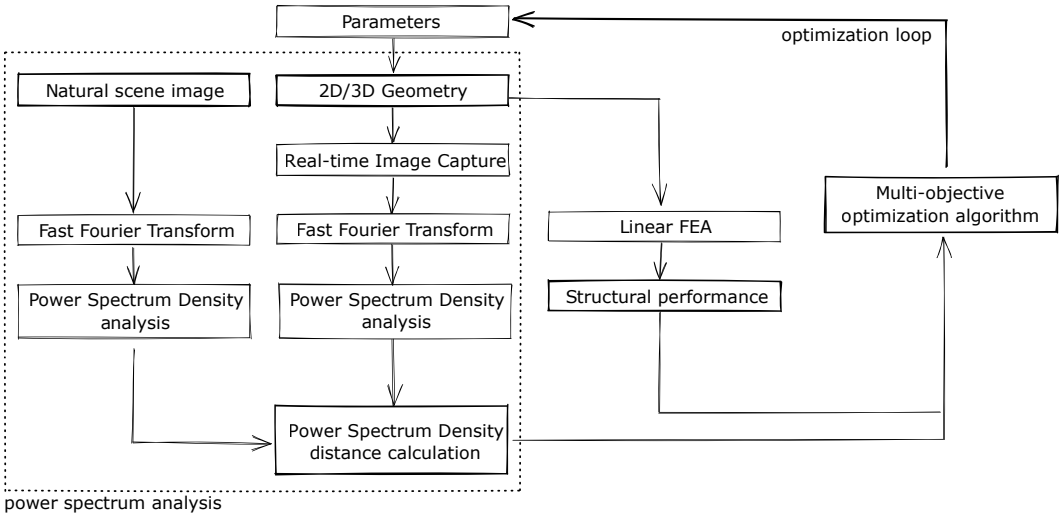

FIG. 4 Proposed optimisation workflow.

The process works with any type of parametrically generated 2D or 3D geometry by capturing 2D bitmaps during each design iteration, transforming the bitmaps with the FFT algorithm, and comparing the result to the power spectrum of an input natural image or image category. This analysis process can be integrated into an automated generative design workflow for design form-finding and optimisation. As such, it can also be combined with other analysis methods to simultaneously improve a structure for multiple objective goals. In the current research, we successfully combined the method with FEM linear structural analysis, which is further discussed in the presented experiments.

2.1 DEVELOPMENT OF THE ANALYSIS METHOD

To solve the problem of real-time PSA for the case of structural design optimisation, a custom software tool was developed with C# programming language. The decision was made to develop the software tool as a plugin for 3D software Rhinoceros and the algorithmic design plugin Grasshopper, chosen for the basic design environment as the most commonly used and versatile software tools for 3D and algorithmic design creation. Their interoperability allows the integration of various plugins and standalone applications, which proved useful for combining the PSA with our C++ FEM software tool for linear structural analysis and automating the whole process through optimisation solvers for single and multi-objective optimisation (MOO).

Different approaches for power spectrum similarity measurement were implemented and their performance was assessed for the specific case. As similarity measurement techniques in image processing and analysis vary by many different methods and approaches, computer image analysers must usually choose the most appropriate option in the context of the actual problem they are trying to solve. One of the most typical similarity measurement approaches in image analysis is the Euclidean distance measurement. It is a fast and simple method by which we can calculate the distance of respective pixel values or equally sized square grid sectors of 2 bitmaps of the same size (FIG.5 (A-B) Euclidean distance). It performs fast, and experiments showed that the results are useful and efficient.

However, in the case of natural scene recognition, we are mostly concerned with the directionality of the power spectrum. To extract the spectral profile of an image useful for scene analysis and classification, a suitable option is to average the power spectrum by orientations (Simoncelli & Olshausen, 2001). The azimuthally averaged power spectrum density (AAPSD) calculator that we devised works by dividing the power spectrum matrix by azimuthal angles into equally sized pie-shaped sectors (FIG. 5 (A-B) AAPSD distance). The number of sectors controls the resolution to which we want to study directionality in the power spectrum. The size of the sectors can be limited between minimum and maximum radii, with the maximum radius being half the width of the 2D spectrum. This allows us to limit the analysed frequencies in the power spectrum, eliminating spectral artefacts occurring at both very low and very high frequencies. The corner regions outside the maximum radius are also excluded from the calculation. The power density in the analysed sectors is then derived by averaging the values inside each of them. The resulting plot shows spectral power (averaged) by radii, which can be used for the final distance calculation.

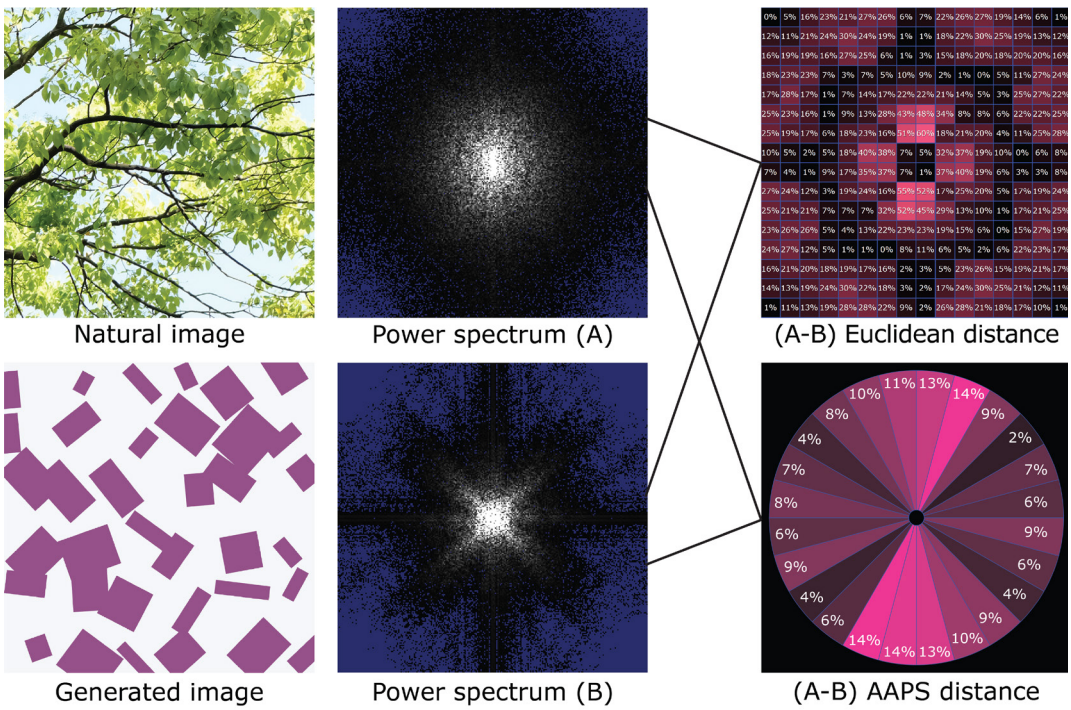

FIG. 5 Power spectrum density distance calculation methods.

Both Euclidean and AAPSD distance calculation methods were tested for the purpose of automatic design optimisation based on power spectrum similarity. FIG. 5. illustrates the difference between the Euclidean distance and the AAPSD distance calculation between two images – one of a natural structure and one of a computer-generated pattern. The AAPSD method can be considered a much more accurate similarity measurement tool in the context of this research, which is why it was applied in the following experiments.

2.2 DEVELOPMENT OF THE OPTIMISATION METHOD

The geometrical optimisation of building envelopes, informed by structural and environmental performance analyses, poses a complex design challenge that can be approached as a black-box problem, where the system's internal workings are not explicitly known or utilised in the optimisation process; rather, only the input parameters and the resulting outputs are considered. This approach allows for flexibility and generality, as the same optimisation techniques can be applied to a wide range of engineering and architectural design problems, facilitating the exploration of complex design spaces and the identification of optimal solutions based on single or multiple, often competing, criteria.

As detailed in the previous section, our integrated analysis tools automatically assess the fitness performance of a computer-generated geometry by calculating an AAPSD distance metric. To successfully integrate this analysis process into an optimisation technique, the proposed methodology necessitates three main steps. First, define the problem phase space by parameterising the façade design and making the numerical parameters accessible to the algorithm. Second, evaluate the fitness function of the design using the proposed PSA tool and, if deemed necessary, integrate FEM analysis to account for structural feasibility and safety, defining a MOO problem. Third, implement an algorithm that iteratively updates the geometry parameters, optimising the design based on the evaluated design performance on the single or multiple objectives.

To test the robustness of the proposed generative design methodology, five distinct optimisation techniques were selected and applied in this research. Initially, for the single-objective optimisation focusing on power spectrum distance minimisation, a general Genetic Algorithm (GA) was used (Rutten, 2013). This popular metaheuristic technique, inspired by biological evolution and relying on mutation and selection, centres on the core idea of heritability, where the algorithm maintains a population of individuals and selectively culls and recombines them to form successive generations. To support the results and ensure repeatability, the analysis method was also tested with four additional optimisation techniques.

A surrogate model-based optimisation method using the Radial Basis Function (RBF) was selected as a second optimisation solver to demonstrate the flexibility of the analysis process and its ability to work with a different class of black-box optimisation algorithms. The RBFOpt (Costa & Nannicini, 2018; Nannicini, 2021) is a powerful derivative-free solver efficient for highly nonconvex, unconstrained mixed-variable problems, which in some cases can outperform GAs, requiring considerably fewer simulation runs (Wortmann & Nannicini, 2016). Another alternative method to evolutionary computations selected for the optimisation methodology is the Particle Swarm Optimisation (PSO) algorithm, based on Swarm Intelligence (SI). Inspired by biological systems like bird flocking, which relies on collective behaviours for optimisation, PSO was chosen for its superior performance in solving single-objective high-dimensional problems compared to some evolutionary algorithms (Cichocka, 2017).

In architectural design and engineering, MOO is often more necessary than single-objective optimisation. Furthermore, most professionals prefer full control over the process, making a human-in-the-loop approach ideal (Cichocka, 2017). Thus, we chose two GAs capable of executing MOO: the Cluster-oriented Genetic Algorithm (COGA) and the Strength-Pareto Evolutionary Algorithm (SPEA). COGA quickly identifies high-performance regions through clustering, allowing focused searches and user interaction to control weighting between objectives (Bonham & Parmee, 2004). An optimisation tool based on the COGA algorithm facilitates the interactive-evolutionary design (Harding & Brandt-Olsen, 2018). SPEA was selected for its efficiency in finding optimal solutions on the Pareto front (Zitzler & Thiele, 1998) and providing higher accuracy than other algorithms (Zitzler, 1999), with Pareto dominance being key for comparing multi-objective solutions. Implemented through a flexible parametric design framework (Vierlinger & Hofmann, 2013), it provided the most favourable results in the following case studies.

3 EXPERIMENTS

During this research, multiple experiments, both for single- and multi-objective optimisation, were conducted using the proposed optimisation workflow FIG.4. Two façade design proposals were chosen for validating the method and illustrating the optimisation process.

3.1 SINGLE-OBJECTIVE OPTIMISATION EXPERIMENT

A double-skin glass façade structure model was selected for a single-objective optimisation experiment. The proposed model consists of a standard curtain wall with glass panels and a second layer of semi-translucent shading elements. These elements are rectangular and come in 5 different size types – 300/300mm, 300/600mm, 600/600mm, and 600/1200mm, and two different levels of opacity – 20% and 60%. Their proposed material is the highly durable glass type Leoflex™ (AGC, 2014), the strength of which was tested through various methods (Oliveira Santos, 2018), and whose light weight and high bending strength make it suitable for the application. Standardised metal spider-type connectors hold the panels tilted at a 5-degree angle, which allows them to be rotated to any degree without interfering with each other. This joint connects the panels to the main façade structure mullions, which makes the location of the panels at fixed points.

The power spectrum of an image of a natural structure was considered one optimisation goal – in this case, the sunlight passing through the leaves of a Japanese maple tree. The scattering of the leaves and their oblique orientations, as well as the different levels of translucency, create a distinct flicker noise pattern typically occurring in natural scenes.

An 8 by 8 meters partial model of the façade with 64 shading panels is studied for the optimisation experiment. The geometry is generated based on three initial parameters – the type of each panel regarding size and proportions (300/300mm, 300/600mm, 600/600mm, or 600/1200mm), the rotation angle defined by the connector element (0 to 360 degrees, with an axis of rotation perpendicular to the façade surface plane), and the opacity of the used material (20% or 60% with 0% being fully transparent and 100% being fully opaque). These parameters are made accessible to the optimisation algorithm and are used to generate the design iterations.

The geometry is visualised using real-time rendering for fast performance. The generative algorithm automatically adjusts the initial parameters, and each newly created geometry triggers the real-time image capturing, saving the image to an external location. Each image is then processed with FFT, which returns its power spectrum. The power spectrum is then azimuthally averaged, and PSD values are compared to the respective input natural image PSD values. The cumulative distance measured in percentage serves as the fitness value, which the optimisation solver uses to adjust the input parameters for subsequent design iterations.

The initial test was performed using the general GA. Starting with a randomly generated set of ten design solutions, the algorithm proceeds to breed them over 20 generations, producing a total of 200 design solutions. Each solution is evaluated to select the one with the lowest PSD distance from the optimisation goal image. Starting from an initial PSD distance of 36.8%, the algorithm achieved a 71.76% improvement, reducing the PSD distance to 10.39%. This result supports the thesis that the devised PSA tool can be effectively integrated within a general optimisation framework.

To assess the validity of the proposed methodology, we expanded the case study by conducting four additional experiments. Using the same geometrical parameters and design conditions, we examined the optimisation of the façade model using the other four techniques detailed in the previous section. All five algorithms were set to produce and evaluate 200 iterations each. In all five cases, the proposed PSA tool successfully informed the optimisation process. Both the RBFOpt and PSO outperformed the GA, introducing significant improvements in the PSD distance and delivering results more quickly. Although primarily designed for MOO, the COGA and SPEA still managed to deliver favourable outcomes in this single-objective optimisation context. The results from the COGA were comparable to those of the general GA, while the SPEA produced the most successful outcomes of the entire case study. TABLE 1 summarises these findings.

TABLE 1 Comparison of the results of the single-objective optimisation experiment achieved by five distinct optimisation algorithms under the same conditions.

Optimization Algorithm	Optimal solution in 200 iterations (AAPSD difference in %)	Improvement from initial state (in %)
GA	10.39	71.76
RBFOpt	9.64	73.81
PSO	7.14	80.6
COGA	10.41	71.71
SPEA	5.99	83.96

The case study produced 1000 different design iterations through five distinct optimisation techniques. The most favourable outcome was located in Generation 19 (out of 20) in the SPEA optimisation and introduced a 6-fold improvement (from 36,8% to 5.99%) from the initial unoptimised geometry. The initial geometry, the optimised geometry projections and the natural goal image, and their respective power spectra are displayed in FIG 6., along with a rendered 3D model of the structure. The design of the structure is automatically optimised to align with the natural phenomenon, not directly in the spatial domain, but through the statistics of the frequency domain, which have proven impact on visual perception and comfort. The algorithm produces many possible design solutions, and each of them is analysed for power spectrum similarity with the natural image. Any of these design solutions could be selected by the objective value but also by the subjective decision of the designer, which maximises the freedom and flexibility of the design process.

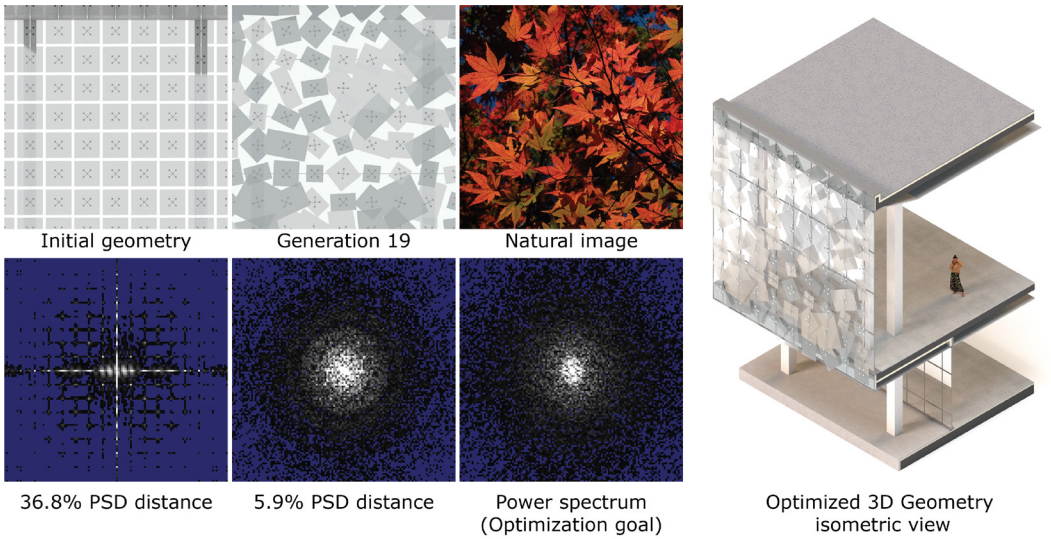

FIG. 6 Single objective optimisation experiment - initial and optimised geometry, optimisation goal - power spectrum analysis results.

3.2 MULTI-OBJECTIVE OPTIMISATION EXPERIMENT

In the second, more complex experiment, the linear structural analysis was implemented to improve structural performance and PSD distance simultaneously. This time, an interlocked timber façade structure model was chosen that could be analysed for PSD difference from a natural image in the same manner as in the first experiment, but also for structural safety based on the finite element method with linear analysis performed by our custom software tool.

An 8 by 8 meters partial model of the façade with 108 linear structural elements is studied for the MOO experiment. The initial geometry features two layers of timber frame structures, spaced 600 mm apart, interconnected by horizontal timber elements that are evenly distributed at a distance of 1300 mm in both directions, forming a 6 by 6 planar array. Optimisation parameters are the locations of the connection points (able to shift from their initial positions by 260 mm in both axes), the length of the timber element in the two layers (from 2500 to 5500 mm), and the angle of their rotation (limited -50 to 20 degrees, with an axis of rotation perpendicular to the façade surface plane, so as to introduce some distinct directionality in the power spectrum of the structure). The minimum and maximum lengths of the linear timber elements are also limited to prevent the generation of excessively long elements prone to buckling. With different lengths and rotations, different intersection points between timber elements occur, so the algorithm automatically divides the elements into their sub-parts. Elements exceeding the 8 by 8 meters bounds of the studied model are automatically trimmed.

The generated line elements are used for the structural analysis of the façade. The supposed structural timber material is Japanese cedar tree. A square cross-section of 160 by 160 mm was determined suitable for the structure and is set for the analysis of all timber elements. Support points are the lower and upper horizontal boundary points of the façade structure. The weight of the elements is measured from their volume and the density of the proposed material. The area of the timber structure is also calculated so that the appropriate wind load can be applied to it. A wind of 34 m/s speed or horizontal load of 100 kgf/m2 is assumed for the sake of the experiment. The calculation happens in each generation and is sent to the structural analysis program

through a custom-programmed Grasshopper interface. Each change in the geometry triggers the plugin, which initiates an instance of the software program, which then performs FEM analysis. The analysis results are then sent back to Grasshopper, allowing the optimisation loop to continue running automatically.

Our FEM software tool calculates the safety ratio of each linear element in accordance with the Japanese structural safety code, with values under 1.0 considered safe and any with values over 1.0 considered critical for structural safety. This ratio is then visualised with a colour scale for easier visual understanding. Elements with a safety ratio under 0.2 are blue, 0.2-0.5 – green, 0.5-0.6 yellow, 0.6-0.99 orange, and the critical elements with a value of 1.0 or over are coloured in red. As the optimisation loop runs, the algorithm seeks geometry with both smaller differences in the AAPSD values and a smaller maximal safety ratio value. Any structure with a maximal safety ratio of over 1.0 can be considered unsafe under the supposed wind load and, therefore, unsuitable to build.

To support the validity of the initial results and ensure repeatability, the experiment was again performed using multiple algorithms. The two algorithms selected for MOO – COGA and SPEA – were tasked with generating 1000 solutions each. In both cases, the optimisation managed to find solutions with significant improvements in the PSD while simultaneously meeting the structural safety objective calculated by FEM. The results are summarised in TABLE 2.

TABLE 2 Comparison of the results of the multi-objective optimisation experiment achieved by two distinct optimisation algorithms under the same conditions.

Optimization Algorithm	Pareto front solution in 1000 iteration		Improvement from initial state (in %)
	AAPSD difference in %	Safety ratio	
COGA	9.27	0.92	68.58
SPEA	5.65	0.93	80.85

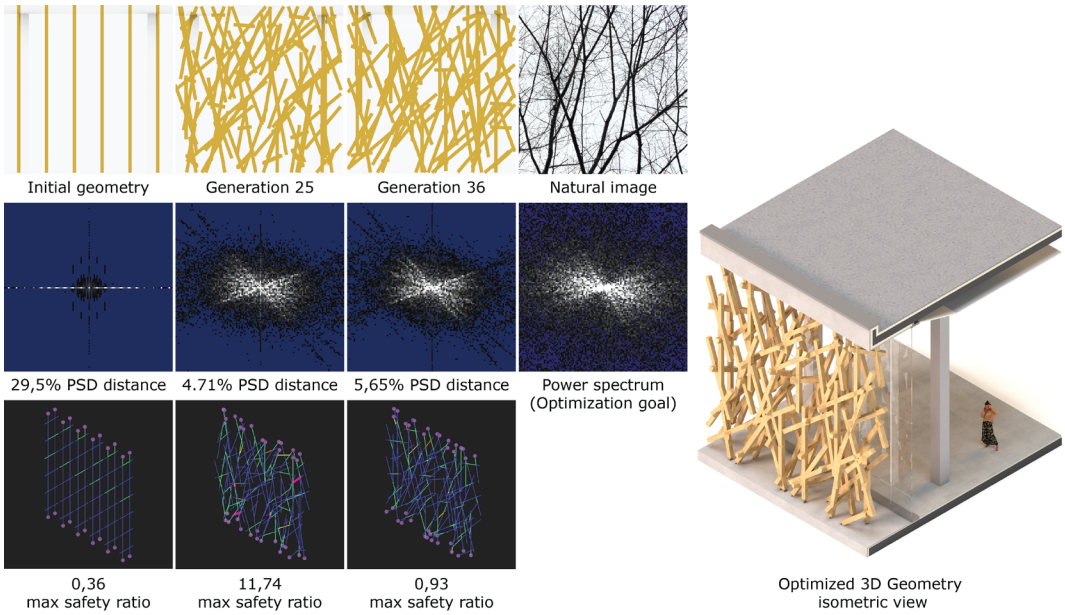

FIG. 7 Multi-objective optimisation experiment - initial and optimised geometry, optimisation goal - power spectrum and structural analysis results.

The most favourable solution in terms of PSD, from the 2000 solutions generated by the two experiments in this case study, was again produced by the SPEA. FIG 7 illustrates key moments of the optimisation process, showcasing the initial geometry of the façade structure, two samples of Generation 25, and Generation 36, and their respective power spectra and safety ratio colours of each of their structural elements calculated by the external FEM tool, as well as the natural goal image (which in this case is an image of multiple tree branches overlapping) and its power spectrum. By Generation 25, we can already observe a significant decrease in the distance between the PSD of the generated geometry and the PSD of the natural goal image (from 29,5% to 4,71%). However, the geometry remains structurally unstable with 15 critical elements and a maximum safety ratio value of 11,74. As the optimisation loop advances with the goal to reduce both values, each consecutive generation is based on the best-performing solutions of the previous one, which is why by Generation 36, a somewhat similar overall geometry can still be observed; however, the number of structurally critical elements is reduced to zero with a maximum safety ratio value of 0,93, which renders the structure safe to build. As expected, the percentage of the PSD difference slightly increased to 5.65%, which is a reasonable trade-off and renders the final solution best considering both optimisation goals.

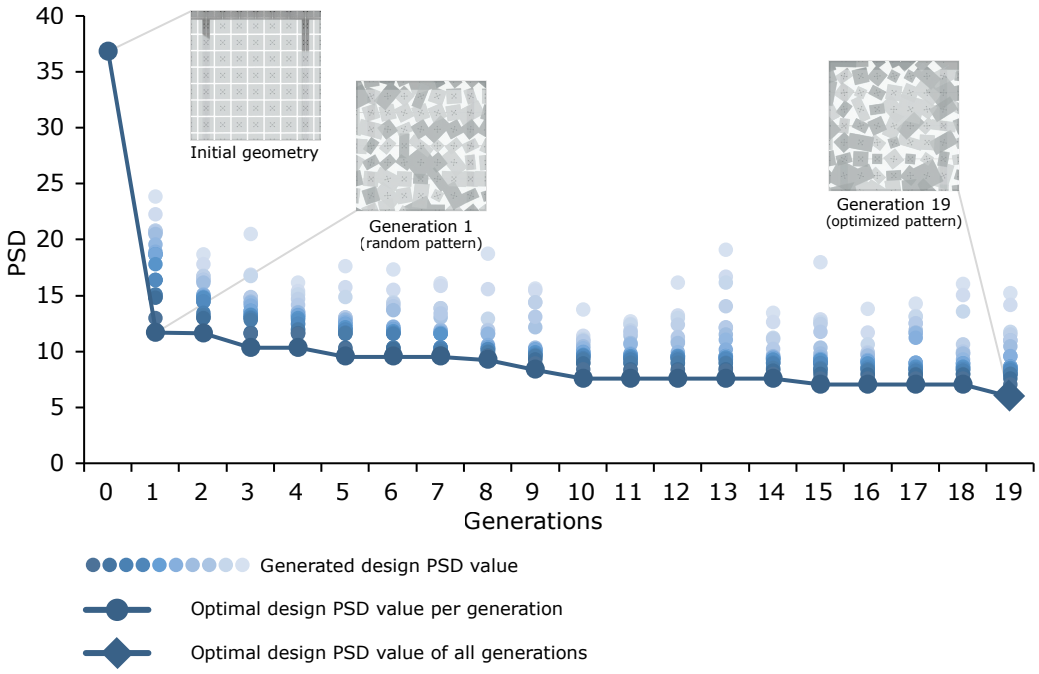

FIG. 8 Single objective optimisation experiment results graph.

4 RESULTS

Considering the data gathered from the presented experiments, we can conclude that PSA can be successfully integrated into façade design optimisation. FIG 8. shows the improvement of the façade structure in the single-objective optimisation experiment from the initial shape to Generation 19.

The generation numbers are plotted on the horizontal axis, and the PSD results from every ten solutions of each generation are plotted on the vertical axis. The line graph connects the lowest distance values, thus illustrating the improvement of the results over each consecutive generation. We can deduct that the mathematical randomness function used for the initial ten solutions in Generation 1 provides results already much closer to those of the natural image goal; however, by continuing the analysis and optimisation loop, a further improvement can be observed to reach a final result of a structure with a PSD distribution of 2 times more similar to the natural input image used as the optimisation goal.

FIG. 9 shows the data from the multi-objective optimisation experiment. Two graphs with the result values for PSD difference and Safety ratio calculation are overlayed with the line graphs representing both values of the optimal solution in the Pareto front in each generation. Fluctuation can be observed in the optimal results through the optimisation process as the algorithm seeks a solution that satisfies both objectives. By Generation 25, the best result of 4.71% in regard to PSD distance was achieved, but the safety ratio value of this solution is 11,74, which renders it unsafe to build. In Generation 39, the optimisation reaches a solution that satisfies the structural safety criterium with a maximum safety ratio of 0.93 while keeping a low PSD distance value of 5,65% from the input natural image set as the optimisation goal.

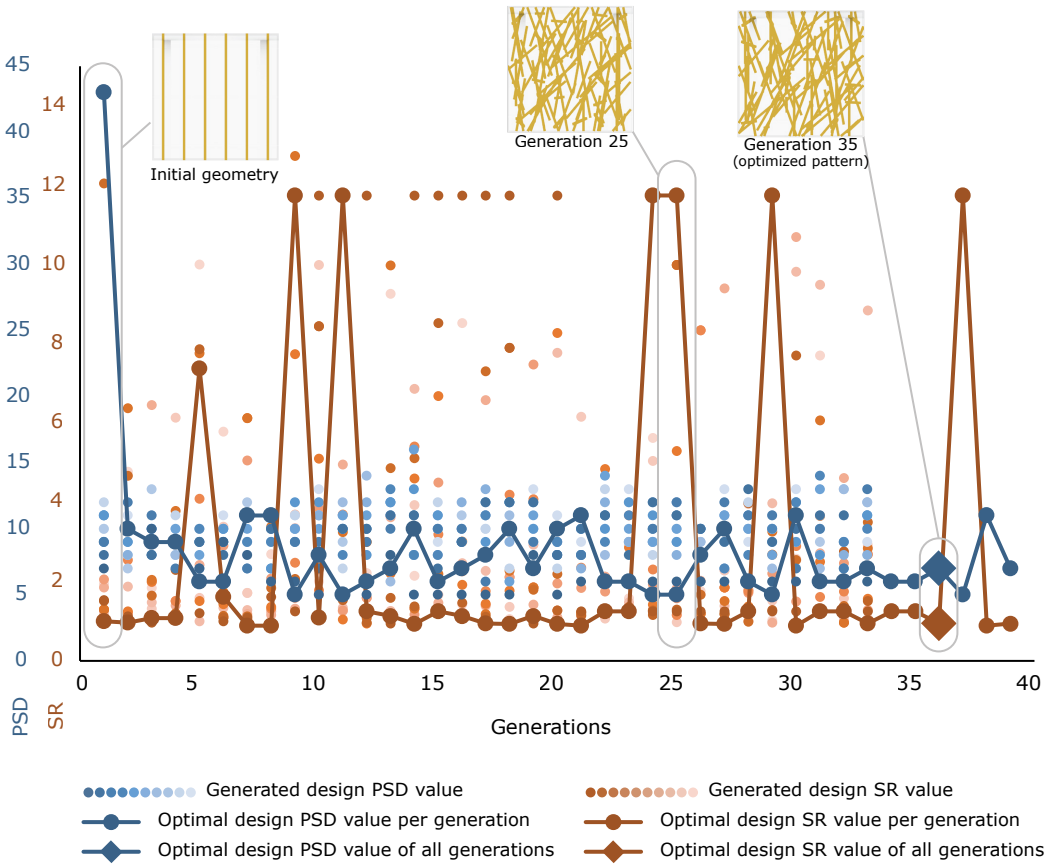

FIG. 9 Multi-objective optimisation experiment results graph

5 CONCLUSIONS AND FUTURE WORK

From the experiments presented here, it can be concluded that power spectrum analysis can be effectively employed to optimise parametrically generated façade geometry. This method, grounded in established digital signal processing techniques and computational design morphogenesis, facilitates the conception of artificial structures that are objectively similar to natural ones without copying them directly. This approach may present a novel way for natural form-finding in façade design and engineering, different from the traditional biomorphic approach, which counts on visual similarity in the spatial domain. The power spectrum density distance calculation can effectively be used to assess façade projections' spectral similarity to a selected natural image goal. Generative design through metaheuristic and model-based algorithms can make use of this computation to automatically optimise geometry and provide an extensive array of design solutions. This method can be combined with other structural analysis methods, such as the Finite Element Method, to create a multi-objective optimisation technique.

In the future development of this research, we aim to include other types of analysis in the multi-objective optimisation workflow. Daylighting analysis, view optimisation, and sun glare mitigation are all suitable objectives that could be combined with power spectrum analysis to pursue efficient, intelligent, comfortable, and aesthetically pleasing design solutions.

We will explore even more natural phenomena and expand our catalogue of natural images with power spectra suitable for optimisation goals. By expanding the natural image database, we can base the optimisation on more statistical data. Three-dimensional Fast Fourier transform may be utilised in the power spectrum analysis of spatial structures.

References

AGC. (2014). Technical Specifications – Leoflex(TM).

Bak, P., Tang, C., & Wiesenfeld, K. (1988). Self-organized criticality. *Phys. Rev. A, 38*(1), 364-374. doi:https://doi.org/10.1103/PhysRevA.38.364

Bonham, C. R., & Parmee, I. C. (2004, 4 2). Developments of the cluster oriented genetic algorithm (COGA). *Engineering Optimization, 36*(2), 249-279. doi:10.1080/03052150410001650160

Brigham, E. O. (1988). *The fast Fourier transform and its applications.* New Jersey: Prentice-Hall Inc.

Choe, B., & Sato, J. (2016). Transparent Structures. *104th ACSA Annual Meeting Proceedings, Shaping New Knowledges.* Association of Collegiate Schools of Architecture. Retrieved 5 7, 2023, from https://www.acsa-arch.org/chapter/transparent-structuresthis-methodology-encouraged-the-fluid-adaptive-growth-of-the-structures-from-cellularmodule-based-models-to-a-full-scale-installation-the-spirit-of-play-and-investigation-wa/

Cichocka, J. M., Browne, W. N., & Rodriguez, E. (2017). Optimization in the Architectural Practice - An International Survey. *CAADRIA 2017: Protocols, Flows, and Glitches*, (pp. 387-396). Suzhou, China. doi:10.52842/conf.caadria.2017.387

Cichocka, J. M., Migalska, A., Browne, W. N., & Rodriguez, E. (2017). SILVEREYE – The Implementation of Particle Swarm Optimization Algorithm in a Design Optimization Tool. In G. Çağdaş, M. Özkar, L. F. Gül, & E. Gürer (Eds.), *Computer-Aided Architectural Design. Future Trajectories* (Vol. 724, pp. 151-169). Singapore: Springer Singapore. doi:10.1007/978-981-10-5197-5_9

Cooley, J. W., Lewis, P. A., & Welch, P. D. (1969). The Fast Fourier Transform and Its Applications. *EEE Transactions on Education, 12*(1), 27-34. doi:doi: 10.1109/TE.1969.4320436.

Costa, A., & Nannicini, G. (2018, 12). RBFOpt: an open-source library for black-box optimization with costly function evaluations. *Mathematical Programming Computation, 10*(4), 597-629. doi:10.1007/s12532-018-0144-7

David, S. V., Vinje, W. E., & Gallant, J. L. (2004). Natural Stimulus Statistics Alter the Receptive Field Structure of V1 Neurons. *Journal of Neuroscience, 24*(31), 6991-7006. doi:10.1523/JNEUROSCI.1422-04.2004

Fernandez, D., & Wilkins, A. (2008). Uncomfortable Images in Art and Nature. *Perception, 37*, 1098 - 1113. doi:10.1068/p5814

Field, D. J. (1987). Relations between the statistics of natural images and the response properties of cortical cells. *Journal of the Optical Society of America. A, Optics and image science, 4*(12), 2379–2394. doi:https://doi.org/10.1364/josaa.4.002379

Gircys, M., & Ross, B. J. (2019). Image Evolution Using 2D Power Spectra. *Complexity, 2019*, 21. doi:https://doi.org/10.1155/2019/7293193

Gisiger, T. (2001). Scale invariance in biology: coincidence or footprint of a universal mechanism? *Biological Reviews*, 161-209. doi:https://doi.org/10.1017/S1464793101005607

Graham, D. J., & Field, D. J. (2007). Statistical regularities of art images and natural scenes: spectra, sparseness and nonlinearities. *Spatial vision, 21*(1-2), 149–164. doi:10.1163/156856807782753877

Hagerhall, C. M., Purcella, T., & Taylor, R. (2004). Fractal dimension of landscape silhouette outlines as a predictor of landscape preference. *Journal of Environmental Psychology, 24*(2), 247–255. doi:10.1016/j.jenvp.2003.12.004

Harding, J., & Brandt-Olsen, C. (2018, 6). Biomorpher: Interactive evolution for parametric design. *International Journal of Architectural Computing, 16*(2), 144-163. doi:10.1177/1478077118778579

Heusler, W., & Kadija, K. (2018). Advanced design of complex façades. *Intelligent Buildings International*, 220-233. doi:10.1080/17508975.2018.1493979

Huang, Y., & Niu, J.-l. (2016). Optimal building envelope design based on simulated performance: History, current status and new potentials. *Energy and Buildings, 117*, 387-398. doi:https://doi.org/10.1016/j.enbuild.2015.09.025.

Juricevic, I., Land, L., Wilkins, A., & Webster, M. (2010). Visual discomfort and natural image statistics. *Perception, 39*, 884-99. doi:10.1068/p6656.

Kaplan, S., Kaplan, R., & Wendt, J. (1972). Rated preference and complexity for natural and urban visual material. *Perception & Psychophysics, 12*, 354–356. doi:10.3758/BF03207221

Kengo Kuma and Associates. (2013). Sunny Hills Japan. Aoyama, Tokyo, Japan. Retrieved from Kengo Kuma and Associates.

Ko, W., Kent, M., Levitt, B., & Betti, G. (2021). A Window View Quality Assessment Framework. *LEUKOS, 18*, 1-26. doi:10.1080/15502724.2021.1965889.

Larson, G. W., & Shakespeare, R. (1998). *Rendering with Radiance.* Michigan: Morgan Kaufmann.

Matusiak, B., & Klöckner, C. (2015). How we evaluate the view out through the window. *Architectural Science Review, 59*, 1-9. doi:10.1080/00038628.2015.1032879

Melmer, T., Amirshahi, S. A., Koch, M., Denzler, J., & Redies, C. (2013). From regular text to artistic writing and artworks: Fourier statistics of images with low and high aesthetic appeal. *Frontiers in human neuroscience*(7), 106. doi:10.3389/fnhum.2013.00106

Nagy, G., & Osama, N. (2016). Biomimicry, an Approach, for Energy Effecient Building Skin Design. *Procedia Environmental Sciences, 34*, 178-189. doi:10.1016/j.proenv.2016.04.017

Nannicini, G. (2021, 2 11). On the implementation of a global optimization method for mixed-variable problems. *Open Journal of Mathematical Optimization*, 1-25. doi:10.5802/ojmo.3

O'Hare, L., & Hibbard, P. (2011). Spatial frequency and visual discomfort. *Vision research, 51*, 1767-77. doi:10.1016/j.visres.2011.06.002.

Oliva, A., Torralba, A., Guerin-dugue, A., & Herault, J. (1999). Global Semantic Classification of Scenes using Power Spectrum Templates. *Challange of Image Retrieval.* New Castle. doi:10.14236/ewic/CIR1999.9

Oliveira Santos, F., Louter, C., & Correia, J. R. (2018). Exploring Thin Glass Strength Test Methodologies. *Challenging Glass Conference Proceedings*, (pp. 713-724). doi:https://doi.org/10.7480/CGC.6.2192

Olshausen, B., & Field, D. (1996). Emergence of simple-cell receptive field properties by learning a sparse code for natural images. *Nature, 381*, 607-9. doi:10.1038/381607a0

Párraga, C. A., Troscianko, T., & Tolhurst, D. (2000). The human visual system is optimised for processing the spatial information in natural visual images. *Current biology*, 35-8. doi:10.1016/S0960-9822(99)00262-6

Pastore, L., & Andersen, M. (2022). The influence of façade and space design on building occupants' indoor experience. *Journal of Building Engineering, 46*. doi:10.1016/j.jobe.2021.103663

Redies, C., Hasenstein, J., & Denzler, J. (2007). Fractal-like image statistics in visual art: similarity to natural scenes. *Spatial Vision, 21*((1-2)), 137–148. doi:10.1163/156856807782753921

Ruderman, D. L. (1994). The statistics of natural images. *Network: Computation in Neural Systems, 5*(4), 517-548. doi:doi:10.1088/0954-898X_5_4_006

Ruderman, D. L., & Bialek, W. (1994, Aug). Statistics of natural images: Scaling in the woods. *Phys. Rev. Lett., 73*(6), 814--817. doi:https://link.aps.org/doi/10.1103/PhysRevLett.73.814

Rutten, D. (2013). Galapagos: On the Logic and Limitations of Generic Solvers. *Architectural Design, 83*(2), 132-135. doi:10.1002/ad.1568

Sato, J. (2010). *Jun Sato: Items in Jun Sato Structural Engineers.* Tokyo, Japan: INAX Publishing.

Schaaf, A. v., & Hateren, J. v. (1996). Modelling the Power Spectra of Natural Images: Statistics and Information. *Vision Research, 36*(17), 2759-2770. doi:https://doi.org/10.1016/0042-6989(96)00002-8.

Simoncelli, E. P., & Olshausen, B. A. (2001). Natural image statistics and neural representation. *Annu. Rev. Neurosci., 24*, 1193-1216. doi:10.1146/annurev.neuro.24.1.1193. PMID: 11520932

Spehar, B., & Taylor, R. (2013). Fractals in Art and Nature: Why do we like them? *Proceedings of SPIE - The International Society for Optical Engineering.* doi:10.1117/12.2012076

Spehar, B., Clifford, C. W., Newell, B. R., & Taylor, R. P. (2003). Universal aesthetic of fractals. *Computers & Graphics, 27*(5), 813–820. doi:https://doi.org/10.1016/S0097-8493(03)00154-7.

Stals, A., Jancart, S., & Elsen, C. (2016). How Do Small and Medium Architectural Firms Deal with Architectural Complexity? A Look Into Digital Practices. *eCAADe 2016: Complexity & Simplicity*, (pp. 159-168). Oulu, Finland. doi:10.52842/conf.ecaade.2016.2.159

Szendrő, P., Vincze, G., & Szasz, A. (2001). Pink-noise behaviour of biosystems. *European Biophysics Journal, 30*, 227-231. doi:https://doi.org/10.1007/s002490100143

Tabadkani, A., Roetzel, A., Li, H. X., & Tsangrassoulis, A. (2021). Daylight in Buildings and Visual Comfort Evaluation: the Advantages and Limitations. *Journal of Daylighting, 8*, 181-203. doi:10.15627/jd.2021.16

Tolhurst, D., Tadmor, Y., & Chao, T. (1992). Amplitude spectra of natural images. *Ophthalmic and Physiological Optics, 12*, 229-232. doi:10.1111/j.1475-1313.1992.tb00296.x

Torralba, A., & Oliva, A. (2003). Statistics of natural image categories. *Network: Computation in Neural Systems*, 391-412. doi:10.1088/0954-898X_14_3_302

Ulrich, R. S. (1983). Aesthetic and affective response to natural environment. In *Behavior and the natural environment* (pp. 85–125). New York: Plenum Press. doi:10.1007/978-1-4613-3539-9_4

Verbeeck, K. (2006). *Randomness as a Generative Principle in Art and Architecture.* Massachusetts Institute of Technology. Retrieved 5 20, 2023, from https://dspace.mit.edu/handle/1721.1/35124

Vierlinger, R., & Hofmann, A. (2013). A Framework for Flexible Search and Optimization in Parametric Design. *Design Modelling Symposium.* Berlin. doi:10.13140/RG.2.1.1516.8727

Vincent, J. (2009). Biomimetic patterns in architectural design. *Architectural Design*, 74-81. doi:10.1002/ad.982

Wienold, J., & Christoffersen, J. (2006). Evaluation methods and development of a new glare prediction model for daylight environments with the use of CCD cameras. *Energy and Buildings, 38*, 743-757. doi:10.1016/j.enbuild.2006.03.017.

Wortmann, T., & Nannicini, G. (2016). Black-Box Optimisation Methods for Architectural Design. *CAADRIA 2016: Living Systems and Micro-Utopias - Towards Continuous Designing*, (pp. 177-186). Melbourne, Australia. doi:10.52842/conf.caadria.2016.177

Zitzler, E. (1999). *Evolutionary Algorithms for Multiobjective Optimization: Methods and Applications.* Zurich: Swiss Federal Institute of Technology.

Zitzler, E., & Thiele, L. (1998). *An Evolutionary Algorithm for Multiobjective Optimization: The Strength Pareto Approach.* Zurich: Swiss Federal Institute of Technology.

Integration of a 3D-Printed Façade Unit in a Curtain Wall System: Prototyping and Assessment

Francesco Milano[1*], Ringo Perez Gamote[2], Nik Eftekhar Olivo[3], Valeria Piccioni[4], Po Yen Chen, Caitlin Gallagher, Arno Schlueter[4], Benjamin Dillenburger[3], Andreas Luible[2], Fabio Gramazio[1], Matthias Kohler[1*]

* Corresponding author: milano@arch.ethz.ch
1 Gramazio&Kohler Research, ITA, ETH Zurich, Switzerland
2 HSLU, Luzern, Switzerland
3 Digital Building Technologies, ITA, ETH Zurich, Switzerland
4 Architecture and Building Systems, ITA, ETH Zurich, Switzerland

Abstract

Plastic materials, known for their lightweight, formability, transparency, and durability, are the state of the art for building façade applications. Recent advances in Large-Scale Robotic 3D Printing (LSR3DP) have enabled the production of bespoke, translucent façade components. While research has largely focused on individual panel properties, there is a gap in developing a comprehensive strategy for integrating these components into a complete façade system. This paper explores the potential of combining custom 3D-printed façade elements with standard curtain wall connections. Quantitative analysis involves constructing and testing a 1 m x 1 m LSR3DP façade assembly for air and water tightness, benchmarking its performance against a conventional curtain wall. Qualitatively, the approach is evaluated through a mock-up, highlighting the architectural possibilities of blending standard and non-standard façade elements. The findings demonstrate that this hybrid system is both technically viable and opens new design possibilities for architects and façade engineers.

Keywords

Façade design, 3D printing, Computational design, Digital fabrication

DOI

http://doi.org/10.47982/jfde.2024.325

1 INTRODUCTION

1.1 BACKGROUND

Plastics are a broad set of synthetic materials that use polymers as the main ingredient (Engelsmann et al., 2010). They are characterised by specific properties – such as lightweight, good weather resistance, high strength, and excellent forming characteristics – which make them particularly interesting for building façade applications (Herzog et al., 2004). Plastic façades have been the state of the art in building and construction since the 1950s and remain a focus of ongoing innovation. Over the past decade, different research projects emerged exploring the possibility of using 3D printing to produce building façade components (Leschok et al., 2023) (Naboni & Jakica, 2022) (Mungenast, 2019) (Fleckenstein et al., 2023). Within this field, a research subset consists of using Large-Scale Robotic 3D Printing (LSR3DP) to produce bespoke, translucent façade components out of plastic (Seshadri et al., 2021) (Cheibas, 2023) (Cheibas, Perez Gamote, et al., 2023) (Cheibas, Piccioni, et al., 2023) (Cheibas, Lloret-Fritschi, et al., 2023) (Piccioni, Leschok, Lydon, et al., 2023) (Piccioni, Leschok, Grobe, et al., 2023). LSR3DP consists of a fused deposition modelling (FDM) system composed of a material extruder mounted on the flange of a 6-axis robotic arm. This technology can produce large-scale components and is characterised by great kinematic possibilities compared to cartesian alternatives (Al Jassmi et al., 2018). Compared to other plastic processing techniques (standard extrusion, moulding, cutting, and milling), LSR3DP entails multiple advantages. (i) It can produce bespoke geometries at no extra cost. (ii) It is fully automatic and, therefore, not labour-intensive. (iii) It is materially effective, being additive rather than subtractive. (iv) It is suitable for producing complex geometries (Strauß, 2013). Different experiments on translucent LSR3DP façade components have already been conducted. Next to the opportunity to expand design possibilities and create novel architectural effects, researchers have been focusing on how this technology can be used to foster efficient façade design, creating highly integrated systems tailored to specific climatic contingencies. In most cases, parameters such as the global geometry or the level of transparency are tuned to optimise solar gain, light transmission, and glare, while the internal articulation is designed to regulate heat and load transfer.

1.2 STATE OF THE ART

Seshadri et al. propose an experimental methodology to optimise the outside geometry of a façade module in relation to solar radiation (Seshadri et al., 2021). The process is based on parametric design, daylight simulation, and topology optimisation. Piccioni et al. explore the possibility of selectively admitting or blocking solar radiation in a translucent polymeric panel by adjusting different parameters in the 3D printing process. The study demonstrates that by varying printing speed, printing temperature, and layer height, optical properties like different levels of transparency, translucency, and haze can be obtained (Piccioni, Leschok, Grobe, et al., 2023). Piccioni et al. also explore the effect of a 3D-printed component's internal geometry on its thermal insulation properties. The study demonstrates how thermal transmittance changes (ranging from 1.7 to 1 W/m^2K) as a function of the internal cavity distribution and size (Piccioni, Leschok, Lydon, et al., 2023). Cheibas et al. propose a conceptual workflow in which the global geometry of a façade, 3D printed out of translucent thermoplastics, is tailored to integrate environmental parameters (Cheibas, Lloret-Fritschi, et al., 2023). Another study demonstrates how different 3DP patterns produced on the panel's outside surface can influence the levels of translucency and, therefore, be used to create bespoke daylight and shading effects (Cheibas, Piccioni, et al., 2023).

1.3 RESEARCH GAP

To date, studies on translucent LSR3DP façades have primarily concentrated on designing and evaluating individual façade components, but more development needs to be done in producing a comprehensive façade construction strategy. In particular, limited developments exist on the interface between neighbouring components and how such a façade would coherently integrate into the larger building ecosystem (load-bearing structure, slabs, roof). Cheibas et al. explored an integrated snap connection strategy inspired by classic unitised curtain walls (Cheibas, Perez Gamote, et al., 2023) (Cheibas, 2023). The exploration was followed by producing a façade prototype, which was tested for air permeability and water tightness. The prototype didn't meet the requirements of the current standards and could not be classified. From a fabrication perspective, integrating performative male-female connections along the edges of an LSR3DP panel is challenging due to the technology's low resolution and the impossibility of creating temporary supports. The problem of how to sensibly combine translucent LSR3DP façade panels in a coherent façade assembly is, therefore, still unsolved. The present work aims to find an answer to this particular question.

1.4 OVERARCHING APPROACH

Connections play a crucial role in a building façade, as they must fulfil a wide array of delicate functions, such as ensuring waterproofing and air tightness, preventing condensation, avoiding thermal bridges, accommodating thermal dilatation and movements of the base structure. To meet high-quality standards, the building industry has progressively developed highly engineered solutions based on dry-mounted components (Knaack et al., 2007). The hypothesis presented in this article is that some of these solutions can be used to assemble translucent LSR3DP façade panels. This pragmatic approach "liberates" the 3D-printed component from the burdensome task of integrating performative connections and delegates the functionality to a highly tested and specifically designed solution. The present work focuses on one particular solution, namely a standard post and beam curtain wall system. The post and beam curtain wall system is traditionally used in combination with infill panels (either IGUs or opaque panels). It usually includes (i) a structure consisting of mullions and transoms, (ii) a clamping mechanism made of two aluminium profiles screwed to one another, (iii) a set of EPDM gaskets, which interpose between the aluminium profiles and the infill panels (FIG. 1A). In the present framework, the infill panels are substituted by bespoke LSR3DP panels (FIG. 1B). The result is a hybrid façade, which combines the customisation possibilities of 3DP with the performance reliability of standard curtain wall systems. For simplicity, from now on, this concept will be addressed as "3D printed Curtain Wall System" (3DPCWS).

FIG. 1 A) Standard post and beam curtain wall system B) Initial prototype constructed to assess the idea of combining standard curtain wall connections and LSR3DP façade panels.

This concept has been assessed by performing two different and complementary experiments.

(i) The first experiment aimed to evaluate the 3DPCWS from a functional standpoint. In particular, it aims to understand whether the standard curtain wall connection system still upholds its performance when the traditional infill panel is replaced with a bespoke 3D-printed component. Standard systems are meant to be combined with panels whose surfaces are flat. The gasket is designed to compress evenly against the flat panel under the force of the pressure plate, reducing air infiltration and preventing water penetration. A 3D-printed surface, however, features a certain rugosity derived from the deposition of the material, one layer on top of the other. As a consequence, if the flexibility of the gasket is unable to fill the groves of the layered surface, air and water can penetrate, compromising the performance of the façade itself. This possibility has been verified through an experiment consisting of constructing and testing a 1 m^2 façade mock-up. The mock-up has been tested for air permeability (SN EN 12153:2000 (*EN 12153*, 2000)) and water tightness (SN EN 12155:2000 (*EN 12155*, 2000)) in the facilities of Lucerne University of Applied Science and Arts (HSLU). Other technical requirements, such as wind and fire resistance, are not addressed in this study, as they fall within the capabilities of 3D printing technology. Wind resistance can be managed through an infill panel design with sufficient structural strength, while fire resistance is primarily determined by the properties of the materials selected. The Testing Laboratory Building Envelope and Civil Engineering of Lucerne University of Applied Sciences and Arts is authorised by the Swiss accreditation body (STS 0209) for air permeability and water tightness tests according to SN EN 13830:2003 (*EN 13830*, 2003). The experiment aims for a quantitative result.

(ii) The second experiment aimed to evaluate the 3DPCWS from an architectural perspective. It consists of developing a design case study that is able to express the system design potential. The case study corresponds to a single-storey building façade. It materialises in a large-scale demonstrator that integrates a façade mock-up and an enclosed space that offers the visitor an architectural experience. The development of the case study involved (i) the design of a timber substructure, (ii) the design of two LSR3DP façade panels, (iii) the façade connection detailing using different standard curtain wall solutions, (iv) the fabrication of the different components, (v) the demonstrator assembly. The process of developing a design case study aims to produce a qualitative rather than quantitative result.

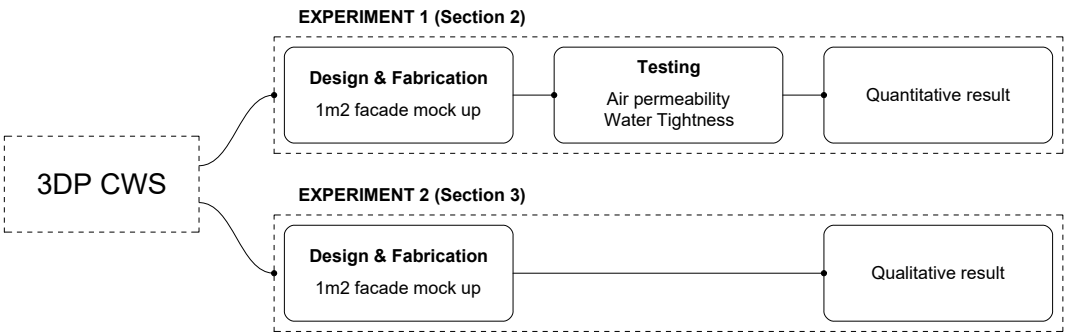

FIG. 2 Diagram summarising the process designed to validate the overarching approach.

2 EXPERIMENT 1 – AIR PERMEABILITY AND WATER TIGHTNESS TEST

2.1 METHOD

The following section describes the experiment that has been designed to assess the 3DPCWS from a functional perspective. The experiment tests the connections of a façade assembly for air permeability and air tightness. The aim of the test is not to give a resolutive answer but rather a preliminary indication of whether this approach can be used for industrial applications. Based on this study, further tests will need to be conducted to validate solutions developed for specific architectural projects. The following chapters include a description of the test specimen (2.1.1), a description of the testing facility (2.1.2), and information about the testing procedure (2.1.3 - 2.1.4).

2.1.1 LSR3D printed specimen and façade assembly

Air permeability and water tightness tests are generally performed on non-standard façade solutions to allow their use in specific architectural projects. The testing procedure – defined by SN EN 12153:2000 (*EN 12153*, 2000) and SN EN 12155:2000 (*EN 12155*, 2000) – requires testing the solution in the same configuration that will be used in the building assembly. In the present case, however, the test is not framed in the contingency of a specific architectural project but rather in a preliminary research scheme aimed at defining whether the approach has potential for architectural applications. This consideration has driven the design of the LSR3DP testing façade panel, conceived as a unitary 1 m x 1 m flat component (FIG.3A, 3B). The panel is characterised by a thickness of 50 mm, which is close to the maximum limit allowed by the selected standard curtain wall connection system (RAICO THERM+ H-I (*RAICO*, 2024)). The panel has an inside and an outside surface, separated by a folded zigzag infill, which provides structural rigidity. In the 3D printing process, the three elements that constitute the geometry emerge from one continuous toolpath. All design operations were executed using the software Rhinoceros 3D (*Rhinoceros 3D*, 2024).

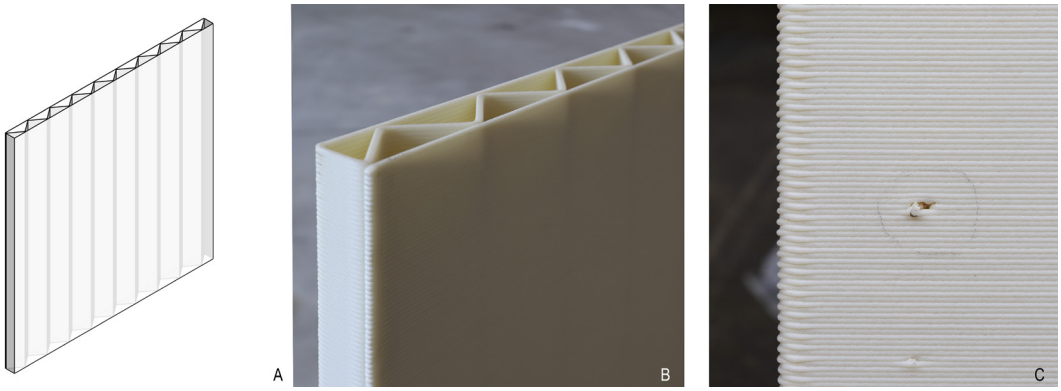

FIG. 3 A) Panel 3D model; B) 3D printed panel; C) Detail showing both the imperfection on the panel surface, corrected with silicon, and the increased rugosity on the panel's left and right edges due to material over-extrusion.

The façade panel was produced by SAEKI (*SAEKI Robotics*, 2024). The company received the panel 3D model from the author and created the robotic toolpath necessary for 3D printing. Production has been carried out using a custom-made LSR3DP set-up. The material chosen was ABS with 20% glass fibre. The choice of a non-transparent polymer was driven by wanting to 3D scan the panel after production to assess the precision of the 3D printing; an operation that would be more challenging in the case of transparent objects. The material extruder features three customisable heating zones for temperature control, which were set to 175, 190, and 225°C. The 3D printing toolpath featured a layer height of 2 mm, and the extruder material flow was tuned to achieve a 5 mm layer width. The superposition of the 3D model used for 3D printing and the one obtained through 3D scanning revealed no major deviation in the panel's global geometry. The panel surface presented minor (mm scale) imperfections due to fabrication errors (FIG. 3C). As the experiment focuses on the panel's edges interface, those imperfections were filled with a small amount of silicon to guarantee a perfectly tight panel surface. The left and right edges of the panel presented irregularities due to material over-extrusion. Although possibly harmful to the system performance, in this case, the irregularities were accepted as relatively common to the manufacturing technique and representative of LSR3DP elements (FIG. 3C).

The standard connection system selected for the experiment is RAICO THERM+ H-I (*RAICO*, 2024) (FIG. 1, FIG. 4). The system is an approved curtain wall solution specifically designed to interface the glazing with an internal load-bearing structure (steel, aluminium, timber…). Considering that the material has no influence on the experiment result, the timber option was selected for simplicity. The system features two drainage levels and pressure equalisation between the façade's interior and exterior space. It can adapt to different timber profile sizes, can be combined with panels up to 64 mm thick, and can hold panels up to 600 kg in weight. Performance-wise, combined with normal glazing, it guarantees a U value down to 0.76 W/(m^2K), air permeability classification AE (>600) according to SN EN 12152:2002 (*EN 12152:2002*, 2002), and water tightness classification RE 2100 according to SN EN 12154:1999 (*EN 12154:1999*, 1999).

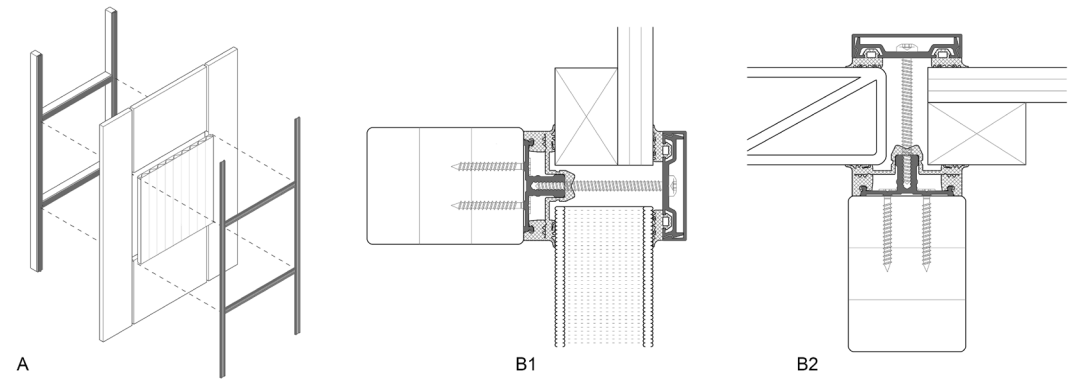

FIG. 4 A) Diagram of the façade assembly to be tested; B1) RAICO THERM+ H-I horizontal connection (transom); B2) RAICO THERM+ H-I vertical connection (mullion).

2.1.2 Description of the testing set-up

The main element of the set-up consists of a full-scale experimental rig from HSLU, which allows the testing of a façade assembly for air permeability and water tightness according to SN EN 12153:2000 (*EN 12153*, 2000) and SN EN 12155:2000 (*EN 12155*, 2000). The rig consists of a 1.5 m deep, 2 m wide

and 2.5 m high chamber. On one of the walls, the chamber has a door that allows access to the interior space for inspection. The opposite wall features a 2000 x 2500 mm opening, on which façade prototypes can be mounted and tested (FIG. 5). A system consisting of centrifugal fans, piping, and valves allows for air pressure control inside the chamber. Changeover flaps can switch the direction of the volume flow to create positive and negative test pressures. A negative test pressure in the chamber simulates the wind pressure on the outer side of the façade. In contrast, a positive test pressure in the chamber simulates wind suction on the outer side of the façade.

Outside the chamber, a water spray system is mounted, pointing at the position where the testing specimen gets installed. The system consists of spray nozzles arranged in a bar with a spacing of 400 mm. The nozzles are mounted 250 mm away from the façade and provide 120° cone-shaped water distribution. When active, the water spray system creates a constant water film on the surface of the specimen.

A set of measuring devices completes the set-up. In particular, (i) the differential pressure inside the chamber is assessed by three sensors (IDP 100, ICS Schneider Messtechnik, with measuring ranges respectively of ± 1000, ± 5000, and ± 10000 Pascal, max. deviation limit of 5% from the measured value). The sensors are located in the test chamber and are connected to the test chamber via pressure hoses so that the static pressure is determined independently of the air supply. (ii) The volume flow rate is measured by one transducer (TA 10 165 GE, measuring range 20 – 600 m^3/h, max. deviation limit of 5% from the measured value). (iii) The water flow is measured and adjusted by control valves (EP020R+MP, Belimo, measuring range 6-40 l/min, max. deviation limit of 10% from the measured value.) The measuring equipment is calibrated every two years according to the specifications of ISO 17025:2018 "General requirements for the competence of testing and calibration laboratories". The test facility is approved for accredited testing according to SN EN 13830:2003 (*EN 13830*, 2003).

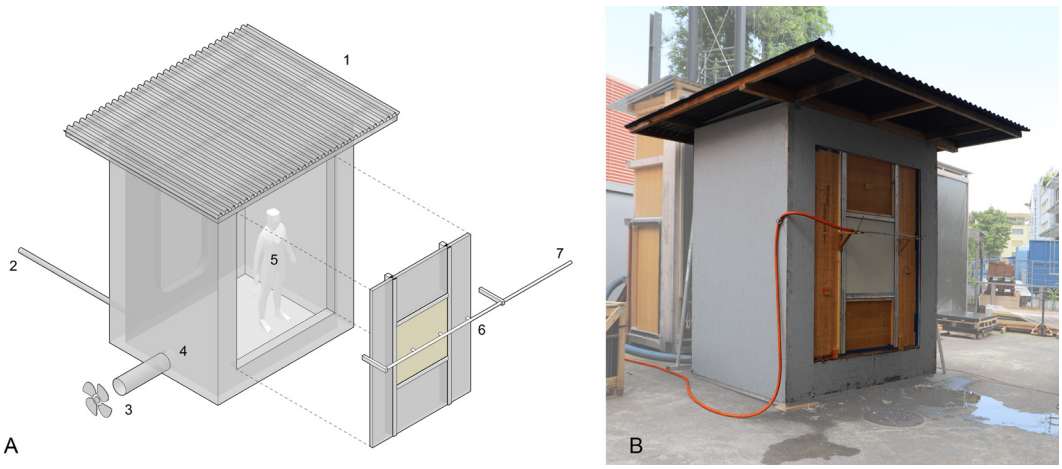

FIG. 5 A) Parts which compose the testing set-up. 1: Pressure cabine; 2: Pressure sensor; 3: Centrifugal fan; 4: Flow rate sensor; 5: Inspector; 6: Spray system; 7: Contro valve; B) Picture of the HSLU Testing Set-up in use.

The 3DP façade panel was installed in the centre of the HSLU experimental rig's opening (FIG. 5, FIG. 9A, FIG. 9B). The initial opening dimensions were adapted to the size of the panel by placing two timber mullions (GL24h, size: 60 x 100 x 2500 mm) spanning the whole aperture height, spaced centrally one meter away from one another. Among the mullions, two transoms were interposed,

also with a spacing of 1 m (GL24h, size: 60 x 100 x 945 mm). Around the panel, the aperture was closed using plywood sheets cut to size (FIG. 4). In the present configuration, consisting of continuous mullions interposed by transoms, the system is meant to channel any water seeping through the façade inside the mullions gasket and drain it through the lower aperture.

2.1.3 Air permeability test

The test was performed according to SN EN 12153:2000 (*EN 12153*, 2000). It consists of determining the airflow Q (mm^3/h), which passes through the façade assembly at specific pressure levels, and comparing it with the benchmark values defined by the standard. Before the test, three positive pressure pulses of 660 Pa are applied to stabilise the chamber; each pulse is held for a minimum of 3 seconds. The test itself consists of applying pressure inside the chamber, with sequentially increasing values corresponding to 50, 100, 150, 200, 300, 450, and 600 Pa. Each pressure level is held for a minimum time of 10 seconds. At each pressure level, the set-up allowed measuring Q_1 (m^3/h), meaning the global airflow passing through the testing chamber. This value is averaged over the measurement time and includes the airflow through façade assembly Q plus the chamber leakage Q_0. The chamber leakage was measured before starting, following the guidelines of EN 12153:2000 (*EN 12153*, 2000), which consists of performing an initial measurement after airtight-sealing the specimen. This procedure ensures that no air leakage is encountered at the junction between the plywood perimeter panels and the curtain wall system. Q is determined as Q_1-Q_0. The procedure is repeated two times, the first one with a positive pressure inside the chamber and the second one with a negative pressure (FIG. 6A). The air permeability of the façade can be assessed both in relation to the surface area of the façade fixed element (q_A) and in relation to the linear meter of closed joints (q_L). The first is calculated as:

$$q_A = Q/A = (Q_1\text{-}Q_0)/A(m^3/hm^2)$$

while the second is calculated as:

$$q_L = Q/L = (Q_1\text{-}Q_0)/L\ (m^3/hm^2)$$

A is the total specimen area, corresponding to 1 m^2, and L is the connection length, corresponding to 4 m.

The air permeability performance requirements and classifications for curtain walls are defined in the SN EN 12152:2002 (*EN 12152:2002*, 2002).

During the test, any airflow infiltration through the connections could be visualised by producing smoke at the interface between the panel and the gasket. This test was performed by a person standing inside the chamber while the pressure was applied, allowing the inspector to understand whether the filtration is uniform (i.e. structural to the system) or concentrates at specific points (i.e. due to errors during the façade assembly).

2.1.4 Water tightness test

The test was performed according to SN EN 12155:2000 (*EN 12155*, 2000). It consists of verifying that the façade is impermeable to water at specific negative pressure levels. In this case, positive pressure is not relevant, as wind suction on the façade doesn't increase the risk of water penetration (FIG. 6B). Before the test, three negative pressure pulses of 660 Pa are applied; each pulse is held for a minimum of 3 seconds. The test itself consists of two phases. First, the spraying system is activated, and the façade is completely sprayed with water for 15 min without any pressure inside the testing chamber. Second, pressure is applied inside the chamber, with sequentially increasing values corresponding to 50, 100, 150, 200, 300, 450, and 600 Pa. Each pressure level is held for a minimum time of 10 seconds. For each pressure level, an inspector inside the chamber checks whether water penetrates the assembly.

The amount of water to be sprayed is calculated as the façade element area multiplied by 2 l/(min·m^2). Therefore, the amount of water required for testing the façade assembly described above was:

$$T_{water} = 1m^2 * 2l/(min*m^2) = 2l/min$$

The water tightness performance requirements and classifications for curtain walls are defined in the SN EN 12154:1999 (*EN 12154:1999*, 1999).

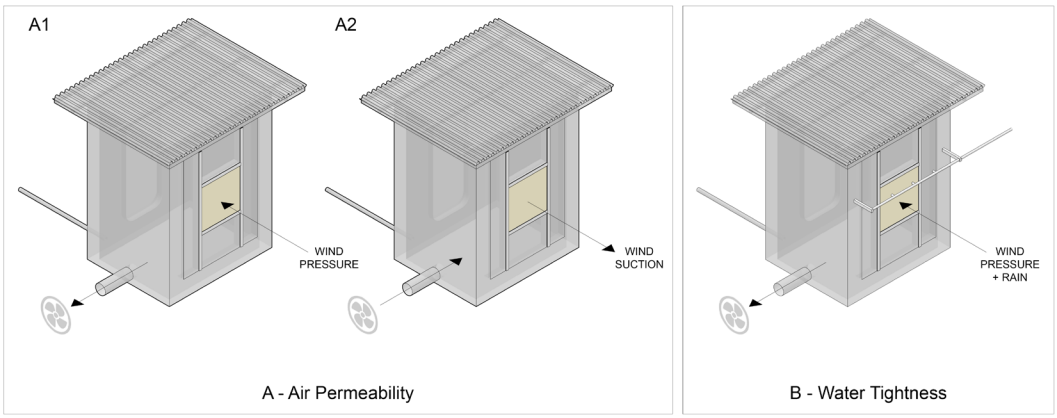

FIG. 6 Tests performed in the HSLU testing rig. A1) Air permeability with positive pressure, simulating air suction on the façade assembly; A2) Air permeability test with negative pressure, simulating wind pressure on the façade assembly; B) water tightness test with negative pressure, simulating wind pressure on the façade assembly.

2.2 RESULTS

2.2.1 Air permeability test

This chapter summarises the result of the air permeability test described in Chapter 2.1.3. The test lasted for about 24 minutes. FIG. 7 shows the progressively increasing pressure applied in the testing chamber, both in the positive and negative directions.

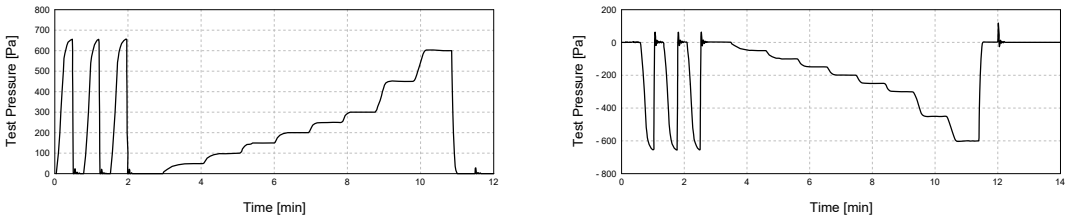

FIG. 7 A) Diagrams showing the positive pressure applied in the testing chamber progressively increasing over time. B) Diagrams showing the negative pressure applied in the testing chamber progressively increasing over time.

At specific pressure values (± 50, 100, 150, 200, 250, 300, 450, 600 Pa), the average airflow through the façade assembly Q (m^3/h) was measured. From those values, the façade permeability is derived, both in relation to the area of fixed element (q_A) and in relation to the linear meter of closed joints (q_L). Q and q_A have equal values because the specimen surface area corresponds to 1 m^2. Table 1 shows the values of Q, q_A, and q_L measured at each pressure level for both positive and negative pressure.

	Negative pressure								Positive pressure							
Test pressure [Pa]	**-600**	**-450**	**-300**	**-250**	**-200**	**-150**	**-100**	**-50**	**50**	**100**	**150**	**200**	**250**	**300**	**450**	**600**
Q (m3/h)	1.683	2.191	1.537	0.919	0.903	0.444	0.52	0	0.269	0.41	0.343	0.808	0.901	1.211	1.605	1.817
qA (m3/hm2)	1.683	2.191	1.537	0.919	0.903	0.444	0.52	0	0.269	0.41	0.343	0.808	0.901	1.211	1.605	1.817
qL (m3/hm)	0.421	0.548	0.384	0.23	0.226	0.111	0.13	0	0.067	0.103	0.086	0.202	0.225	0.303	0.401	0.454

TABLE 1 Table showing, for each positive and negative pressure level: 1) The m^3 of air flowing through the façade assembly per hour (Q). 2) The m^3 of air flowing through the façade assembly per hour relative to the façade surface area (qA). 3) The m^3 of air flowing through the façade assembly per hour reactive to the façade linear meter of closed joints (qL).

The results were assessed according to the SN EN 12152:2002 (*EN 12152:2002*, 2002), which classifies façade air permeability within four categories of increasing efficiency level (A1, A2, A3, A4). For each category, the standard defines the maximum air permeability value allowed at each pressure level. FIG. 8A, 8B, 8C, and 8D show the results in relation to the categories thresholds. To achieve a certain category classification, the value points corresponding to all pressure levels (positive and negative) have to be below the corresponding category line in the diagram. For categories A1, A2, and A3, only pressure values up to ± 150, ± 300 and ± 450, respectively, are relevant.

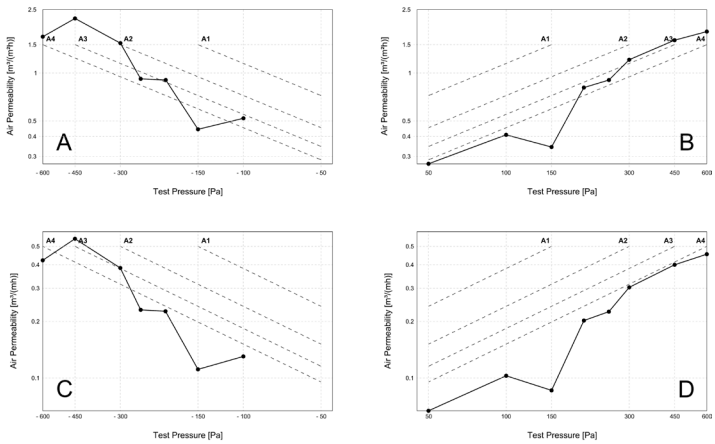

FIG. 8 Diagrams showing the results of the air permeability test in relation to the benchmark values defined by SN EN 12152:2002. A and B show qA values for negative and positive pressure, respectively. C and D show qL values for negative and positive pressure, respectively.

When evaluated with the "air flow through the area of fixed element" criteria (q_A), the façade specimen classifies as A1, as the value of 1.537 m^3/m^2h corresponding to the pressure level -300 Pa is just above the threshold for category A2, which is 1.5 m^3/m^2h. When evaluated with the "air flow through closed joints" criteria (q_L) however, the façade classifies in category A2, as all the values are below the threshold for category A2. The façade does not classify as A3, as the values corresponding to the pressure levels -300 and -450 Pa are above the A3 threshold. For q_A and q_L, the evaluation criteria resulting in the better category can be selected. Therefore, the façade specimen classifies as A2.

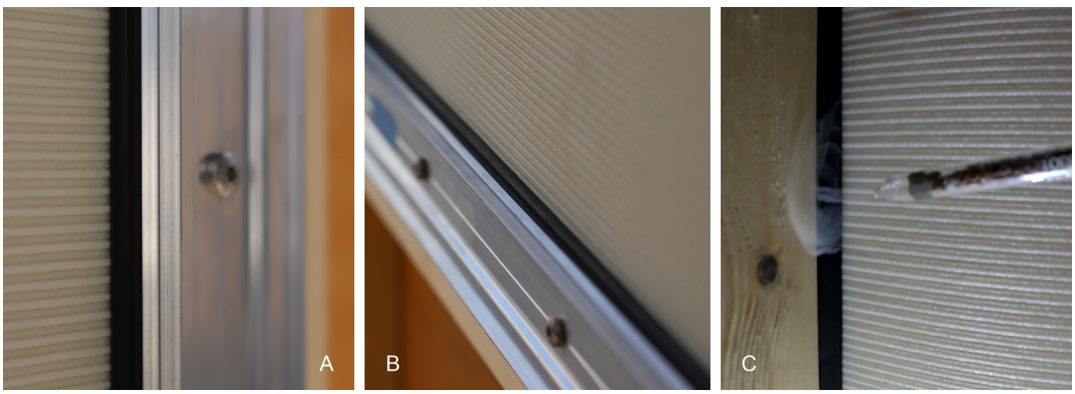

FIG. 9 A) Test vertical connection (mullion); B) A) Test horizontal connection (transom); C) Visualization of the airflow. With positive pressure, the smoke gets "sucked" through the vertical connection. This phenomenon does not occur at the horizontal connection.

During the test, the airflow through the connections was visualised by producing smoke at the interface between the 3DP panel and the gasket. At the top and bottom sides, no air movement could be observed. On the left and right edges, however, a flow in the horizontal direction was clearly visible (FIG. 9C), suggesting that the layered texture of the 3DP panel, to some extent, affects the functionality of the vertical gaskets. The air movement was uneven through the edge, suggesting that some imperfection in the façade assembly might have also come into play.

2.2.2 Water tightness test

This chapter summarises the result of the air permeability test described in chapter 3.1.4. The test had a total duration of 55 minutes. FIG. 10 shows the negative pressure in the testing chamber, progressively increasing during the test, and the constant water flow sprayed on the outside of the specimen.

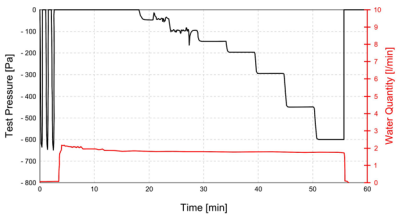

FIG. 10 Diagrams showing the negative pressure applied in the testing chamber progressively increasing over time and the constant water flow sprayed on the outside of the façade.

For the whole test duration, three people stood inside the testing chamber, inspecting the façade assembly. No water penetration was observed throughout the duration of the test. The results were assessed according to the SN EN 12154:1999, which classifies façades' water tightness within four categories of increasing efficiency level (R4, R5, R6, R7). The façade specimen is classified in category R7.

3 EXPERIMENT 2 – EXPLORING THE SYSTEM'S ARCHITECTURAL POTENTIAL

The previous chapter describes the experiment designed to validate the concept of a 3DPCW from a functional standpoint. The experiment aimed for a quantitative result, namely, the system classification of air permeability and water tightness. This analysis is not without limitations. On the one hand, being a preliminary study, it produces numerical information on one single CW system (RAICO THERM+ H-I), even though countless standard CW systems exist on the market and could be used with the same approach. On the other hand, focusing on functionality, the study leaves behind the possibility of exploring the architectural and tectonic potential of this novel approach. The process described in the following chapter has been specifically designed to fill this gap and should be considered as a complementary study. The approach is rather oriented to a qualitative result. In this case, the vocabulary of standard CW solutions has been expanded, considering that all solutions adapted to LSR3DP façade panels would function similarly. Also, the focus has been shifted to demonstrating the design possibilities offered by the novel façade system.

3.1 METHOD

The experiment presented in this section consists of the design and fabrication of a large-scale demonstrator. The large-scale demonstrator corresponds to a single-storey building façade mock-up, including two organically shaped LSR3DP panels. The panels have a rectangular outline, each measuring 2 m in height, 1 m in width, and having a variable thickness from 10 mm to

35 mm. Within the mock-up, the panels span from floor to ceiling and are reciprocally connected by a central mullion. Behind the façade, the roof and the floor extend for 1 m, creating a 2 m^2 accessible space. The total height of the mock-up was set at 2 m rather than a regular floor height (2.4 m to 2.7 m) to limit the panel's 3D printing time. All the components composing the façade's structure (floor, roof, mullion, upper and lower façade horizontal edges) are made of timber. The detailing of the interface between the panels and the timber substructure was carried out using the solution set offered by the company RAICO®. Three different details were developed: the connection between the panels and the roof (FIG. 11B1), the connection between the panels and the floor (FIG. 11B3), and the reciprocal connection between the panels (FIG. 11B2).

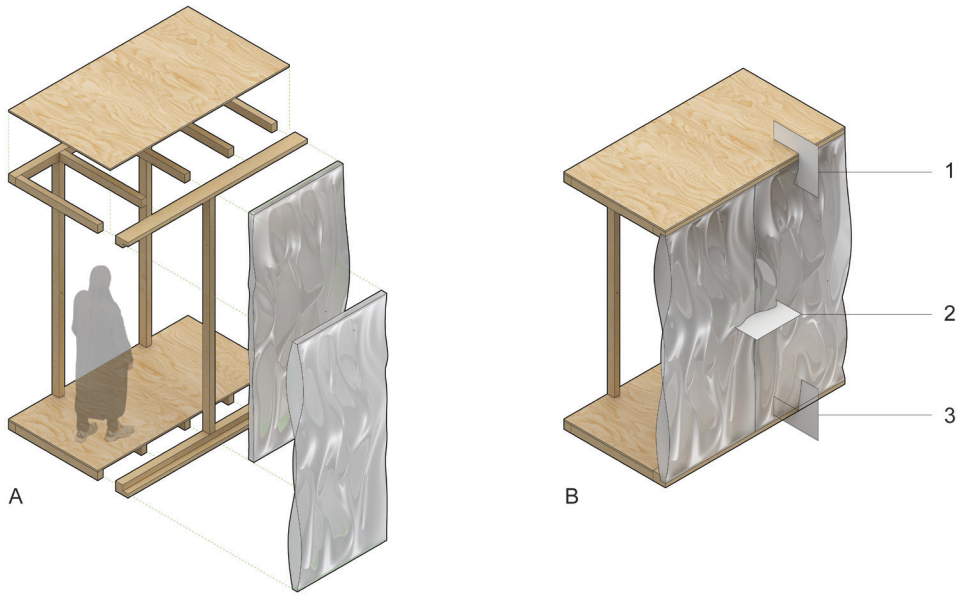

FIG. 11 A) demonstrator constructive logic; B) types of connections studied: 1: façade - roof connection; 2: panel to panel connection; 3: façade to floor connection.

3.2 RESULTS

3.2.1 Design of the LSR3DP panels

One of the advantages of 3D printing is the possibility of tailoring the geometry and targeting specific material performances. It has been shown, e.g., that different panel infills lead to different thermal performances (Piccioni, Leschok, Lydon, et al., 2023) as different degrees of light transmission and solar gain can be achieved through different printing patterns on the outside surface (Piccioni, Leschok, Grobe, et al., 2023) (Cheibas, Piccioni, et al., 2023). The present study, however, does not focus on building physics but rather on the panel's connections and the system tectonic. Therefore, in the design of the two mock-up panels, both infill and surface patterns have been simplified to reduce material use and printing time. Besides this fact, the connection strategy outlined here is

compatible with the guidelines offered in the aforementioned studies, focusing on producing high-performance LSR3DP façade panels (e.g. maximizing the number of air cavities within the infill to improve the panel U value).

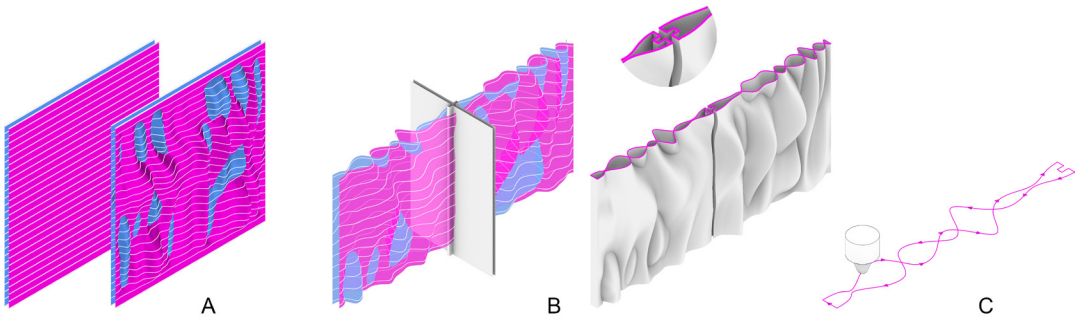

FIG. 12 3DP panels design logic. A) Perlin noise applied to two parallel surfaces; B) Production of the connection detail; C)Toolpath consisting of one continuous smooth curve.

A first guideline for the current design process was based on exploring new aesthetics allowed by 3DP, creating a geometry that could not be made by any other means. Given those prerequisites, the concept for the façade global geometry resulted in a volume defined by two intersecting free-form surfaces (FIG.12A). The design process was held within Rhinoceros 3D and Grasshopper, a 3D modelling environment that allows parametric operations. The global façade geometry is created by applying a Perlin noise (Perlin, 1985) distortion to a couple of rectangular, flat, parallel B-rep surfaces. The multiple intersections between the two surfaces are meant to provide rigidity to the panel. A second design criterion for the current demonstrator has been production speed optimisation. To allow higher velocity during printing, avoiding vibration and consequential quality loss, the 3D printing toolpath needs to avoid kinks and sharp edges. When sliced horizontally, the chosen geometry results in a series of smooth cross-sections (FIG.12C).

3.2.2 Connection detailing

In the previous experiment, the façade concept consisted of continuous mullions separated by transoms. In the present case, a different configuration was explored. The façade scheme consists of two continuous transoms on the upper and lower limits of the façade, between which the mullions are interposed. In the present configuration, the system is meant to channel any water seeping through the façade inside the lower transom gasket and drain it through specific apertures.

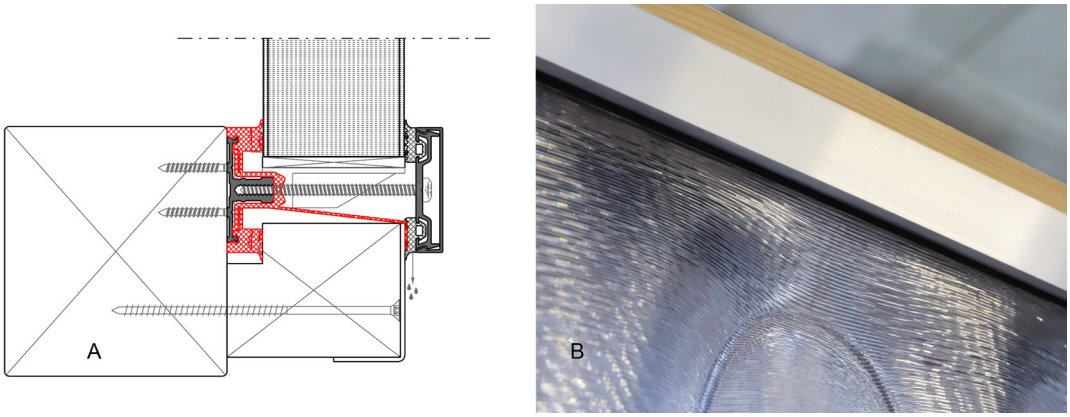

FIG. 13 A: façade-floor connection detail; B: Close-up of façade-roof connection in the final demonstrator.

For the panel's horizontal connections, corresponding to the façade's upper and lower edges, the same connection type was adopted as used in experiment 1 (RAICO THERM+ H-I). The pattern characterising the panels was designed to progressively fade towards the upper and lower edges, transitioning smoothly from an organic surface to a flat one. This way, the flat portion of the panel could be effectively clamped between the two aluminium profiles and EPDM gaskets of the standard CW system (FIG. 13). For the lower detail, a special gasket was chosen to create an internal gutter able to collect and evacuate any water seeping through the connections and draining through the mullions (FIG. 13A, element in red).

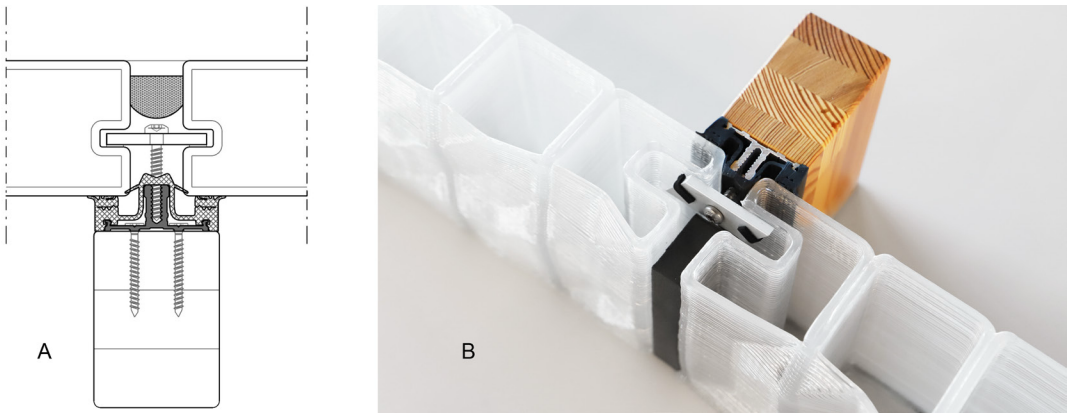

FIG. 14 A: Panel-to-panel vertical connection detail; B: Panel-to-panel vertical connection, prototype (wet or dry sealant missing).

A different solution was adopted for the vertical connection. The curvy pattern characterising the façade design is continuous throughout the two panels. Respecting the pattern continuity required a strategy to limit the visual impact of the vertical connection. This goal was achieved by hiding the fixation to the timber mullion within the thickness of the panel. This involved adopting a different solution compared to the one used in experiment 1. The solution consists of a special curtain wall detail based on an aluminium profile, EPDM gasket, punctual fasteners (toggles), and wet or dry sealant (RAICO THERM+ H-I Structural glazing SG2). This detail is commonly used to avoid additional frames on the outside of the façade and to achieve a flush glass surface. The toggles are generally inserted in a groove specifically manufactured in the IGU or panel edge. A similar groove was designed and produced on the left and right edge of the 3D-printed panel (FIG. 14). The 3D-printed infill panel does not require structural silicone bonding for its functionality. This presents a clear advantage over traditional SG glass systems, which rely on bonding performance control, testing, and other stringent requirements.

3.2.3 Fabrication of the LSR3DP panels

For the 3D printing to be executed, the geometrical information of the 3D model needed to be translated into a toolpath, meaning a series of positions the robot has to reach progressively during fabrication. This operation was performed within Rhinoceros and Grasshopper, the same parametric environment used for all design operations. The workflow consisted of (i) slicing the 3D model vertically to obtain parallel polylines (the 3D printing layers) spaced 2 mm apart; (ii) dividing the polylines into points, spaced approximately 5 mm apart; (iii) assigning to each point an XY plane, which the robot could interpret as a position instruction. The communication between the 3D modelling environment and the machine was established through COMPAS_RRC (*COMPAS RRC*, 2024) using a JavaScript Object Notation (JSON) as an intermediary file format.

The two LSR3DP panels were produced in the Robotic Fabrication Lab of ETH Zurich. The 3DP set-up consisted of a CEAD thermoplastic extruder (CEAD, 2024) attached to an ABB 4600 robotic arm, which, in turn, was attached to a gantry system. This particular configuration allowed for the great cinematic possibilities required to 3D print large-scale components. The CEAD extruder works with different types of thermoplastics and must be fed with material in the form of pellets. For the present case, transparent Polyethylene Terephthalate Glycol (PETG) was employed. The material has a low warping tendency and is, therefore, widely used in LSR3DP applications. Before fabrication, the material was dried for 4 h at 60°C in a VisMec Dryplus 50 dryer to remove moisture. The extruder features four customisable heating zones for temperature control and a custom-made cooling device that releases compressed air of 0.6 bar pressure. The heating zones were set respectively to 215, 225, 235, and 245°C, and the cooling device was turned on during printing. A 3 mm nozzle was used for extrusion, and the material flow was regulated to achieve a wall thickness of 5 mm.To reduce the risk of warping and improve the adhesion between the panels and the 3D printing groundwork during fabrication, a 50 mm brim layer was added at the base of the panels. The toolpath length of the two panels corresponded to 2556 m and 2831 m. Since the robot velocity was set to 70 mm/s, printing time resulted in 10 hours and 8 minutes for the first panel and 11 hours and 14 minutes for the second panel. For safety reasons, the set-up was run in manual mode, meaning, an operator had to hold the safety button on the ABB flex pendant during the whole fabrication process. For this reason, the printing sessions were interrupted multiple times, leading to imperfections in the panel's 3D-printed surface. The weight of the 3DP panels resulted in 31.4 kg for the first and 34.8 kg for the second panel, meaning an average of 16.5 kg/m^2. Each panel could easily be handled by two people during the assembly operations.

3.2.4 Fabrication of the timber substructure and assembly

The timber substructure was produced using conventional carpentry techniques. The roof and the floor were produced using two sheets of plywood 18 mm thick, stiffened by a timber frame made of 80x60 mm planks. The mullion and the two columns supporting the roof were produced using 80x60 mm timber planks. In contrast, the upper and lower façade limits, which are characterised by a more complex cross-section, were produced by glueing multiple planks of different cross-sections. The different timber components were assembled using a nailer powered by a compressor. After the construction of the timber substructure, the façade system (aluminium profiles, EPDM gaskets, pressure plates, 3DP panels...) was assembled in a timeframe of two hours (FIG. 15).

FIG. 15 2 m x 2 m x 1 m single-storey building façade mock-up consisting of two 3DP façade panels integrated into a timber substructure with off-the-shelf curtain wall connections

4 CONCLUSION

The present study focuses on the problem of connections in LSR3DP façades. It builds upon the general hypothesis that experimental solutions can benefit from hybridisation with standard, highly tested products to find an easier way into real-world architecture. In this framework, the study introduces the idea of using conventional curtain wall connections to join highly customised 3DP façade panels. The concept was evaluated both from a functionality and from a design standpoint.

In the first instance, an experiment was performed to classify the system for air permeability and water tightness.

Regarding air permeability, the system was classified in category A2 according to SN EN 12152:2002. The standard CW system used in the experiment (RAICO THERM+ H-I), when combined with IGUs or opaque panels, is classified in a higher category (AE (>600)). This means that the substitution of IGUs with LSR3DP does indeed have a slightly negative impact on the connection's performance, presumably due to the horizontal grooves in the 3DP surface derived from the layered deposition of the material. Besides the performance loss, A2 classification should be considered a positive result, acknowledging that this is a preliminary study aimed to define whether this approach can be used in architectural projects. Façades classified as A2 can, in fact, be used in architecture where the expected wind dynamic pressure is moderate. The use of SN EN 12152:2002 classified system in relation to wind dynamic pressure is regulated by the SIA 329 (*SIA 329*, 2018) (*SN 520329*, 2018). In case a project requires it, further studies will need to address the improvement of the system's air permeability performance. In this regard, three alternative approaches are suggested. First, the test could be repeated, increasing the pressure on the clamping mechanism. This could be achieved by,

e.g. increasing the number of screws that connect the pressure plate to the mullions and transoms. Second, a custom gasket could be developed, characterised by greater thickness and higher flexibility. Third, special attention could be paid to the fabrication of the panel's edges, adjusting parameters dynamically (e.g. velocity) to achieve a smoother interface with the gasket. As stated in section 2.2.1, the performance loss concerns only the connections that meet the 3D-printing layers perpendicularly; therefore, those measures could be limited to those particular points.

Regarding water tightness, the system was classified in category R7 according to SN EN 12154:1999. R7 is a highly performative category, and it is suitable for the majority of architectural projects. The standard CW system used in the experiment (THERM+ H-I), in combination with IGUs, is certified by RAICO as RE 2.100, meaning it can withstand water penetration with a pressure up to 2100 Pa. Verifying whether the system performs equally to the same pressure level in combination with LSR3DP façade panels is outside the scope of this study. In terms of water tightness, the system does not require any improvement or further testing.

In the second instance, an experiment consisting of a design case study was developed to assess the system from a broader perspective. From an aesthetical standpoint, the hybrid tectonic, which arises from the combination of conventional façade construction on the one hand and digitally designed and fabricated custom elements on the other, offers an exciting territory for designers to explore. In this regard, the present work aims to present a general methodology and inspire further research. Future works on this line could either use the façade solutions detailed in this paper, exploring new designs and functionalities for the 3D-printed panels or abstract the overarching logic and adapt it to other solutions provided by the façade construction industry (e.g. unitised façade system). Moreover, future research should tackle how this approach could be adapted to the different situations of increased complexity which commonly arise in building façade design (corner detail, presence of apertures like doors and windows).

Another consideration concerns the interdependence – implicitly entailed in this approach – between the geometrical freedom provided by LSR3DP and the limits imposed by the underlying substructure. With 3D printing, one can easily produce façade panels characterised by a curved boundary. However, increasing the complexity of the panel boundary naturally means producing the same effect on the underlying substructure, a condition which might not always be desirable due to fabrication constraints. This fact needs to be carefully taken into account in the design phase. The demonstrator presented in this paper studied the case of a simple façade composed of straight mullions and transoms arranged in a planar configuration. The geometrical complexity allowed by 3D printing has been celebrated by producing a custom texture on the panel surface rather than creating a complex global geometry. Future studies should go beyond this condition and explore more complex configurations characterised by single or double curvature. A first option worth exploring in this framework is a façade whose global geometry is defined as a ruled surface. This condition could still be achieved using straight mullions and transoms. A further step in this direction would be introducing curved elements for the substructure. This might be possible with different state-of-the-art technologies depending on the materiality of the components. This option would allow taking full advantage of the geometrical complexity allowed by 3DP in creating complex shapes for the panels and consequentially expand the set of architectural typologies achievable by this means (e.g. domes, grid-shells).

Acknowledgements

ETH RFL: Michael Lyrenmann, Philppe Fleishmann, Luca Petrus. ETH MAS dFab: Aejmelaeus-Lindstrém Petrus. HSLU: Bruno Marty. Raico: Josef Erni, MArtin Eberhard. Saeki: Matthias Leshock

References

Al Jassmi, H., Al Najjar, F., & Mourad, A.-H. I. (2018). Large-Scale 3D Printing: The Way Forward. *IOP Conference Series: Materials Science and Engineering*, *324*. https://doi.org/10.1088/1757-899X/324/1/012088

CEAD. (2024). *CEAD Group*. CEAD | Large Scale Additive Manufacturing. https://ceadgroup.com/

Cheibas, I. (2023). *Additive Manufactured Facade*. https://doi.org/10.3929/ethz-b-000648606

Cheibas, I., Lloret-Fritschi, E., Piccioni, V., Leschok, M., Dillenburger, B., Schlüter, A., Gramazio, F., & Kohler, M. (2023). *Thermoplastic large-scale 3D printing of a light-distribution and fabrication-informed facade panel*. https://doi.org/10.3929/ETHZ-B-000639445

Cheibas, I., Perez Gamote, R., Önalan, B., Lloret-Fritschi, E., Gramazio, F., & Kohler, M. (2023). Additive Manufactured (3D-Printed) Connections for Thermoplastic Facades. In *Trends on Construction in the Digital Era* (Vol. 306, pp. 145–166). Springer International Publishing. https://doi.org/10.1007/978-3-031-20241-4_11

Cheibas, I., Piccioni, V., Lloret-Fritschi, E., Leschok, M., Schlüter, A., Dilllenburger, B., Gramazio, F., & Kohler, M. (2023). Light Distribution in 3D-Printed Thermoplastics. *3D Printing and Additive Manufacturing*. https://doi.org/10.1089/3dp.2023.0050

COMPAS RRC. (2024). https://compas-rrc.github.io/compas_rrc/latest/

EN 12152:2002—Curtain walling - Air permeability - Performance requirements and classification; German version. (2002).

EN 12153:2000—Curtain walling—Air permeability—Test methods; German version. (2000).

EN 12154:1999—Curtain walling - Watertightness - Performance requirements and classification; German version. (1999).

EN 12155:2000—Curtain walling—Watertightness—Laboratory test under static pressure; German version. (2000).

EN 13830:2003—Curtain walling—Product standard; German version. (2003).

Engelsmann, S., Spalding, V., & Peters, S. (2010). *Plastics in Architecture and Construction* (Birkhäuser).

Fleckenstein, J., Bertagna, F., Piccioni, V., Fechner, M., Düpree, M., DAcunto, P., & Dörfler, K. (2023). *Revisiting Breuer through Additive Manufacturing: Passive solar-control design strategies for bespoke concrete building envelope elements*. 527–538. https://doi.org/10.52842/conf.ecaade.2023.1.527

Herzog, T., Krippner, R., & Lang, W. (2004). *Facade construction manual* (1st ed). Birkhauser-Publishers for Architecture.

Knaack, U., Bilow, M., Klein, T., & Auer, T. (2007). *Fassaden: Prinzipien der Konstruktion*. Birkhäuser Verl.

Leschok, M., Cheibas, I., Piccioni, V., Seshadri, B., Schlüter, A., Gramazio, F., Kohler, M., & Dillenburger, B. (2023). 3D printing facades: Design, fabrication, and assessment methods. *Automation in Construction*, *152*, 104918. https://doi.org/10.1016/j.autcon.2023.104918

Mungenast, M. B. (2019). *3D Printed Future Facade*.

Naboni, R., & Jakica, N. (2022). Additive manufacturing in skin systems: Trends and future perspectives. In *Rethinking Building Skins* (pp. 425–451). Elsevier. https://doi.org/10.1016/B978-0-12-822477-9.00004-8

Perlin, K. (1985). *An image synthesizer*.

Piccioni, Leschok, M., Lydon, G., Cheibas, I., Hischier, I., Kohler, M., Gramazio, F., & Schluter, A. (2023). *Printing thermal performance: An experimental exploration of 3DP polymers for facade applications*. https://doi.org/DOI 10.1088/1755-1315/1196/1/012063

Piccioni, V., Leschok, M., Grobe, L. O., Wasilewski, S., Seshadri, B., Hischier, I., & Schlüter, A. (2023). Tuning the Solar Performance of Building Facades through Polymer 3D Printing: Toward Bespoke Thermo-Optical Properties. *Advanced Materials Technologies*. https://doi.org/10.1002/admt.202201200

RAICO. (2024). https://www.raico.de/

Rhinoceros 3D. (2024). https://www.rhino3d.com/

SAEKI Robotics. (2024). https://www.saeki.ch/

Seshadri, B., Cheibas, I., Leschok, M., Piccioni, V., Hischier, I., & Schlüter, A. (2021). Parametric design of an additively manufactured building facade for bespoke response to solar radiation. *Journal of Physics: Conference Series*. https://doi.org/10.3929/ethz-b-000521182

SIA 329. (2018).

SN 520329. (2018).

Strauß, H. (2013). *AM Envelope / The potential of Additive Manufacturing for façade construction*. https://doi.org/10.7480/abe.2013.1.386

JOURNAL OF FACADE DESIGN & ENGINEERING

VOLUME 12 / NUMBER 1 / 2024

SOAP | STICHTING OPENACCESS PLATFORMS
ISSN PRINT 2213-302X
ISSN ONLINE 2213-3038
ISBN 978-94-93439-16-0